ASSESSMENT AND EVALUATION OF PONGAMIA PINNATA OIL AS AN ALTERNATIVE FUEL FOR MINE EQUIPMENT

Thesis

Submitted in partial fulfilment of the requirements for the degree of

DOCTOR OF PHILOSOPHY

by

BALAJI RAO K

DEPARTMENT OF MINING ENGINEERING
NATIONAL INSTITUTE OF TECHNOLOGY KARNATAKA,
SURATHKAL, MANGALORE-575025

July, 2023

D E C L A R A T I O N

by the Ph. D Scholar

I hereby declare that the Research Thesis entitled **“Assessment and Evaluation of Pongamia Pinnata Oil as an Alternative Fuel for Mine equipment”** which is being submitted to the **National Institute of Technology Karnataka, Surathkal** in partial fulfillment of the requirements for the award of the Degree of **Doctor of Philosophy** in **Mining Engineering** is a bonafide report of the research work carried out by me. The material contained in this Research Thesis has not been submitted to any University or Institution for the award of any degree.

Balaji Rao K
(Reg. No.: 177120MN001)
Department of Mining Engineering

Place: NITK, Surathkal
Date: 14.07.2023

CERTIFICATE

This is to certify that the Research Thesis entitled "**Assessment and Evaluation of Pongamia Pinnata Oil as an Alternative Fuel for Mine Equipment**" submitted by **Mr. Balaji Rao K** (**Register Number: 177120MN001**) as the record of the research work carried out by him, is accepted as the Research Thesis submission in partial fulfillment of the requirements for the award of degree of **Doctor of Philosophy.**

Research Guides

Dr. B. M. Kunar
Assistant Professor
Department of Mining Engineering
National Institute of Technology Karnataka,
Surathkal

Dr. Ch. S. N. Murthy
Professor – HAG (Retd.,)
Department of Mining Engineering
National Institute of Technology Karnataka,
Surathkal

19/7/2023

Prof. Harsha Vardhan
Professor, Head and Chairman, DRPC
Department of Mining Engineering
National Institute of Technology Karnataka, Surathkal

Chairman - DRPC
Department of Mining Engineering
National Institute of Technology Karnataka, Surathkal
P.O. Srinivasnagar-575 025, Mangalore.
Karnataka State, India.

DEDICATED
TO
MY FAMILY,
MY TEACHERS AND
MY FRIENDS

ACKNOWLEDGEMENT

I am indebted to my supervisors Dr. B. M. Kunar, Assistant Professor, and Prof. Ch. S. N. Murthy, Professor-HAG, National Institute of Technology Karnataka (NITK), Surathkal, for their excellent guidance and support throughout the research work. Their valued time, constant encouragement, help and review of the entire work during the investigations are invaluable.

I wish to thank all the members of the Research Program Assessment Committee (RPAC), including Prof. M. Govinda Raj, Professor, Department of Mining Engineering, NITK, Surathkal and Dr. Kumar G N, Associate Professor, Department of Mechanical Engineering, NITK, Surathkal for their unbiased appreciation and criticism all through this research work.

I wish to express my sincere thanks to Prof. Harsha Vardhan, Associate Professor, Head and DRPC Chairman, Department of Mining Engineering, NITK, Surathkal and former HODs Dr. M. Auna, Dr. K. Ram Chandar, Prof. M. Govinda Raj and Prof. V. R. Sastry, for providing the departmental facilities, which ensured the satisfactory progress of my research work.

I express my sincere gratitude to, Dr. Anup Kumar Tripathi, Assistant Professor, and Dr. Sandi Kumar Reddy, Dr. Srikant Lamani, Assistant Registrar, Department of Mining Engineering, NITK for their constant encouragement during my research work.

I express my heartfelt thanks to Sri. Santosh, Sri. Surender, Sri Satish, Smt. Bharathi, Smt. Chandrakshi and Smt. Gayathri, Department of Mining Engineering, NITK, Surathkal who helped me in one way or the other during the course of my work. Also, I thank NITK, Surathkal, for providing financial assistance and all the necessary facilities to make this research peaceful. I also thank the Department of Chemical Engg., and Department of Mechanical Engg., NITK, for providing experimental facilities.

I owe my deepest gratitude to The Hutti Gold Mines Limited (HGML), Karnataka, for giving permission to collect data for my research work. I also owe my deepest gratitude to Sri. Prakash, I/c Executive Director, HGML, Karnataka, Sri. Sikender, Sri. Dean Derrick, Sri. Elango Ramchandra, Sri. Kumaresh A, Sri Suresh Tambe, Sri. Prakash Bandenur, Sri. Prashant D, Sri Manjunath Kadler, Sri. Zakeer Hussain, Sri. Safiulla Khan, Sri Manjunath Ellappa, Sri.

Raghavendra, Sri. Ravi Kumar, Sri. Manjunath T S, of HGML, Karnataka for their kind help during collecting data in the Mine.

I would like to thank my friends Dr. Harish Kumar N S, Dr. N V Sarathbabu Goriparti, Dr. Vijay Kumar S, Mr. Harish H, Dr. Gayana B C, Mr. Sridhar S, Dr. Lakshmi Narayana S, Dr. Vijaya Raghavan P Mr. Mohit Bekal, Mr. Eshwaraiah, Dr. Balaraju Jakkula, Dr. Ch. Vijay Kumar, Mr. Bharath Kumar S, Mr. Pudari Harish, Mr. Gurram Dileeep, Mr. Raghunath Reddy, Mr. Sahas Swamy, Mr. Bojja Shiva Kumar, Mr. Ram Mohan Perumalla, Mr. Anil Nayak, Mr. Sasi Kiran, Mrs. Chenna Basamma and Mr. Tejeswaran K M, for their countless help during my research work. I Specially Thank Dr. Jagadish for his help during the experimentation.

I would like to share this moment of happiness with my father Late Mr. K Krishna Murthy, my mother, Late Mrs. Vimala Bai K, my elder Brother Mr. Satish Rao K, my younger brother Mr. Sajjan Rao K, my sisters in law Mrs. Gayathri and Mrs. Sirisha my father in law Mr. K H Jayaprakash, my mother in law Late Mrs. Shobha J P, my wife Mrs. Seema K J, my dearest little masters, Devashree-Kaushal, Humangh-Lisha, and Yashica-Lian Sai, for all the sacrifices and compromises they have made during the tenure of my Ph. D work.

I also thank my cousin brothers, sisters, and elder parents who have been continuously supporting me during the course of my research work.

I am sure I have forgotten someone. I assure you that this is a shortcoming on my part and not on yours. I beg you to forgive me for my oversight.

Place: NITK, Surathkal

Date: 14. 07.2023 (Balaji Rao K)

ABSTRACT

The growing population has demanded to need more power generation. The present era relies mainly on fossil fuels as solid and liquid power sources. The demand for more power can lead to the exhaustion of fossil fuels. This also has given rise to a search for an alternative fuel source. Liquid fuels can readily be supplemented using other alternative fuel sources, including ethanol, natural gas, electricity, hydrogen, propane, methanol, P-series fuels, and biodiesel. Biodiesel can be used as a supplement to diesel in the form of blends. Pongamia pinnata is one of the most popular sources of biodiesel in South India.

In the present study, Pongamia pinnata is introduced as a biodiesel source in different forms, namely raw form, ester form, and combined form. i.e., Raw pongamia oil (RPO), methyl ester of Pongamia oil (MPO), a combinational form of methyl esters of Pongamia and waste cooking oil (MPWO), methyl esters of Pongamia pinnata and waste cooking oil (MWO). Samples were prepared with blends varying from 0% to 30% in increments of 5% volumetrically, and these samples were referred to as base biodiesel blends. A similar set of samples were prepared with an additional 10% volume of ethanol and acetone to the base biodiesel blends by reducing the volumetric contribution of diesel. The total sample size was 75, including diesel.

For each prepared sample, property tests were performed to identify the density, kinematic viscosity, and calorific value. A deviation was computed with reference to diesel. It was found that the RPO showed the largest deviation as far as the properties were concerned, which were found to be 1.66% lower, 13.24% lower, and 1.81% for density, Kinematic viscosity, and calorific value, respectively.

Further, the engine test was carried out on a single-cylinder four-stroke diesel engine. The engine speed was kept constant (1500 rpm), and the engine load varied from 5% to 100% in increments of 25% of the engine load. i.e., the engine speed was maintained constant for each engine load, and the same was followed for all 75 samples. The time taken for 10cc fuel consumption and the corresponding emissions at each engine load was recorded. Four of the emission parameters were observed, namely carbon monoxide (CO), Carbon dioxide (CO_2), unburnt hydrocarbons (UHC), and oxides of Nitrogen (NOx). The mass of fuel consumed

(MF), brake thermal efficiency (BTE), and brake-specific energy consumption (BSEC) were calculated.

The effects of blending on the performance and emissions of the engine were evaluated by plotting a scatter graph. The average deviations of performance and emission parameters were found. The average deviations were measured by referencing each base biodiesel blend and its ethanol and acetone additions. BTE and BSEC of diesel-ethanol (DE) were found to be near to the BTE and BSEC of diesel, with deviations (higher) of 2.59% and 2.33%, respectively. DE is considered the best alternative for diesel in terms of efficiency and energy consumption. RPO is considered the poorest source regarding efficiency and energy consumption, with deviations (Lower) of 32.73% and 4l.4%, respectively. All biodiesel blends showed lower CO and UHC emissions, exhibiting higher CO_2 and NOx. RPE (raw Pongamia-ethanol) blends showed better CO and UHC with deviations (Lower) of 57.47% and 51.1% and poorer CO_2 and NOx with deviations (higher) of 49.16% and 172.67%.

Statistical analysis was performed to predict the performance and emissions of the engine. Regression modelling (multivariate) and ANOVA analysis were used to develop regression equations and identify the significant parameters. The parameters blend, load, density, kinematic viscosity, calorific value, and mass of the fuel consumed were considered input parameters. The output parameters include BTE, BSEC, CO, CO_2, UHC, and NOx. It was observed that the regression models showed a performance of more than 70% R-squared values at a confidence interval of 95% in predicting the performance and emissions of the engine. Blend and load on the engine were considered the most significant parameters.

Prediction studies were also performed using the ANN technique. The number of neurons varied from 4 -10, and a two-layered perceptron neural network was chosen for the analysis. TRAINLM and LEARNGDM were used as training and learning algorithms. The Transfer function is TRANSIG. Each neuron's Root mean squared error (RMSE) value was computed. The best model was evaluated to be the one with the least RMSE. With 375 data sets, 263 were used for training the model, and the remaining 112 were used for testing and validating the model. 50% of the remaining data is shared equally for each testing and validation. An MLPNN network, the optimised model for predicting BTE, BSEC, CO, and NOx, was found to have 6 neurons. The best model for predicting the UHC and CO_2 is the one with 5 neurons with R^2 value of 0.99 for all training, testing, and validation.

Field studies were conducted in one of the esteemed Underground metal mines in southern India. A mine Tipper was selected to conduct the test with 20% of the blends of base biodiesel. Two conditions, idle and high idle, were implemented to study the variations. The four emission parameters studied were NO, NO2, NOx, and CO. The observations were similar to experimentation, and the deviations are estimated. RPO reduced CO emissions of the engine. Alternatively, increasing nitrogen emissions. The deviations of RPO compared to diesel were 29.5% and 50.74%, with diesel at both idle and high idle conditions for CO, respectively. The deviations measured are 29.5% and 33% at both idle and high idle conditions for NOx, respectively.

TABLE OF CONTENTS

LIST OF FIGURES

LIST OF TABLES

NOMENCLATURE

RPO: Raw Pongamia Pinnata Oil

MPO: Methyl esters of Pongamia Pinnata

MWO: Methyl esters of Waste cooking oil

MPWO: Methyl esters of Waste cooking oil and Pongamia pinnata oil

RPA: Raw Pongamia oil with Acetone

RPE: Raw Pongamia oil with Ethanol

MPE: Methyl esters of Pongamia Pinnata with Ethanol

MPA: Methyl esters of Pongamia Pinnata with Acetone

MWE: Methyl esters of Waste cooking oil with Ethanol

MWA: Methyl esters of Waste cooking oil with Acetone

MPWE: Methyl esters of Waste cooking oil and Pongamia pinnata oil with Ethanol

MPWA: Methyl esters of Waste cooking oil and Pongamia pinnata oil with Ethanol

DE: Diesel with Ethanol

DA: Diesel with Acetone

CO: Carbon Monoxide

CO_2: Carbon Dioxide

SO_2: Sulphur Dioxide

NO: Nitrous Oxide

NOx: Oxides of Nitrogen

NO_2: Nitrogen Di oxide

P-Value: Probability Value

T-Value: T-Test Values

R^2 or R-Sq: R-squared Value.

BTE: Brake thermal Efficiency

BSEC: Brake Specific Energy Consumption

BSFC: Brake Specific Fuel Consumption

PP: Pongamia Pinatta

CHAPTER 1

INTRODUCTION

1.1 Alternate fuels

The global fossil fuel crisis and emissions problems have led to the investigation of alternative fuels (Shahir et al. 2014). According to the report “Clean Cities” in June 2009, alternative fuels are any materials or substances that can be used as fuels, apart from fuels like fossil fuels, nuclear materials, and synthetic radioisotope fuels from nuclear reactors. The top eight alternate fuels are ethanol, natural gas, electricity, hydrogen, propane, methanol, P-series fuels, and biodiesel.

1.2 Need for alternate fuels for mining industries

Increased mining activities, frequent use of fossil fuels, and equipment fuelled using petroleum products contribute to the emission of greenhouse gases (GHGs). The mining industry uses diesel equipment, including load haul dumpers (LHD), Side discharge loaders (SDL), shovels, graders, tractors, and explosive vans.

Inflation in diesel prices and the availability of crude oil to produce diesel are significant concerns. The amount of oil exploration for the forthcoming decades may reach the highest peak due to the increasing population of the world and a relative increase in the transportation system relying on the energy sectors for more fuel. As "The Hindu" reported on "26th August 2018", Fortescue Metals of Australia, the world's fourth-largest iron ore miner, considers fuel an inflation driver to increase production margins. With the increase in production, the machinery for a particular mine industry also increases.

The second major concern for using alternative fuels in the mining industry is the environmental problems from diesel use. As per the Central pollution control board (CPCB) guideline on emissions, the sulfur content in diesel was limited to 0.035% in 2010. Further, it was 0.05% during 2005-10, 0.25 during 2000-2005, and 0.5% during 1996-2000. Some alternative fuels possess zero sulfur content; as a form of alternative fuel, biodiesel possesses lesser to zero sulfur content than diesel. Apart from this, the emissions arising from the outlet of diesel engines contain Carbon monoxide (CO) and

Unburnt Hydrocarbons (UHC), which contribute as a part to air pollution (Shahir et al. 2015), thereby enhancing the demand for the use of alternative fuels instead of diesel. The outcome of excess emissions using fossil fuels has resulted in global warming. As per the Indian climate emergency institute, global warming is synonymous with the enhanced greenhouse effect, increasing the number of greenhouse gases surrounding the earth's atmosphere, which leads to the trapping of more and more solar radiation and therefore increases the planet's overall temperature.

The third primary concern to using alternative fuels is that economy is involved in importing fuels, as per the web reports of "Veolia" The economy is classified into two types: conventional economy and circular economy. In a conventional economy, everything is linear from cradle to extraction, production, and disposal. In the circular economy, consumption patterns are designed to mirror the cyclical approach of natural ecosystems. With over 1.3 billion people and a GDP growth of 7% annually, India faces new resources and energy consumption challenges. It has become necessary to control GHG emissions, waste generation, pollution, and erosion of natural capital. That is why the circular economy model is an opportunity for India to reach a long-term prosperity economy. With the implementation of the circular economy, even mine wastes can be recycled to improve the economy further.

1.3 Why Pongamia pinnata (PP) and its forms as alternative fuels

An ecological restoration approach is beneficial for reclaiming land degraded by mining (Srivastava et al. 2014); most degraded lands are used for agriculture and forestry purposes. Trees and shrubs provide permanent vegetation cover on mine-degraded sites with little or no aftercare. Trees can improve soils through numerous processes, including maintenance or increasing soil organic matter (SOM) (Ahirwal et al. 2017). Several fast-growing, nitrogen-fixing, and high bio-masses-yielding tree species were tested for growth on the overburden slope. Pongamia pinnata is one of the best species that can be grown on slopes of the overburden (Singh A. N & Singh J. S. 2006); This implies that Pongamia pinnata trees can be vegetated on degraded lands to improve the productivity of Pongamia pinnata oil.

Pongamia trees can grow on roads, canals, and bordering portions of farmland with minimal care. Its seeds contain 28% to 34% of the oil; they are not edible. Up to 99%

biodiesel is obtained through transesterification. It can grow well in soils of low agricultural productivity, typically characterised by low water availability, low nutrient content, and high salinity (Dwivedi and Sharma 2014).

Alternative fuels are prepared using different edible and non-edible sources, but the fuel prepared to replace diesel must have similar characteristics or be the same as diesel. Many researchers have contributed to large numbers in the development of alternative fuels; Pongamia, as a fuel source, can be used as a supplement to diesel (Dwivedi G. & Sharma M. P. 2014). Pongamia pinnata, as an alternative fuel, is used in different forms. These include raw, ester, and combinational forms. The major difficulty in using the raw oil form is that the oil's viscosity is higher, leading to prolonged ignition and combustion (Zaharin et al. 2017). Hence the present study is carried out by blending the raw form of Pongamia pinata with diesel and other emulsifying agents in various blending ratios.

The other form of using Pongamia pinnata is the ester form. Because of the higher viscosity of vegetable oils, combustion of vegetable oils in IC engines is difficult. There are different processes available for reducing the viscosity of oils. Transesterification converts the oil into biodiesel, yielding max biodiesel (Balat M. and Balat H. 2010). Transesterification converts oil to biodiesel by treating the oil with an alcohol such as methanol, ethanol, and higher alcohols in the presence of an acid (Sulfuric acid) or a base catalyst (sodium hydroxide or potassium hydroxide) and subjected to a temperature.

With the use of a single type of biodiesel produced from various vegetable oils, the economy of the food supply is disturbed. Hence, an even application of biodiesels from multiple sources can provide a better solution (Gui et al. 2008). With this perspective, the present study is proposed to combine biodiesels, preferably methyl esters, from two different sources: waste cooking oil (MWO) and Pongamia pinnata oil (MPO). The advantage of preparing this mixture is that waste cooking oil's raw material cost is less than vegetable oil's yield cost. Also, the advantage of using Pongamia pinnata is that it may not disturb the economy of the food supply to a large extent as it is non-edible. The other benefit of Pongamia pinnata is the derived waste after collecting oil from the seeds, i.e., fertilisers, animal feeds, and medicines for skins. The kernels of Pongamia pinnata seeds can also be used to produce compost, soaps, and other byproducts of glycerin. Combining MWO and MPO can reduce the cost of MPO, as the raw material cost of waste cooking oil is lesser than the MPO yield.

The usage of methyl esters fuels in a diesel engine results in an increased NOx (oxides of nitrogen/ nitrous oxide) emission, decreased unburnt hydrocarbons, and carbon monoxide (Shahir et al. 2015). Further, to regulate the NOx emission, studies by earlier researchers were carried out using different emulsifying agents (Yusri et al. 2017). The present study also involves the emissions investigation using two different emulsifying agents, i.e., ethanol and acetone.

Statistical analysis helps researchers to determine the best optimal solutions for predicting output variables based on the input variables. ANOVA (Analysis of variance) is one such test that allows studying the Effect of parameters on the responses of the output variable, and the analysis indicates whether a particular parameter/ input has significance on output.

Some authors have used the RSM (Response Surface Methodology) approach to find optimum results through the importance of input parameters on output (Saravanan et al., 2017). In the present study, statistical analysis was carried out to understand the Effect of blending and engine loading on the performance and emission of the engine. The present study also identifies the relationship of input parameters: density, kinematic viscosity, calorific value, blend, the mass of fuel consumed, and engine load with response variables, namely specific energy consumption, brake thermal efficiency, and engine emission characteristics.

Artificial neural networks (ANNs) are biologically inspired computer programs that simulate how the human brain processes information. ANNs gather their knowledge by detecting patterns and relationships in data, and they learn (or are trained) through experience, not programming (Agatonovic-Kustrin and Beresford 2000). The ANN comprises hundreds of unique units, artificial neurons, or processing elements (PE) connected with coefficients (weights), constituting the neuronal structure in layers. ANN modelling predicts brake thermal efficiency and brake-specific energy consumption based on emission parameters, blending, and loading (Shivakumar et al. 2011). The present study also predicts energy consumption and brake thermal efficiency using ANN.

1.4 Thesis outline

Based on the literature review and to fulfill the research gap, the thesis is structured as follows:

Chapter 1

The introduction includes the alternative fuels' origin, types, needs, and applications in mining engineering.

Chapter 2

The chapter includes a comprehensive literature review of the topics covered in the proposed research work, including the different fuels, statistical techniques, ANN modelling, and applications in Mining Engineering.

Chapter 3

This chapter presents an experimental methodology, including the equipment and specifications. The chapter also describes the standards applied for measuring the properties of the prepared alternative fuels. A brief description of the experimentation methodology is also illustrated. A draft of the sample preparation chart is also presented.

Chapter 4

The chapter outlines the results of the experimentation. The Effect of loading and blending of alternative fuel in different forms is studied. The chapter also describes the engine performance and emission variations due to adding ethanol and acetone. A comparison study is carried out to identify the deviation in the engine's performance and emissions fueled with biodiesel blends from diesel.

Chapter 5

Presents the development of regression models to predict the performance and emissions of the engine. ANOVA analysis is performed to identify the most significant factors of the model.

Chapter 6

Outlines the ANN method of predicting the engine's performance and emissions. Based on load, blend, and properties of the fuel.

Chapter 7

The chapter introduces the applications and emission studies of implementing biodiesel blends in a Mine tipper.

CHAPTER 2

LITERATURE REVIEW

Over the past two decades, the research has contributed extensive data on alternative fuels and their applications in IC engines. Further, a detailed literature review is carried out to ease and interpret critical factors related to using alternative fuels, emulsification, and additive addition. The literature review is carried out considering four categories, namely.

1) Use of alternatives to diesel fuels in the global scenario.
2) Various emulsifications on diesel and alternative fuels.
3) Applications of biodiesel in Mining Industries.
4) Application of Regression and ANOVA to develop a prediction model for engine performance and emissions.
5) Application of ANN prediction modelling for engine performance and emissions.
6) Use of biodiesel in the mining industry.

2.1 Use of alternatives to diesel fuels in the global scenario

Sureshkumar et al. (2008) investigated the performance and emissions of SCFS diesel engines using Pongamia piannata methyl esters blends. The study concluded that up to 40% blend could be used for better efficiency, fuel consumption, and reduced emissions, similar to diesel.

Qi et al. (2009) studied the performance and emissions of SCFS diesel engines using soybean methyl ester blends. The authors' observation found properties varying from diesel BSEC (Brake specific fuel consumption) was high, similar output power as that of using diesel, emissions CO, UHC, NOx, and smoke were reduced by 27%, 27%, 5% and 52% respectively as compared to diesel.

Godiganur et al. (2009)studied the performance and emissions of a Cummins 6 BTA 5 turbocharged engine using blends of mahua biodiesel. The authors concluded that Mahua biodiesel could be safely blended with diesel up to 20% without significantly affecting the engine performance and emissions and thus could be a suitable alternative fuel for heavy-duty engines.

Kalam et al. (2011)studied the performance and emission of waste cooking oil of palm and coconut oil blends on the MCFS engine. The author concluded that 5% blending coconut and palm fuels showed a reduced brake power of 0.7% and 1.2%, respectively, compared with diesel, reduced CO by 7.3% and 21%, respectively, and decreased HC by 23% and 17%, respectively, with blend zero.

Dhar et al. (2012)used neem oil biodiesel blends to study performance and emission on SCFS engines. The author concluded that lower biodiesel blends (up to B20) could be used in unmodified CI (compression Ignition) engines without compromising engine performance and emission characteristics.

Chauhan et al. (2012) implemented jatropha biodiesel blends to study performance and emission on SCFS engines. The study results showed that the engine performance with biodiesel of jatropha and its blends was comparable to that of diesel fuel. The oxides of nitrogen from jatropha biodiesel during the whole range of the experiment were higher than diesel fuel.

Mallikappa et al. (2012) used cardanol biofuel blends to study the performance and emission of MCFS engines. The authors found that with higher loading, brake thermal efficiency increases. Emission levels were found to be nominal, up to 20% blending.

Habibullah et al. (2014) used Palm (PB), coconut (CB), and Palm+coconut (PBCB) to study the performance and emission of the SCFS engine. The experimental analysis revealed that the combined blend of palm and coconut oil had superior performance and emission over individual Coconut and Palm biodiesel blends. CO and HC emissions were reduced to a great extent at 13.75–17.97%, compared with diesel fuel operation. PB30 showed 5.15% and 18.83% higher CO and HC emissions, respectively, compared with the values for CB30. Meanwhile, PB15CB15 showed lower CO and HC emissions (2.43% and 9.35%, respectively) than PB30 and slightly higher emissions (2.60% and 7.72%, respectively) than CB30 fuel. At the same time, BSEC values were higher (8.55–9.03%) than PB15. CB15 showed slightly higher BTE (1.12%) than PB30 and slightly lower BP and BTE (0.20% and 0.12%, respectively) than CB30 fuel. PB15CB15 showed a 1.22% higher NOx emission than PB30 and a 1.20% lower NOx emission.

Imtenan et al. (2014) used palm-jatropha combined biodiesel blends to study the performance and emissions of the SCFS engine. The study revealed that compared to diesel fuel, the study concluded with reduced carbon monoxide (CO) emissions for PBJB5 and PBJB10 (9.53% and 20.49%). On the contrary, hydrocarbon (HC) emissions for PBJB5 and PBJB10 were reduced by 3.69% and 7.81% compared to diesel fuel.

Palash et al. (2015) included blends of methyl esters of Aphanamixispolystachya blends(APME) to study the performance and emissions of turbocharged MCFS engines. The study found that APME5 and APME10 showed an average 0.9% and 1.81% reduction in torque and 0.9% and 2.1% reduction in brake power (BP). The brake-specific fuel consumption increase was 0.87% and 1.78% compared to diesel. In engine emissions, diesel blends of APME gave an average reduction in carbon monoxide (CO) and hydrocarbon (HC) emissions compared to pure diesel. However, APME blends emitted higher levels of nitrous oxide compared to diesel. It was suggested that APME5 and APME10 could be used as diesel fuel substitutes without any engine modifications.

Perumal and Ilangkumaran (2017) used methyl esters of Pongamia pinnata blends in an SFCS engine to study the performance and emissions of the engine. The study revealed that using PME as fuel reduces carbon monoxide to 8.2% compared to diesel; at the same time, HC was reduced by 8.9%, and a considerable reduction in nitrogen oxides. There was an increase in BSEC of 4.2%, and the thermal efficiency was reduced by 2.4%.

Patel and Sankhavara (2017) reviewed the application of Pongamia pinnata biodiesel blends and their applications in diesel engines. The review concluded that both efficiency and emissions of the diesel engine are comparable with 20% blending.

Damanik et al. (2018)reviewed different sources of biodiesel application in diesel engines. The review concluded that most biodiesel blends significantly decrease carbon monoxide and total unburned hydrocarbon emissions. There is also a decrease in carbon monoxide, nitrogen oxide, and total unburned hydrocarbon emissions. At the same time, the engine performance increases for diesel engines fueled with biodiesels blended with nano-additives. The development of automotive technologies, such as exhaust gas recirculation systems and low-temperature combustion technology, also improves the thermal efficiency of diesel engines and reduces nitrogen oxide.

Leksono et al. (2018) studied Pongamia pinnata's sustainability as a biodiesel source. The study suggests that the leguminous tree Pongamia could be utilized to produce biofuel while restoring degraded land. Its height is 15–20 m, and it can grow in various environmental conditions. Its seeds can generate up to 40% crude oil by weight. It can help restore degraded land and improve soil properties.

2.2 Emulsifying agents with biodiesel

Singh et al. (2010) used Aqueous ethanol and 1-butanol with crude and virgin coconut oil (CCO and VCO) biodiesel blends in an SFCS engine to study the performance and emissions of the engine. The study revealed that SO_2 (Sulfur dioxide) emission for hybrid fuels is reduced by as much as 54% for CCO-based hybrid fuels and 53% for VCO-based hybrid fuels compared to diesel. The viscosity of the hybrid fuels can be decreased and brought merely to the viscosity of diesel using micro emulsification techniques.

Subbaiah and Gopal (2011) included rice bran (RB) oil and ethanol blends in the SFCS engine. The authors' study showed that the maximum brake thermal efficiency was obtained with 2.5% ethanol blended with RB and 6.98% and 3.93% higher than diesel fuel and biodiesel, respectively, at full engine load. A minimum BSFC of 0.339 was observed among the ethanol blends with 2.5% ethanol. The ethanol blending reduced the exhaust gas temperature. The lowest carbon monoxide, hydrocarbons, and unused oxygen emissions were recorded with a 2.5% ethanol blend. The smoke of the biodiesel was reduced by 20% when blended with 7.5% of ethanol. The maximum reduction of smoke was 27.47%, with 2.5% ethanol blending.

Prakash et al. (2013) included bi-oil with jatropha methyl esters(JME) biodiesel blends in an SFCS engine to study the performance and emissions of the engine. The study concluded a significant reduction in nitrous oxide emissions by 2.5% with 5% Bio-oil and 15% JME blended with diesel. The smoke opacity decreased by 25%, 26.7%, 22.1%, and 18.2% for JME and its emulsions compared to diesel at full load.

Palash et al. (2014) introduced di-phenylenediamine with jatropha biodiesel blends in an SFCS engine to study the performance and emissions of the engine. The observation revealed that By the addition of 0.15% (m) DPPD additive in JB5, JB10, JB15, and JB20, the reduction in NOx emissions were 8.03%, 3.503%, 13.65%, and 16.54%, respectively, compared to biodiesel blends without the additive under the full-throttle condition.

Shahir et al. (2014) assessed the feasibility of the diesel–biodiesel–ethanol/bioethanol blend as existing CI engine fuel. The results concluded that the use of diesel– biodiesel–ethanol/bioethanol blend could minimise the use of diesel fuel by approximately 25–30%.

Bora et al. (2015) studied the atomisation characteristics using oleyal alcohol (OA) and ethylene glycol butyl ether with fatty acid methyl esters. The study concluded that droplets increased from 1.88 × 1018 to 6.60 × 1022. The average length of the surface-active agent decreased from 8.8 to 0.26 nm. The introduction of OA and FAME (fatty acid methyl Ester) also increased the gross calorific value (GCV) (from 38.91 to 40.21 MJ/kg).

Rajesh Kumar and Saravanan (2016) introduced Isobutanol (B), and Iso-pentanol (P) blends in an SCFS engine to study the engine's performance characteristics. The study revealed that B40 gives a longer ignition delay, higher peak pressure, and higher premixed heat release rate than P40. B40 has a better effect on the NOx-smoke trade-off when compared to P40. At retarded injection timing (21° crank angle before Top dead centre) and 30% exhaust gas recirculation, B40 presented simultaneous reduction of NOx (↓41.7%) and smoke (↓90.8%) emissions with diesel-like performance. In contrast, P40 simultaneously reduced NOx (↓39.3%) and smoke (↓15%) emissions with a slight drop in performance.

Perumal and Ilangkumaran (2018) used water with Pongamia pinnata methyl ester as blends in the SCFS engine to study engine performance parameters. The result revealed a 9% increase in BSFC and a 5% decrease in BTE (Brake thermal efficiency) with a reduction of around 32% in NOx emission. The smoke was reduced to 7.4%. CO and HC emissions have been reduced to a marginal value of 2.3% and 1%, respectively.

Sidhu et al. (2018) introduced glycerine with biodiesel and diesel blends to study the SCFS engine's performance parameters and emissions. Results showed that with the increase in glycerine concentration, brake-specific fuel consumption and brake-thermal efficiency increased. Regarding emissions, it was seen that carbon monoxide and unburnt hydrocarbon increased, and reductions in exhaust gas temperature and nitrogen oxides were observed.

Ahmad et al. (2018) introduced non-surfactant water (NW) prepared from tap water, rainwater, and seawater to blend with diesel in an SCFS engine. The result showed that NW diesel made from tap water helps the engine reduce NOx by 32%. Rainwater reduced it by 29% and seawater by 19%. Also, all NWs show significantly improved engine performance compared to diesel fuel.

Arunprasad et al. (2020) used a Jatropa and Pongamia biodiesel mixture. The supplements were used with 25, 50, 75, and 100% blendings with diesel. The findings of the engine study showed that The reduction of HC (hydrocarbon), CO (carbon monoxide), smoke emissions, and an increase of NOx (nitrogen oxides) for different loads was observed and compared with diesel at all loads.

2.3 Application of Regression and ANOVA to develop a prediction model for engine performance

Al-lwayzy and Yusaf (2017) used blends of microalgae biodiesel from Chlorella Protothecoides (MCP-B) to estimate diesel engine performance. The analysis of variance (ANOVA) was performed to evaluate the significance of the means of the parameters. The results showed that MCP-B100 produces fewer emissions compared to petroleum diesel. Statistically significant differences were found in engine brake power, torque, BSFC, exhaust gas temperature, CO, O_2, and NOx when MCP-B100 and its mixtures were used compared to PD. The MCP-B100 showed a 7, 4.9, 6.1, 28, 4.2, and 7.4% reduction in stopping power, torque, exhaust gas temperature, CO, CO_2, and NOx, respectively.

Rahim and Rasul (2019) used diesel-tomato seed oil biodiesel (TSOB) blends to determine the performance and emissions of an SCFS diesel engine. The regression models showed that the torque decreases with increasing the engine speed and biodiesel percentage. These results also show that the highest and the lowest SFC are related to B0 and B20, respectively.

Pandian et al. (2011)used regression and ANOVA analysis to predict the performance and emissions of an SCFS diesel engine powered with Pongamia biodiesel blends. The results showed that the opacity of BSEC, CO, HC, and smoke was lower. BTE and NOx were higher at a 2.5 mm nozzle tip protrusion, 225 bar injection pressure, and 30 ° BTDC Injection. The injection system parameters were optimized using the response surface methodology for better performance and lower NO emissions. An injection pressure of 225 bar, an injection timing of 21° BTDC, and a 2.5 mm nozzle tip protrusion were optimal values for diesel fuel operation blended with Pongamia biodiesel in the diesel engine. 7.5 kW test at 1500 rpm.

Amarnath and Prabhakaran (2012) used the genetic algorithm optimisation technique to evaluate the optimised parameters, namely load, compression ratio, injection pressure, and blend. The author used the Karanja methyl esters blend to conduct SCFS engine experiments. Concerning maximum efficiency and minimum emissions, the optimised load, compression ratio, injection pressure, and blend values were 6 kg, 18, 247 bar, and 95%, respectively.

Pohit and Misra (2013) used grey relational analysis and the Taguchi method to optimise studies on an IC engine's performance and emissions. A 50% mixture was found to be the most suitable for use in a diesel engine without significantly affecting engine performance and emissions characteristics. Sivaramakrishnan Kaliamoorthy, and Ravikumar Paramasivam

Kaliamoorthy and Paramasivam (2013) used Taguchi's approach analysis to optimise the Karanja biodiesels engine's performance. The study concluded that BTE, BSFC, and diesel engine emissions depend upon biodiesel blend, compression ratio (CR), nozzle pressure, and injection timing (IT). The results showed that a diesel engine operating at a CR –17.7, pressure 230 bar, IT of 27° BTDC, biodiesel – diesel blends B20, and brake power –3.64 kW achieves the optimum engine performance. The findings of our confirmatory test well support the results.

Ahamad et al. (2018) used the grey Taguchi method to predict the performance parameters. As per the thermal performance evaluation, it is observed that the engine's operating conditions with 30% polanga biodiesel blend at 220 bar injection pressure are similar to the operating conditions with diesel. Taguchi method has been adapted to obtain a rich design matrix for optimization of parameters. The engine’s input parameters are optimized with BTE, UHC, NOx, and smoke multi-response characteristics. Multiple single-to-noise ratios (MSNR) are employed to analyze the performance characteristics from the actual value. In the study, the optimal values of BTE, UHC, NOx, and smoke emissions obtained are 32.59%, 20.3 ppm volume, 551 ppm volume, and 94.2%, respectively, at 30% polanga biodiesel blend with 15◦bTDC fuel injection timing and 200 bar injection pressure.

Rao and Rao (2017) used grey relation analysis to optimise the parameters obtained from mahua methyl esters (MME) biodiesel results in the SCFS engine. It was observed that the experimental results almost coincided with the validation results. The optimal combination observed was 20 kg of load and MME + 3% Methanol as the fuel.

Ahamad et al. (2018) used polanga biodiesel blends to study the performance of an SCFS engine. Further, the Taguchi method was optimised to obtain the best parameters. The study concluded that the optimal values of BTE, UHC, NOx, and smoke emissions obtained are 32.59%, 20.3 ppm volume, 551 ppm volume, and 94.2%, respectively, at 30% polanga biodiesel blend with 15°bTDC fuel injection timing and 200 bar injection pressure.

Thodda et al. (2020) used acetylene and diesel as fuel in dual mode to test the engine's performance. A multi-objective optimisation was conducted using the RSM To evaluate optimized parameters. The results showed a high flow rate of acetylene injection of 6 lpm, higher IP of 240 bar, CR of 18, and IT of 23ºCA BTDC arrived as the optimum operating conditions.

Simsek and Uslu (2020) studied the effects of mixing three sources of biodiesel (canola, waste vegetable oil, and safflower on the performance and emissions of the SCFS engine. Optimisation studies using response surface methodology were also conducted to find optimum BTE, BSFC, and emissions. The optimum BTE, BSFC, NOx, CO, HC, and smoke responses were 19.782%, 385.790g/kWh, 436.951ppm, 0.0272%, 33.639 ppm, and 0.167%, respectively.

Aneeque et al. (2021) studied the impact of additives N-octanol and N-butanol with Calophyllum inophyllum biodiesel on the engine's performance and emissions. The response surface methodology (RSM) optimisation revealed that the optimised thermal efficiency and emission were obtained at full and minimum loads, respectively. N-octanol addition hindered emission at all loads, while N-butanol reduced it at higher loads.

2.4 Application of ANN prediction modelling for engine performance

Ghobadian et al. (2009) studied the implementation of artificial neural network (ANN) modelling of a diesel engine using waste cooking biodiesel fuel to predict the engine's brake power, torque, specific fuel consumption, and exhaust emissions. The experimental results revealed that blends of the waste vegetable oil methyl ester with diesel fuel improve engine performance and emission characteristics. An ANN model was developed based on the engine's standard back-propagation algorithm. A multi-layer perception network (MLP) was used for non-linear mapping between the input and output parameters. Different activation functions and several rules were used to assess the percentage error between the desired and the predicted values. It was observed that the ANN model could predict the engine performance and exhaust emissions quite well with correlation coefficient (R) 0.9487, 0.999, 0.929, and 0.999 for the engine torque, SFC, CO, and HC emissions, respectively. The prediction MSE (Mean Square Error) error was between the desired outputs as measured values, and the simulated values were obtained as 0.0004 by the model.

Sarıtas et al. (2010) used an artificial neural network to predict performance using diesel fuel, biodiesel, B20, and bioethanol–diesel fuel having different percentages (5%, 10%, and 15%). Biodiesel was mixed to be used in a developed artificial neural network. Mixtures were also controlled for their fuel properties, and motor experiments were performed to collect the reference values. Power, moment, hourly fuel consumption, and specific fuel consumption were estimated using the artificial neural network developed using reference values. Estimated values and experiment results are compared. As a result, from the performed statistical analyses, the realised artificial intelligence model is an appropriate model to estimate the engine's performance used in the experiments., the reliability value was found to be 99.94% ($p = 0.9994$ and $P > 0.05$) after conducting statistical analysis.

Kannan et al. (2013) predicted the Effect of injection pressure and injection timing on a diesel engine's performance, emission, and combustion characteristics fuelled with waste cooking palm oil-based biodiesel using the artificial neural network (ANN) model. Experiments were carried out in a single-cylinder, four-stroke direct injection diesel engine at a constant speed of 1500 rpm and full load (100%) conditions to acquire data for training and testing in the proposed ANN. The experimental results showed that waste-cooking palm oil methyl ester improved engine performance, emission, and combustion characteristics at 280 bar and 25.5o BTDC injection pressure. An ANN model was developed using the data acquired from the experiments. Training of ANN was performed based on a back-propagation learning algorithm. The multi-layer perceptron (MLP) network was used for mapping non-linear input and output parameters. Among the various networks tested, the network with two hidden layers and 11 neurons gave a better correlation coefficient for engine performance, emission, and combustion characteristics. The ANN model was validated with the test data not used for training and was very well correlated.

Cirak and Demirtas (2014) Implemented an artificial neural network (ANN) model to predict the torque of a diesel engine. Experiments on the performance of a diesel engine using biodiesel produced from canola and soybean oils through transesterification were carried out to acquire data for training and testing of the proposed ANN. An MCFS test engine was fuelled with biodiesel and euro diesel mixture fuels with various percentages of biodiesel % amounting to half the CB with SB and operated at different loads engine speeds, coolant temperatures, biofuel mixtures, exhaust temperature, etc. Levenberg Marquardt algorithms for the engine were developed using experimental data for training as a non-linear system has been accepted. The performance of the ANN was validated by comparing the prediction dataset with the experimental results. It was observed that the ANN model could predict the engine performance quite well with a correlation coefficient of R 0.98 for the engine torque, respectively. The prediction MSE (Mean Square Error) error was between the desired outputs as measured values, and the simulated values were obtained as 0.0002 by the model.

Shukri et al. (2015)studied engine performance using a mixture of palm oil methyl ester blends with diesel oil as biodiesel in a diesel engine and optimised engine performance using artificial neural network (ANN) modelling. To acquire data for training and testing of the proposed ANN, a four-cylinder, four-stroke diesel engine was fuelled with different palm oil methyl ester blends as biodiesel and operated at different engine loads. The properties of biodiesel produced from waste vegetable oil were measured based on ASTM standards. The experimental results revealed that palm oil methyl ester blended with diesel fuel improved engine performance. An ANN model was developed based on the Levenberg-Marquardt algorithm for the engine. Logistic activation was used for mapping between the input and output parameters. It was observed that the ANN model could predict the engine performance quite well with correlation coefficients (R) of 0.996684, 0.999, 0.98964, and 0.998923 for the in-cylinder pressure, heat release, thermal efficiency, and volume, respectively.

Rao et al. (2017) investigated the performance and emission characteristics of SCFS indirect diesel injection (IDI) engine fueled with Rice Bran Methyl Ester (RBME) with Isopropanol additive. The investigation is done through experimental data analysis and artificial neural network (ANN) modelling. The study used IDI engine experimental data to evaluate nine engine performance and emission parameters, including exhaust gas temperature (EGT), Brake Specific Fuel Consumption (BSFC), Brake Thermal Efficiency (B.The), and various emissions like Hydrocarbons (HC), Carbon monoxide (CO), Carbon dioxide (CO_2), Oxygen (O_2), Nitrogen oxides (NO_X) and smoke. The standard backpropagation algorithm was the optimum choice for the ANN modeling for training the model. A multi-layer perception(MLP) network was used for non-linear mapping between the input and output parameters. It was found that ANN was able to predict the engine performance and exhaust emissions with a correlation coefficient of 0.995, 0.980, 0.999, 0.985, 0.999, 0.999, 0.980, 0.999, and 0.999 for EGT, BSFC, BTE, UHC, O_2, CO_2, CO, NO_X, smoke, respectively.

Karami et al. (2019)used diesel-tomato seed biodiesel (TSOB) blends to determine the performance and emissions of an SCFS diesel engine. The ANN model can predict the engine performance parameters and emissions without running costly and time-consuming experiments with the histogram error of 0.004 and R = 0.96.

Sajjadi et al. (2016) reviewed the application of ANN for studying engine behaviour in implementing biodiesel in diesel engines. The study concluded that using ANN with trained, tested, and validated data was introduced to determine a diesel engine's performance and emission characteristics fueled with biodiesel-based fuel. In general, the ANN model could supply a relatively high determination coefficient compared to predicted results and experimental data, showing that the ANN model could have an excellent ability to predict engine behaviours with an accuracy higher than 95%.

Simsek et al. (2022) used waste animal fat oil and predicted the engine response using ANN. The developed ANN model could predict engine responses with mean absolute percentage error (MAPE) in the range of 3.787e10.730%. MAPE values for RSM were obtained between 2.004 and 11.461%.

2.5 Application of biodiesel in the field of mining

Tiffany (2016) studied the importance of biodiesel for underground mines. She concluded that using exhaust filters for Particultae matter (PM)-control will result in ambient PM reductions exceeding 65%. Mine operators would need to use straight biodiesel with catalytic converters to get comparable reductions. Biodiesel will need to fall below \$2.00/gal to be competitive with filters for coal mines and below \$1.25/gal for metal mines. However, biodiesel has advantages that filters do not. Using biodiesel in mines would be easy to implement and would not require miner training. There are no new maintenance procedures required.

Debia et al. (2017) compared exposure levels within and between the mines as well. They studied the various ways of assessing Diesel Exhaust (DE) exposures, such as respirable combustible dust (RCD), elemental carbon (EC), and total carbon (TC); DE exposures in employees at two underground gold mines were assessed. Measurements were made of the ambient air and the personal breathing zone (PBZ). The respirable percentage RCD, EC, and TC, and the worker's breathing zone are all measured concurrently throughout a whole shift (ECR and TCR). In addition to the ambient measurements of ECR, TCR, and RCD, a submicron aerosol fraction of EC and TC (less than 1 mm) was also detected (EC1 and TC1). The average ambient readings for RCD, ECR, and TCR are 240 mg/m3, 150 mg/m3, and 210 mg/m^3, respectively. The average PBZ results in TCR, ECR, and RCD were 150 mg/m^3, 84 mg/m^3, and 190 mg/m3, respectively. ECR and EC1 exhibit a very strong association, with a calculated Pearson correlation coefficient between the two log-transformed concentrations of 0.99 (p 0.01), indicating a significant link. Between ECR and EC1, there were no reported differences. The load haul-dump (LHD), jumbo drill operators, and traditional miners have the highest exposures. Truck and LHD operators have significant exposure variations between mines (p 0.01). The average TCR/ECR ratio for PBZ and ambient results is 1.6 and 1.3, respectively.

Lutz et al. (2017) conducted a diesel and biodiesel exposure study in underground mines. Using a load-haul-dump vehicle, personal exposure monitoring was performed in a non-operational, hard rock underground mine. Eight-hour time-weighted average (TWA8) exposure concentrations of ultra-low sulfur diesel and 75% biodiesel/25% diesel blend (B75) fuels were compared. The use of a blend of 75% was linked to relative percent reductions in median respirable (r) diesel particulate matter (DPM) and nitrogen dioxide of 22 and 28%, respectively, and increases in median total DPM and nitric oxide TWA 8 exposure doses of 25 and 23%, respectively, when compared to diesel. Diesel was linked to a slightly lower mean surface area concentration and higher total geometric mean mass concentration. The blend of 75% might lessen DPM exposures.

Tiffany (2016) studied the importance of biodiesel for underground mines. She concluded that the use of exhaust filters for particulate matter (PM) control will result in ambient PM reductions exceeding 65%. Mine operators would need to use straight biodiesel with catalytic converters to get comparable reductions. Biodiesel costs need to fall below $2.00/gal to be competitive with filters for coal mines and below $1.25/gal for metal mines. However, biodiesel has advantages, such as applying biodiesel in mines would be easy to implement. It would not require much training for the workers.

2.6 Research gap

Alternative fuel is most necessary for the replacement/ accomplishment of depleting mineral fuel for future sustainability. It is needed to compensate for the economy of using vegetable oils. The literature gaps identified include the need for alternative fuel for demanding future energy generation in mining industry, sustainability, and cost optimization.

The best suggestion would be to use a combination of two or more sources of alternative fuels. Hence, waste cooking oil is used as an additional source to compensate for the cost of yielding raw Pongamia oil. The literature review reveals that studies on Pongamia pinnata and other such oils qualify to a larger extent. The governing authorities regularised it under the Indian biofuel policy 2015, stating that a blend of 20% is to be implemented with diesel for future sustainability and optimal performance.

The mine environment plays a significant role in enhancing the health condition of the workers. Biodiesel implementation can undoubtedly contribute to regulating engine emissions compared to diesel, especially carbon monoxide. Biodiesel can be sustainable with the addition of alcohol and other emulsifying agents. Ethanol, as one such additive, can be used to attain the sustainability of biofuels. Ethanol and acetone are the two agents used in this study to evaluate engine performance and emission characteristics.

CHAPTER 3

OBJECTIVES, METHODOLOGY, EXPERIMENTATION AND ALTERNATIVE FUEL PROPERTIES

3.1 Introduction

This chapter describes the details of the experimental setup and the instruments and standards involved. Also, the properties are listed down.

3.2 Objectives

Objectives of the proposed research work are:

1 To prepare blended alternative fuels using Pongamia pinnata and waste cooking oil (WCO) in the form of methyl esters, a combination mixture of Pongamia pinnata and WCO methyl esters (50:50 by volume), raw form of Pongamia pinnata and emulsification using acetone and ethanol.

2 To determine and study the physico-thermal properties, namely density, kinematic viscosity, and calorific value of diesel and the blends of prepared alternative fuels.

3 To study the performance and emissions of a single-cylinder four-stroke diesel engine using diesel and blended alternative fuels.

4 To determine the relationship between the physico-thermal properties of the prepared alternative fuels with the performance and emissions of the four-stroke diesel engine using statistical and artificial neural network techniques.

5 To study the Effect of the blends of RPO, MPO, MWO, and MPWO on emissions of the mining equipment. as per the Indian biofuel regulation 2010.

3.3 Methodology

1. The flow chart of the research methodology is shown in figure 3.1.

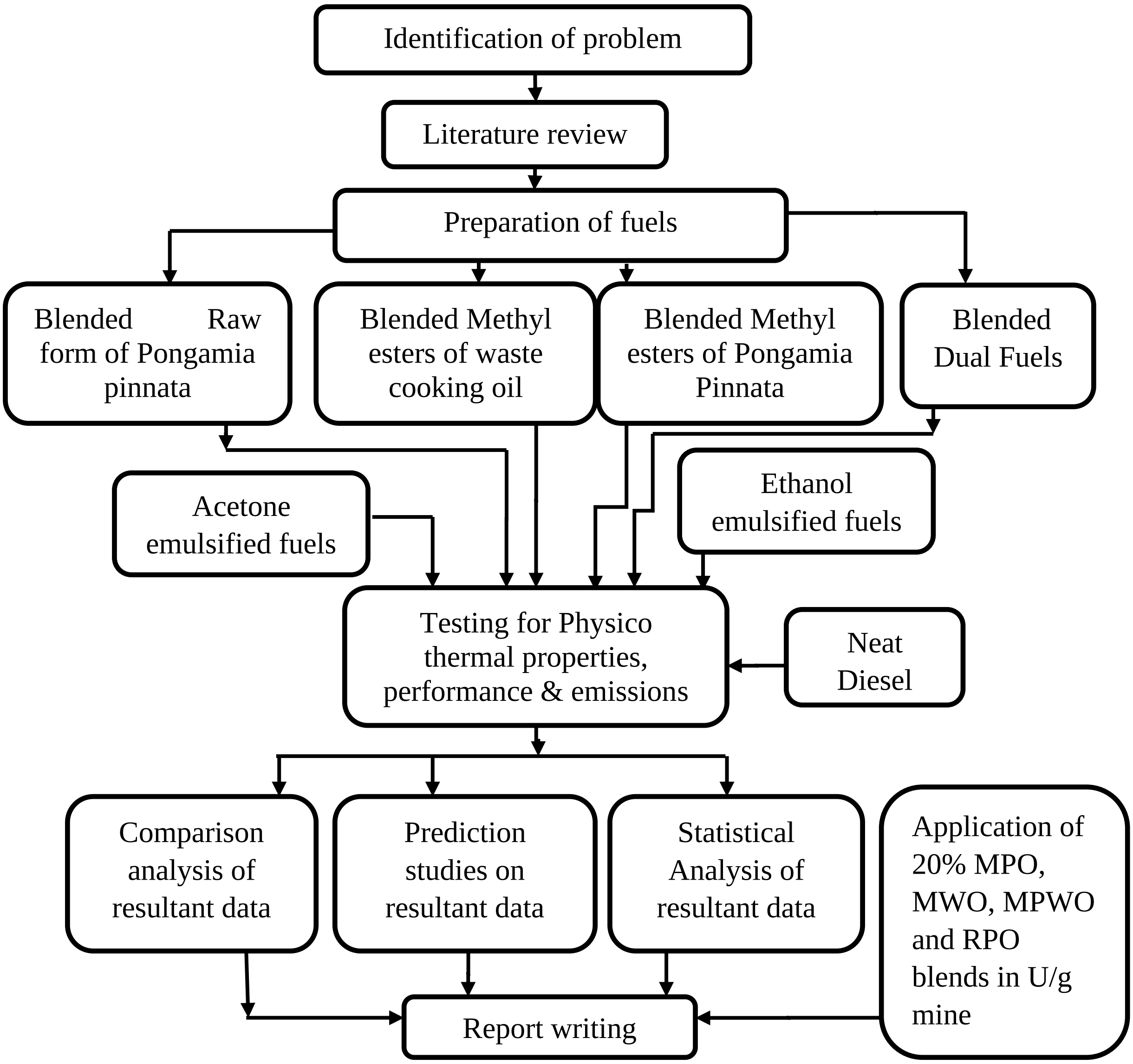

Figure 3.1 Flow chart of the research methodology

2. Carried out a detailed literature review; on different kinds of alternative fuels, including their preparation, usage, performance prediction, and emission from diesel engines.
3. Prepared alternative fuels using raw Pongamia pinnata oil, methyl esters of WCO (Ehsan and Chowdhury 2015), and Pongamia pinnata oil (Babu et al. 2009).

   Alternative fuels are prepared as described below.

   a) Methyl esters of Pongamia pinnata (MPO) and waste cooking oil (MWO) in blended ranges from 5% to 30% with an increment of 5% by volume with diesel.
   b) A mixture of MPO and MWO (50%:50%, by volume) MPWO is prepared; in blends ranging from 5% - 30% with an increment of 5% by volume.

c) Raw Pongamia pinnata oil (RPO); in blends ranging from 5% - 30% with an increment of 5% by volume with diesel.

d) Similarly, Adding 10% by volume of ethanol by reducing the quantity of diesel; for diesel and the samples discussed in Points a, b, and c. Respectively, the samples are labeled as DE, RPE, MPE, MWE, and MPWE.

e) The subjection of the fuels listed in points a, b, and c, to further addition using acetone by a '10% by volume by reducing the quantity of diesel; for diesel and the samples discussed in Points a, b, and c. the samples are labeled as DA, RPA, MPA, MWA, and MPWA, respectively. The chart for specimen preparation is shown in figures 3.2 to 3.6.

4. Determining physico-thermal properties such as density, kinematic viscosity, and calorific value for the prepared alternative fuels. The standards used in the estimation of properties are listed in Table 3.1.

5. Performance and emission studies are conducted on a single-cylinder 4-stroke water-cooled direct injection diesel engine using the prepared alternative fuels described under point 2. The specifications of the engine are shown in Table 3.2. The schematic diagram for the test set-up is shown in Figure 3.7, and the pictorial view of the engine is shown in Figure 3.8. The procedure for engine testing is as follows:

   a) The condition chosen for the engine test includes maintaining a constant engine speed of 1500 rpm for each varied engine load from 0 % to 100% in increments of 25%. The experiment is carried out for all prepared alternative fuel samples.

100% Diesel	10% Ethanol 90% Diesel	10% Acetone 90% Diesel

Figure 3.2 Preparation of ethanol and acetone added to diesel sample

5% RPO 95% Diesel	10% RPO 90% Diesel	15% RPO 85% Diesel	20% RPO 80% Diesel	25% RPO 75% Diesel	30% RPO 70%
5% RPO 10% Ethanol 85% Diesel	10% RPO 10% Ethanol 80% Diesel	15% RPO 10% Ethanol 75% Diesel	20% RPO 10% Ethanol 70% Diesel	25% RPO 10% Ethanol 65% Diesel	30% RPO 10% Ethanol 60% Diesel
5% RPO 10% Acetone 85% Diesel	10% RPO 10% Acetone 80% Diesel	15% RPO 10%Acetone 75% Diesel	20% RPO 10% Acetone 70% Diesel	25% RPO 10% Acetone 65% Diesel	30% RPO 10% Acetone 60% Diesel

Figure 3.3 Preparation of RPO, ethanol, and acetone-added RPO biodiesel blends

b) The time for 10 Cc fuel consumption and the emission parameters, namely, carbon monoxide (CO), carbon dioxide (CO_2), unburnt hydrocarbon (UHC), and oxides of nitrogen (NOX), is recorded at each loading condition for each blend. AVL 444 exhaust gas analyser is used. The specifications of the analyser are listed in Table 3.3.

5% MPO 95% Diesel	10% MPO 90% Diesel	15% MPO 85% Diesel	20% MPO 80% Diesel	25% MPO 75% Diesel	30% MPO 70% Diesel
5% MPO 10% Ethanol 85% Diesel	10% MPO 10% Ethanol 80% Diesel	15% MPO 10% Ethanol 75% Diesel	20% MPO 10% Ethanol 70% Diesel	25% MPO 10% Ethanol 65% Diesel	30% MPO 10% Ethanol 60% Diesel
5% MPO 10% Acetone 85% Diesel	10% MPO 10% Acetone 80% Diesel	15% MPO 10%Acetone 75% Diesel	20%MPO 10% Acetone 70% Diesel	25% MPO 10% Acetone 65% Diesel	30% MPO 10% Acetone 60% Diesel

Figure 3.4 Preparation of MPO, ethanol, and acetone added to MPO biodiesel blends.

5% MWO 95% Diesel	10% MWO 90% Diesel	15% MWO 85% Diesel	20% MWO 80% Diesel	25% MWO 75% Diesel	30% MWO 70% Diesel
5% MWO 10% Ethanol 85% Diesel	10% MWO 10% Ethanol 80% Diesel	15% MWO 10% Ethanol 75% Diesel	20% MWO 10% Ethanol 70% Diesel	25% MWO 10% Ethanol 65% Diesel	30% MWO 10% Ethanol 60% Diesel
5% MWO 10% Acetone 85% Diesel	10% MWO 10% Acetone 80% Diesel	15% MWO 10%Acetone 75% Diesel	20% MWO 10% Acetone 70% Diesel	25% MWO 10% Acetone 65% Diesel	30% MWO 10% Acetone 60% Diesel

Figure 3.5 Preparation of MWO, ethanol, and acetone added to MWO biodiesel blends

5% MPWO 95% Diesel	10% MPWO 90% Diesel	15% MPWO	20% MPWO	25% MPWO 75% Diesel	30% MPWO 70% Diesel
5% MPWO 10% Ethanol 85% Diesel	10% MPWO 10% Ethanol 80% Diesel	15% MPWO 10% Ethanol 75% Diesel	20% MPWO 10% Ethanol 70% Diesel	25% MPWO 10% Ethanol 65% Diesel	30% MPWO 10% Ethanol 60% Diesel
5% MPWO 10% Acetone 85% Diesel	10% MPWO 10% Acetone 80% Diesel	15% MPWO 10%Acetone 75% Diesel	20% MPWO 10% Acetone 70% Diesel	25% MPWO 10% Acetone 65% Diesel	30% MPWO 10% Acetone 60% Diesel

Figure 3.6 Preparation of MPWO, ethanol, and acetone added to MPWO biodiesel blends

c) The performance parameters, namely mass of fuel consumed (MF), brake power (BP), brake thermal efficiency (BTE), and brake-specific energy consumed (BSEC), are computed using equations 3.1 to 3.4.

Table 3.1 ASTM standards in the determination of the physico-thermal properties of the fuels.

Sl.No	Type of the Physico-Thermal Property	ASTM Standard
1	Density	ASTM D-941
2	Kinematic Viscosity at 40°C	ASTM D-445/17A
3	Calorific value	ASTM D-240

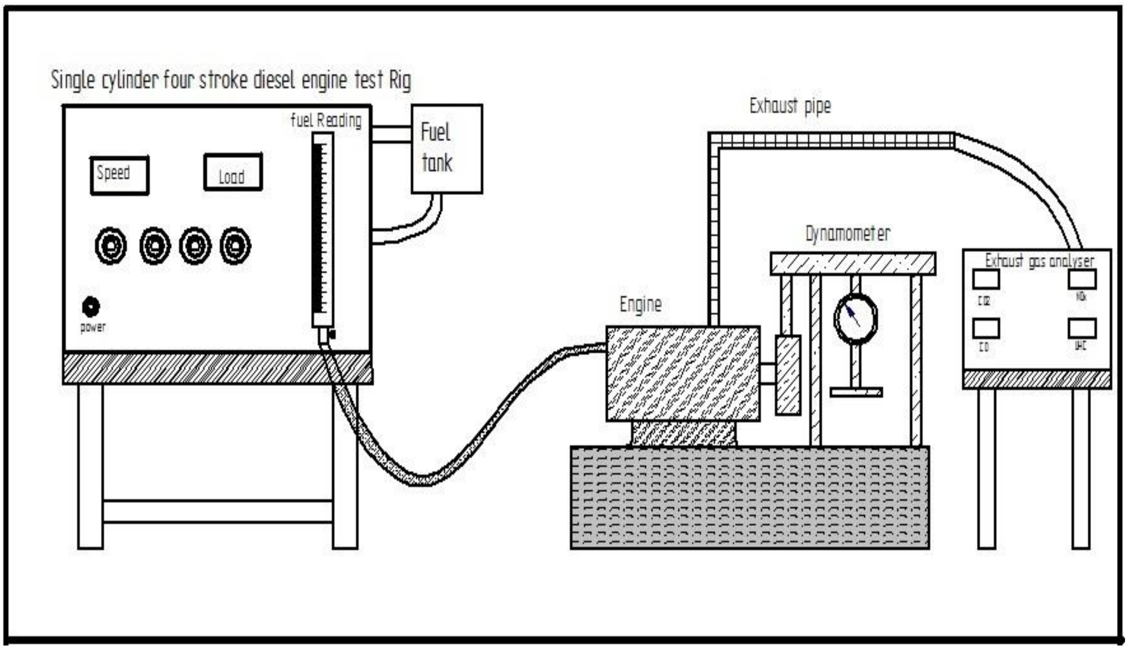

Figure 3.7 Schematic representation of engine set-up

Figure 3.8 Pictorial view of the engine test set-up

Table 3.2 Specification of the engine used in the present research

Type	Four-stroke direct injection diesel engine
Engine	Kirloskar-TV 1
Type of cooling	Water cooling
Bore	80 mm
Stroke	110 mm
Displacement volume	553 cc
Piston (standard)	Hemispherical
Compression ratio	1:16.5
Rated power	5.2 kW at 1500 rpm
Fuel oil	Commercial high-speed diesel
Type of governor	Mechanical centrifugal type
Lubrication system	Forced feed

Table 3.3 Specifications of the AVL 444 exhaust gas analyser

S.No.	Details	Specifications
Exhaust Gas Analyzer Measuring Ranges		
1	Oxygen (O_2)	0 – 25.00% vol
2	Carbon monoxide (CO)	0 – 15.00% vol
3	Carbon dioxide (CO_2)	0 – 20.00% vol
4	Hydro carbon (HC)	0 – 20,000 ppm n-hexane
5	Nitrogen oxide (NOx)	0 – 2,000 ppm
6	Excess Air calculated According to Brett Schneider'sTemperature	-40°C to +650°C
7	Oxygen (O_2)	0.1% or 3%
8	Carbon monoxide (CO)	0.06% or 5% of the measured value
9	Carbon dioxide (CO_2)	0.5% or 5% of the measured value
10	Hydro carbon (HC)	12 ppm or 5% of the measured value
11	Nitrogen oxide (NOx)	5 ppm or 5% of the measured value
12	Temperature (T>250^{o}C)	1% (T<150^{o}C) 2% (T<250^{o}C)
Resolution		
13	Oxygen (O_2)	0.01%
14	Carbon dioxide (CO_2)	0.1%
15	Carbon monoxide (CO)	0.01%
16	Hydro carbon (HC)	1 ppm
17	Nitrogen oxide (NOx)	1 ppm

$$MF \text{ in Kg/s} = (10 * D)/(1000 * T) \qquad (3.1)$$

Where, MF is the mass of fuel consumed in Kg/s

D- Density, g/cc

T-time for 10 cc fuel consumption, seconds

$$BP = 2\,\pi NT/\ 60000 \text{ in KW} \qquad (3.2)$$

where BP- Brake power, KW

N-Speed of the engine, rpm

T- Engine torque, N-m

$$BTE= (BP/(MF* CV*1000))*100$$

where BTE- Brake thermal efficiency in %

CV-Calorific Value, MJ/Kg

$$BSEC= (MF*CV/BP) \qquad (3.4)$$

where BSEC- Brake specific energy consumtion in KJ

6. Evaluate the effects of blending and loading each alternative fuel blend on the engine's performance and emissions.
7. Carry out a regression analysis for the results of multivariate data to identify and understand the relationships between the fuel properties, loads, and blends with the performance and emissions of the engine using multivariate regression analysis and ANOVA.

   a) The output variables chosen include BTE, BSEC, CO, CO_2, UHC, and NOX. Engine load, fuel blends, the mass of fuel consumed, and the properties, namely density (D), kinematic viscosity (KV), and calorific value (CV), are considered input parameters.

   b) The significant parameters (P-Value) and their contributions (F- Value) are tested under ANOVA analysis.

   c) The regression equation and performance of the model (R-Squared) are tested under regression analysis

   d) Minitab V19 is used to carry out both ANOVA and Regression analysis.
8. Carry out prediction studies on the performance and emission of the engine using the ANN technique.

   a) The output and input parameters are chosen as in Point 6 (a).

   b) The analysis is performed using MatLab 2019 a. NNTOOL command to start the analysis. The input and output variables are fed to the MatLab workspace.

   c) A network with two hidden layers is created for the hidden layer for the input and the output layer. A feed-forward back-propagation network is used to develop the model.

d) TRAINLM and LEARNGDM are used as the training and learning algorithm. The transfer function is TRANSIG.

e) The number of neurons varies from 4 to 12 in increments of 1. To observe and arrive at the optimised model. The root Mean square error (RMSE) is computed, and the optimised model is then suggested based on the least RMSE.

8. An evaluation study on the implementation of base biodiesel blends as per the Indian biofuel policy on the equipment used in an underground mine was carried out on a tipper of the Hutti Gold Mine Ltd., Karnataka. Emissions, namely CO, NO (nitrous oxide), NO2 (nitrogen dioxide), and NOx (oxides of nitrogen).

9. Reporting and concluding the effects of blending each alternative fuel blend on the engine's emissions and variations measure with reference to diesel in a mining tipper. The specifications of the mine tipper are shown in Table 3.4

Table 3.4 Specifications of the mine tipper

Make	Tata
Max. Engine Output	100 kW @ 2400 r/min
Max. Torque	490 Nm @ 1400 r/min
No. Of Cylinders	Six (Inline)
Engine Capacity	5675 CC

3.4 Properties of the prepared alternative fuels

A preliminary investigation of the characteristics of prepared fuels is assessed. The study aims to verify that fuel standards are being met and is very beneficial in determining the best combination that might be added to diesel fuel. Three major properties, namely Density, Kinematic viscosity, and calorific value, are studied. The average deviation concerning diesel of all prepared samples is estimated. The average deviations concerning diesel are tabulated in Table 3.5. A comparison plot is shown for ethanol and acetone additions in bar graphs. The effect of ethanol and acetone additions are shown as scatter plots for each sample. A comparison study was carried out to determine the effects of mixing two methyl esters and properties deviations with reference to MPO.

Table 3.5 Average deviation of the physico-thermal properties of prepared samples.

Sample	Deviation (in %)		
	Density	Kinematic viscosity	Calorific value
DA	0.73	0.25	-0.30
DE	0.97	0.51	-2.20
MPO	-1.54	-8.59	1.95
MPA	-0.77	-7.19	1.48
MPE	-1.27	-5.58	1.22
MWO	-1.21	-6.35	0.59
MWA	-0.71	-5.88	0.77
MWE	-0.63	-5.33	-0.54
MPWO	-1.41	-9.35	1.41
MPWA	-0.67	-7.91	0.63
MPWE	-0.71	-7.06	-0.80
RPO	-1.66	-13.24	1.81
RPA	-1.39	-10.36	1.30
RPE	-1.11	-6.77	0.60

3.4.1 Density

Density is a vital physical fuel property that signifies how much fuel an engine uses and how much power it can make. It affects the working of the engine and how much pollution it puts out (Ramírez Verduzco 2013). If one type of fuel is much denser, more mass goes into the combustion chamber for the same amount of space. Generally, the fuel density increases with increased biodiesel blending due to the biodiesel's lower carbon and hydrogen content (Hoekman and Robbins 2012). Ethanol and acetone addition to the base biodiesel blends improves the quality of base biodiesel blends (Jimenez and Svolj 2010). The lower the density of the fuel higher would be the fuel quality.

Figure 3.9 shows the Effect of ethanol and acetone on diesel. However, the improvements in diesel density due to ethanol and acetone additions are found to be 0.73% and 0.97%, respectively. Figure 3.10 shows the Effect of mixing two methyl esters. Adding MPO to MWO, improvements in density are found for MPO; MPWO shows a 0.11% improvement in density. Figure 3.11 to 3.14 shows the Effect of ethanol addition and acetone addition on RPO, MPO, MWO, and MPWO. Adding ethanol and acetone has improved the density of the base biodiesel samples. However, the most significant deviation is found with RPO with a variation of 1.66%. Hence, RPO can be considered a poor source as far as density is concerned.

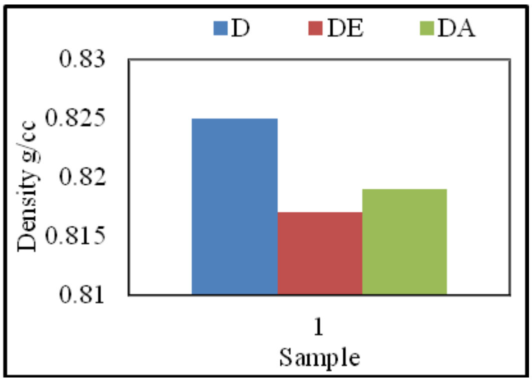

Figure 3.9 Effect of ethanol and acetone blending on the density of diesel

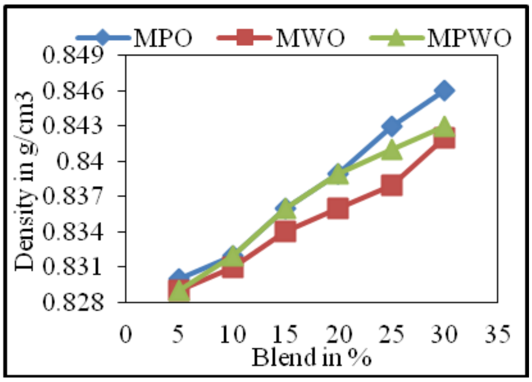

Figure 3.10 Comparison of density of MPWO with MPO and MWO blen

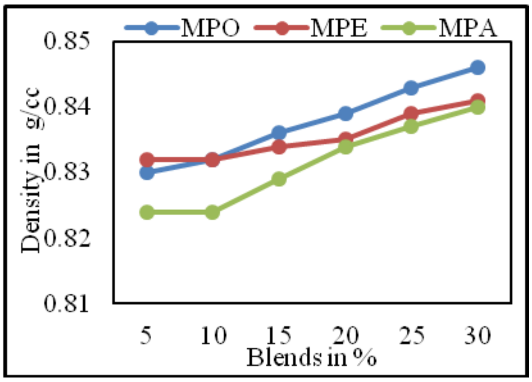

Figure 3.11 Effect of ethanol and acetone blending on the density of MPO blends

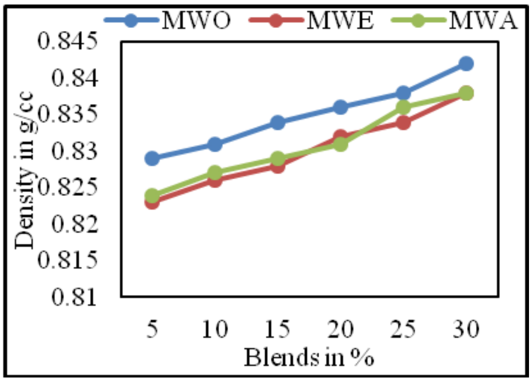

Figure 3.12 Effect of ethanol and acetone blending on the density of MWO blends

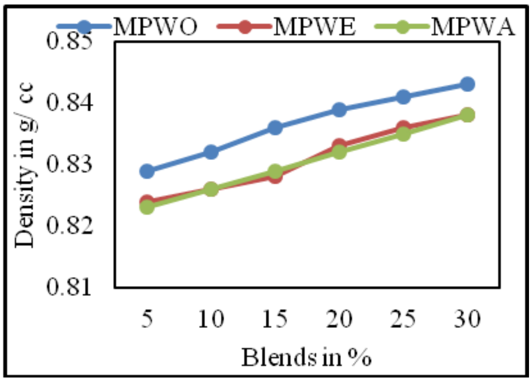

Figure 3.13 Effect of ethanol and acetone blending on the density of MPWO blends

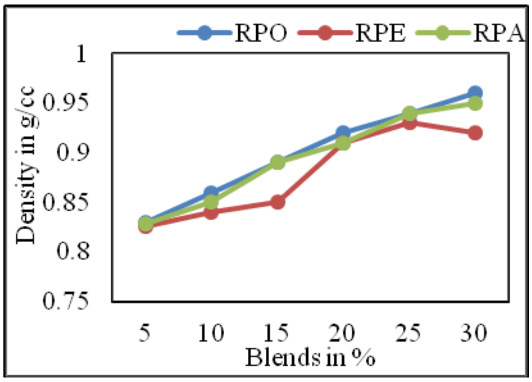

Figure 3.14 Effect of ethanol and acetone blending on the density of RPO blends

3.4.2 Kinematic viscosity (KV)

An essential characteristic of fuel is kinematic viscosity, which directly affects fuel atomization's effectiveness and the spray's fuel droplet size. A lower kinematic viscosity improves the fuel's ability to spray better. Diesel's properties may deteriorate by adding biodiesel blends (Hoekman and Robbins 2012). This may be due to Influencing factors such as chain length, position, number, nature of double bonds, and oxygenated moieties (Knothe and Steidley 2005). Ethanol and acetone additions improve diesel's kinematic viscosity (Wu-gao et al. 2005) and base biodiesel blends (Mahalingam et al. 2018). This is because of the lower kinematic viscosity of ethanol on the biodiesel blends. However, ethanol shows better improvement in the improvement of kinematic viscosity compared to acetone.

Figure 3.15 shows the Effect of adding acetone and ethanol on diesel fuel's kinematic viscosity. Both ethanol and acetone decrease the kinematic viscosity of diesel. The measured deviation of DE and DA with reference diesel is 0.25% and 0.51%, respectively.

Fig 3.16 depicts the Effect of combining the two methyl esters, MPO and MWO; adding MWO to MPO tends to reduce the kinematic viscosity of the MPO blend sample. This is because of the lower viscosity of MWO, which affects the reduction. The improvement achieved by MPWO compared to MPO addition is 2.96%. Figures 3.17 to 3.20 illustrate the significance of ethanol and acetone additions to MPO, MWO, MPWO, and RPO blended samples. Ethanol and acetone show reduced kinematic viscosity. The largest deviations are found with RPO, which is 13.24% higher than diesel. Hence, RPO is considered a poor source regarding kinematic viscosity.

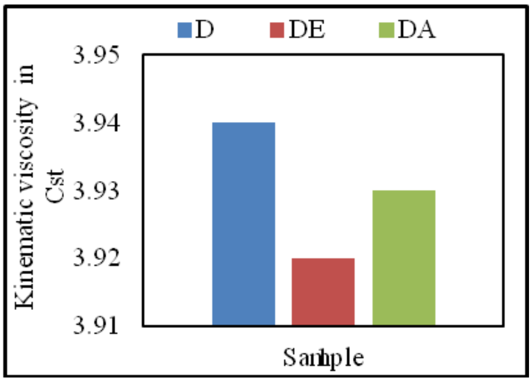

Figure 3.15 Effect of ethanol and acetone blending on the KV of diesel

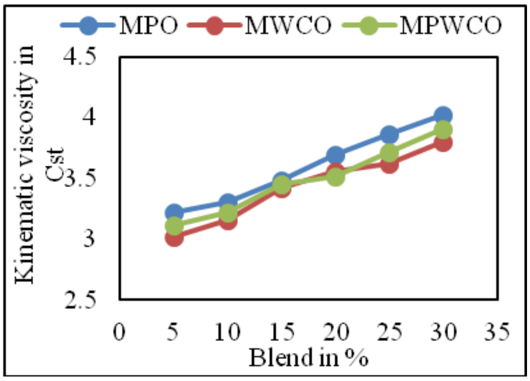

Figure 3.16 Comparison of KV of MPWO with MPO and MWO blends

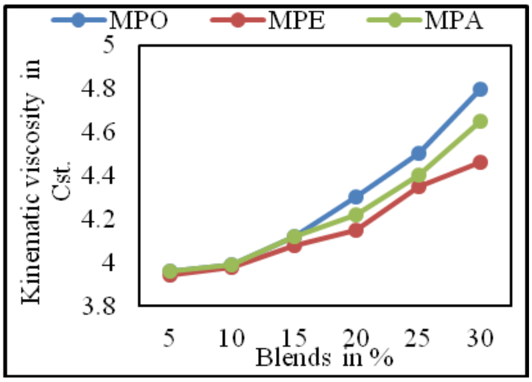

Figure 3.17 Effect of ethanol and acetone blending on the KV of MPO blends

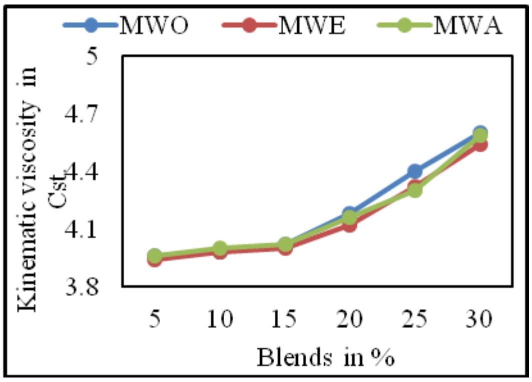

Figure 3.18 Effect of ethanol and acetone blending on the KV of MWO blends

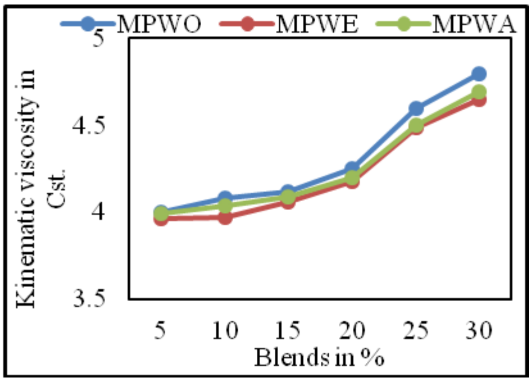

Figure 3.19 Effect of ethanol and acetone blending on the KV of MPWO blends

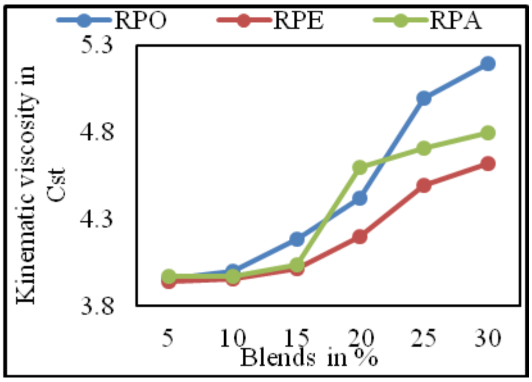

Figure 3.20 Effect of ethanol and acetone blending on the KV of RPO blends

3.4.3 Calorific value (CV)

Figure 3.21 shows how adding acetone and ethanol affects the diesel fuel's calorific value. Both ethanol and acetone can improve the calorific value of diesel. This is due to the higher calorific values of ethanol and acetone. The improvements in the calorific value of diesel compared to the blend samples are 1.72% and 1.99% for ethanol and acetone additions, respectively.

Fig 3.22 depicts the Effect of combining the two methyl esters, MPO and MWO; adding MWO to MPO tends to increase the calorific value of the MPO blend sample.

The improvements achieved by MPO due to MWO addition are 0.696%.

Figures 3.23 to 3.26 illustrate the effects of ethanol and acetone additions to RPO, MPO, MWO, and MPWO blended samples. The largest deviation with increased calorific value is found with RPO at 1.81%. Hence, RPO is considered the poorest source with reference to diesel.

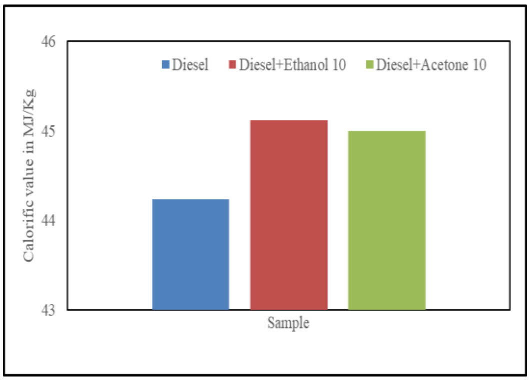

Figure 3.21 Effect of ethanol and acetone blending on the CV of diesel

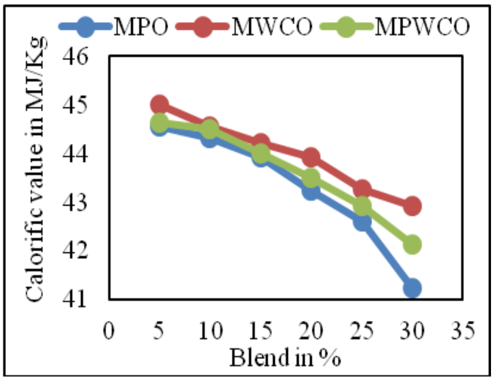

Figure 3.22 Comparison of the CV of MPWO with MPO and MWO blends

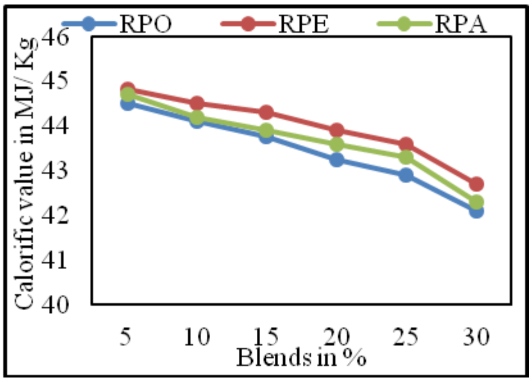

Figure 3.23 Effect of ethanol and acetone blending on the CV of RPO blends

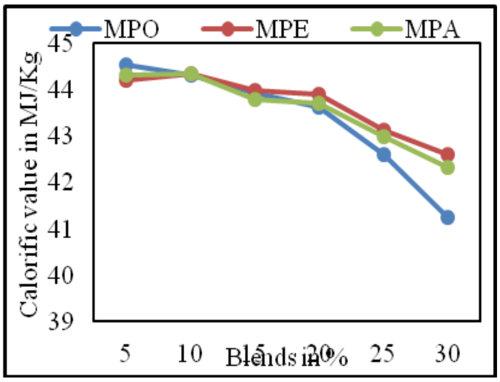

Figure 3.24 Effect of ethanol and acetone blending on the CV of MPO blends

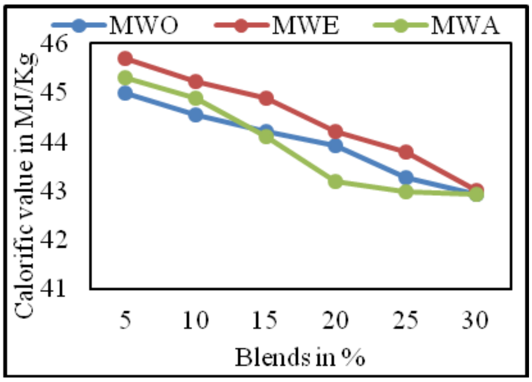

Figure 3.25 Effect of ethanol and acetone blending on the CV of MWO blends

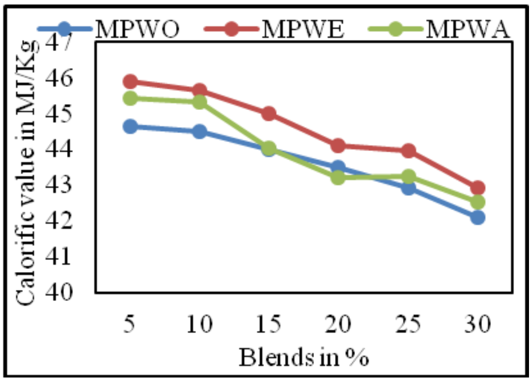

Figure 3.26 Effect of ethanol and acetone blending on the CV of MPWO blends

Calorific value is the number of calories generated when a unit amount of substance is completely oxidised. Calorific value decides the efficiency of an energy source per unit weight. The calorific value of biodiesel blends decreases with an increase in blend percentage (Wakil et al. 2015). The higher the calorific value better would be its fuel characteristics. Ethanol shows improvements in the calorific value of biodiesel blends (Hussan et al. 2013). However, the calorific values of ethanol-added biodiesel blend remain lower than diesel (Sharanappa and Navindgi 2017). With an increase in biodiesel blending, the calorific value decreases. The biodiesel blends' lower calorific values are due to the fuel's higher oxygen content (Kaisan et al. 2020).

CHAPTER 4

EXPERIMENTAL ANALYSIS

This study considers two performance parameters (BTE and BSEC) and four emission parameters (CO, CO_2, UHC and NOx); the parameters are evaluated and tabulated as shown in Appendix -I. The significance of mixing two methyl esters, namely the Pongamia pinnata and waste cooking oil, and the Effect of ethanol and acetone's addition on the engine's efficiency and emissions are studied. The following sections illustrate the significance of the individual parameter. In this study, the estimated parameters are compared as follows.

Case-1: The Effect of constant ethanol and acetone addition individually to the diesel is compared with diesel

Case-2: MPWO is compared with MPO and MWO for each blend.

Case-3: The Effect of ethanol and acetone blended samples on performance and emissions of the engine, i.e., RPE, MPE, MWE, MPWE, and RPA, MPA, MWA

An average deviation of the blends of each prepared biodiesel sample is estimated concerning diesel and is tabulated in Table 4.1.

Table 4.1 Average deviation of prepared samples with diesel.

Sample	Average variation (in %)					
	BTE	BSEC	CO	CO_2	UHC	NOx
DA	-2.5974	2.33	17.6471	-12.775	7.69231	-35.345
DE	-3.22	1.99	20.915	-18.062	11.5385	-43.75
MPO	16.0552	-7.66	35.5914	-18.209	30.8608	-107.9
MPA	12.9502	-7.69	33.4409	-22.54	33.5165	-117.39
MPE	8.60832	-3.84	35.5914	-28.634	39.3773	-122.45
MWO	11.9742	-5.13	32.9032	-11.821	24.8168	-77.407
MWA	9.00614	-5.22	39.8652	-35.857	34.0945	-86.277
MWE	5.04766	-0.35	44.5708	-50.101	39.8535	-98.21
MPWO	13.8112	-7.4	32.9032	-16.079	27.1978	-93.032
MPWA	12.1888	-6.32	37.0065	-27.289	38.6572	-98.458
MPWE	4.02742	-0.54	32.5551	-25.31	37.7109	-99.253
RPO	32.7324	-41.4	52.7452	-33.693	45.5632	-144.05
RPA	30.4258	-37.69	55.1079	-39.627	48.2294	-163.97
RPE	26.5956	-31.46	57.4706	-49.165	51.1079	-172.68

Mixing two methyl esters has improved both performance and emissions of the poorer source ester (Sanjid et al. 2014; Sridhar et al. 2017).

4.1. Engine performance parameters

4.1.1 Brake thermal efficiency

Figure 4.1 illustrates the Effect of adding acetone and ethanol to diesel on the BTE of the engine. The figure shows a positive Effect of ethanol-diesel (Khalife et al. 2017) than acetone-diesel. It may be because of the higher CV of ethanol than acetone. The variation in BTE of the diesel engine due to 10% ethanol and 10 % acetone additions is found to Be 3.2% and 2.6%, respectively.

Figures 4.2 to 4.7 show the effect of combining two methyl esters, MPO and MWO. Combining MPO with MWO can improve the efficiency of MPO. The average achievement in the efficiency of MPWO as compared to MPO for blending up to 30% by volume is 13.9%.

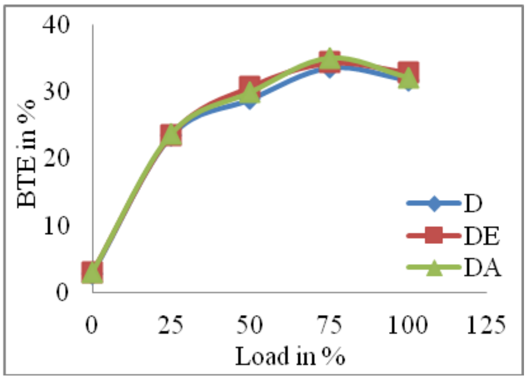

Figure 4.1 Effect of ethanol and acetone blended diesel on the BTE of engine

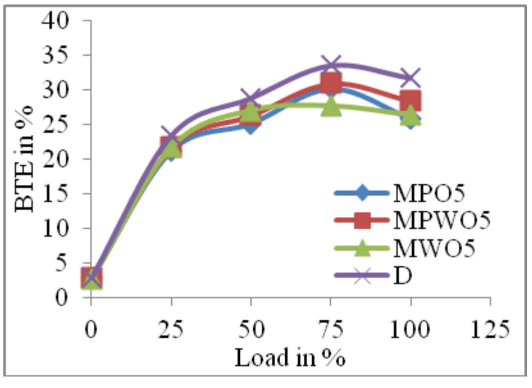

Figure 4.2 Effect of combining MPO and MWO on the BTE of the engine at 5% blending

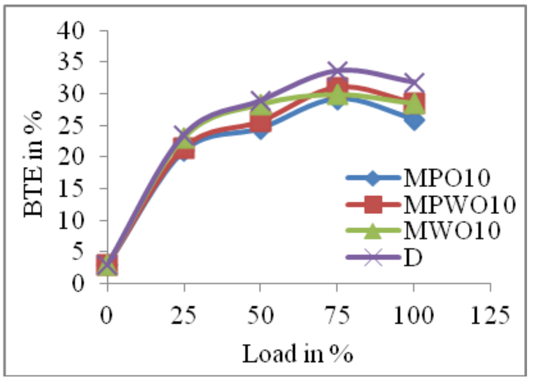

Figure 4.3 Effect of combining MPO and MWO on the BTE of the engine at 10% blending

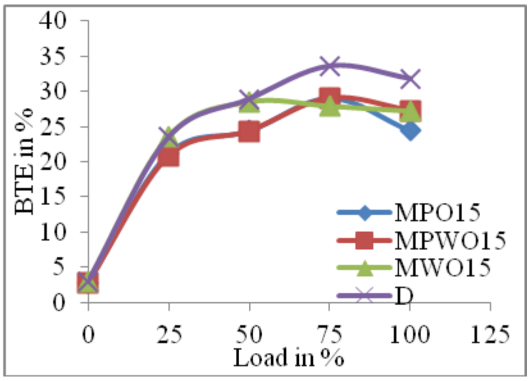

Figure 4.4 Effect of combining MPO and MWO on the BTE of the engine at 15% blending

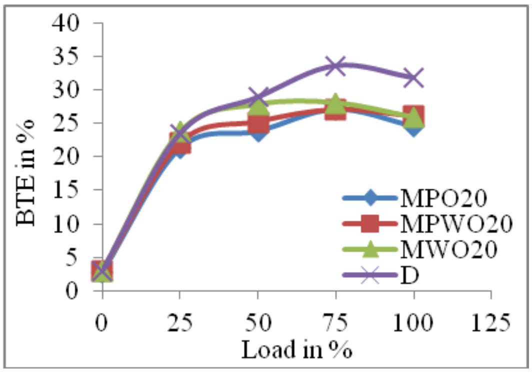

Figure 4.5 Effect of combining MPO and MWO on the BTE of the engine at 20% blending

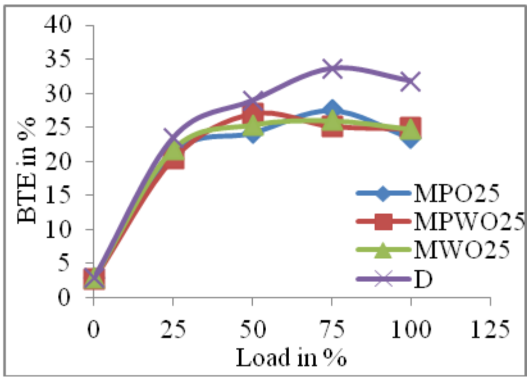

Figure 4.6 Effect of combining MPO and MWO on the BTE of the engine at 25% blending

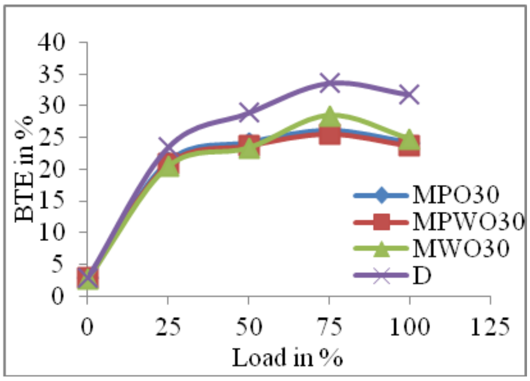

Figure 4.7 Effect of combining MPO and MWO on the BTE of the engine at 30% blending

Adding ethanol and acetone to the RPO blends has improved the engine's efficiency compared to biodiesel blends. Figures 4.8 to 4.13 shows the variational plot of load versus the BTE of the engine for various blends of raw biodiesel and ethanol acetone and additions. It is observed that the ethanol and acetone addition to the raw biodiesel blends behaves similarly to that of biodiesel blends with variations in engine load. The average reduction in the engine's efficiency of RPO, RPA, and RPE compared to that of the diesel blends is 32.73%, 30.43%, and 26.60%, respectively.

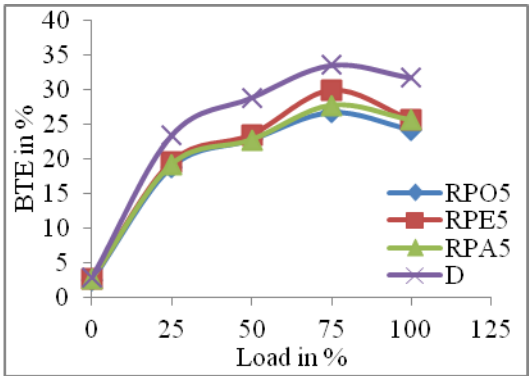

Figure 4.8 Effect of ethanol and acetone addition on the BTE of the engine with 5% blending of RPO

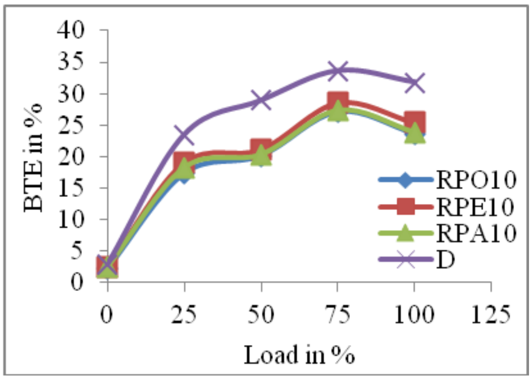

Figure 4.9 Effect of ethanol and acetone addition on the BTE of the engine with 10% blending of RPO

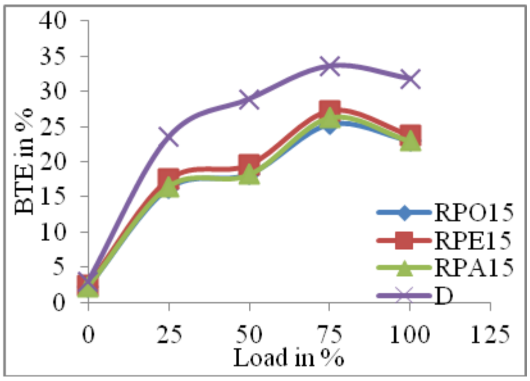

Figure 4.10 Effect of ethanol and acetone addition on the BTE of the engine with 15% blending of RPO

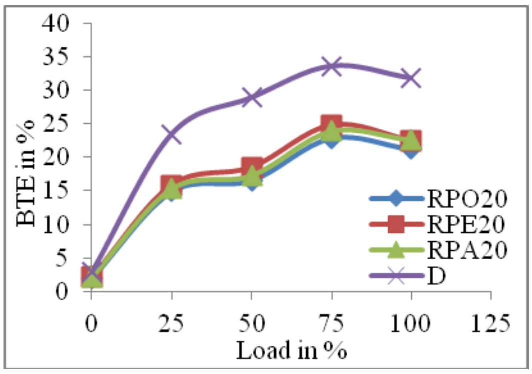

Figure 4.11 Effect of ethanol and acetone addition on the BTE of the engine with 20% blending of RPO

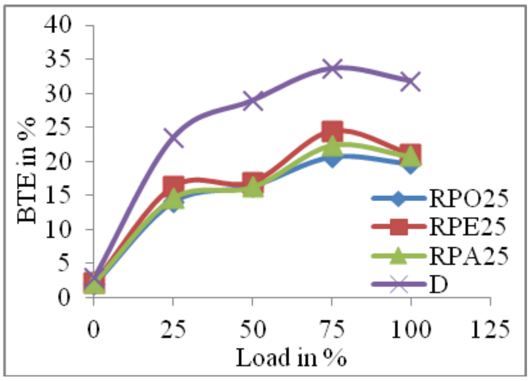

Figure 4.12 Effect of ethanol and acetone addition on the BTE of the engine with 25% blending of RPO

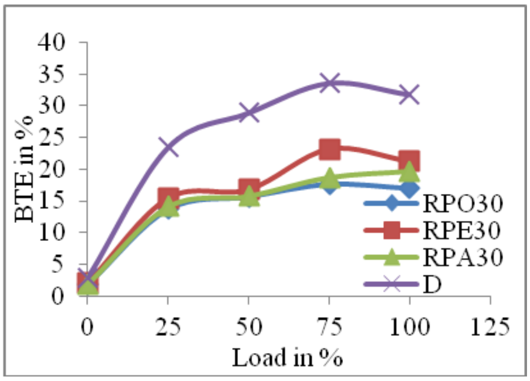

Figure 4.13 Effect of ethanol and acetone addition on the BTE of the engine with 30% blending of RPO

Figures 4.14 to 4.19 show the variational plot of load versus the BTE of the engine for various blends of raw biodiesel and additions of ethanol and acetone. Adding ethanol (Shrivastava et al. 2021) and acetone to the MPO has improved the engine's efficiency compared to MPO biodiesel blends. Also, the ethanol and acetone addition to the raw biodiesel blends is similar to that of biodiesel blends with engine load variations. The average reduction in the engine's efficiency of MPO, MPA, and MPE compared to the diesel blends is 16.06%, 12.95%, and 8.6%, respectively.

Ethanol and acetone additions to the biodiesel blends of MWO have also shown an improvement in engine efficiency compared to biodiesel blends. Figures 4.20 to 4.25 show the plot of load versus BTE of the engine for various biodiesel blends of MWO, ethanol, and acetone additions. Similar behaviour is found with all the samples at each blend of ethanol and acetone (Dhanarasu et al. 2021). An average deviation with the BTE of engine fuelled with MWO, MWA, and MWE is 11.97%, 9.01%, and 5.05% compared to diesel.

Similarly, ethanol and acetone additions to the biodiesel blends of MPWO have also shown an improvement in engine efficiency compared to biodiesel blends. Figures 4.26 to 4.31 show the plot of load versus BTE of the engine for various biodiesel blends of MPWO, ethanol, and acetone additions. Similar behaviour is found with all the samples at each blend of ethanol and acetone. An average deviation with the BTE of engines fuelled with MPWO, MPWA, and MPWE is 13.81%, 12.19%, and 4.03%, respectively, compared to diesel.

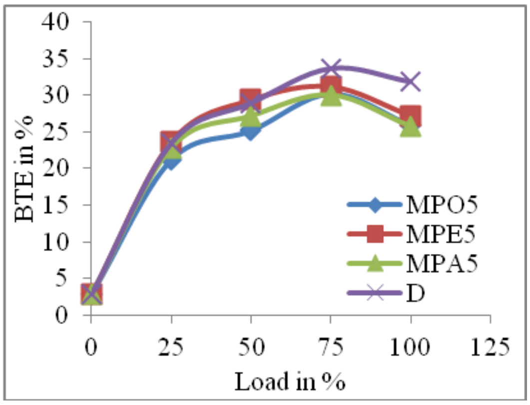

Figure 4.14 Effect of ethanol and acetone addition on the BTE of the engine with 5% blending of MPO

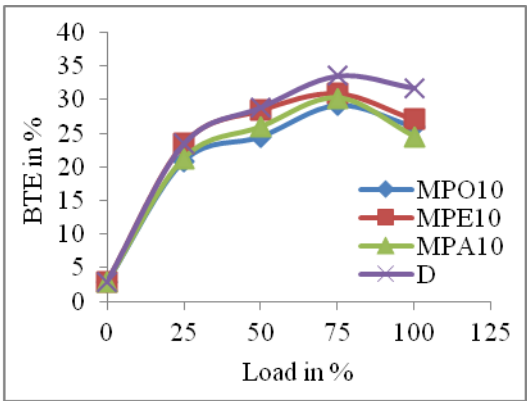

Figure 4.15 Effect of ethanol and acetone addition on the BTE of the engine with 10% blending of MPO

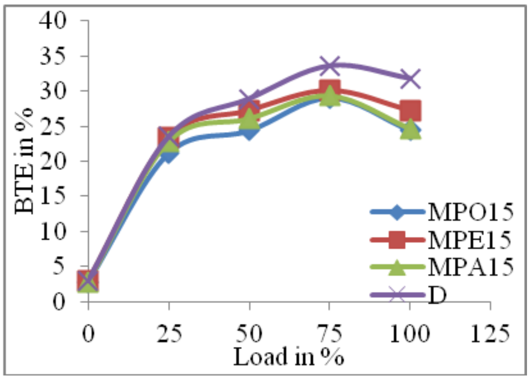

Figure 4.16 Effect of ethanol and acetone addition on the BTE of the engine with 15% blending of MPO

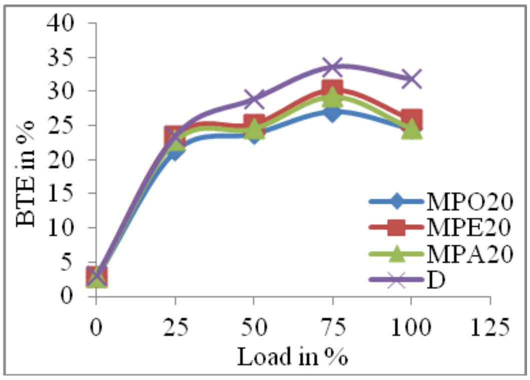

Figure 4.17 Effect of ethanol and acetone addition on the BTE of the engine with 20% blending of MPO

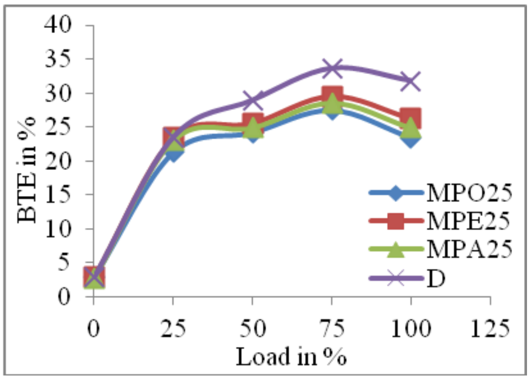

Figure 4.18 Effect of ethanol and acetone addition on the BTE of the engine with 25% blending of MPO

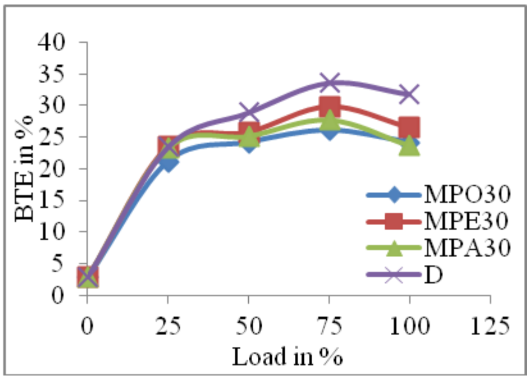

Figure 4.19 Effect of ethanol and acetone addition on the BTE of the engine with 30% blending of MPO

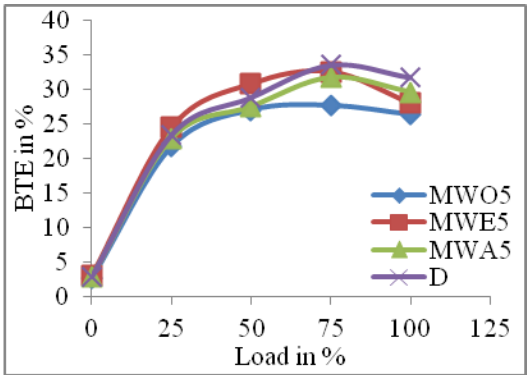

Figure 4.20 Effect of ethanol and acetone addition on the BTE of the engine with 5% blending of MWO

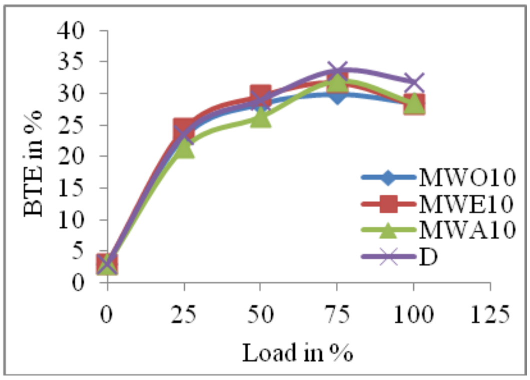

Figure 4.21 Effect of ethanol and acetone addition on the BTE of the engine with 10% blending of MWO

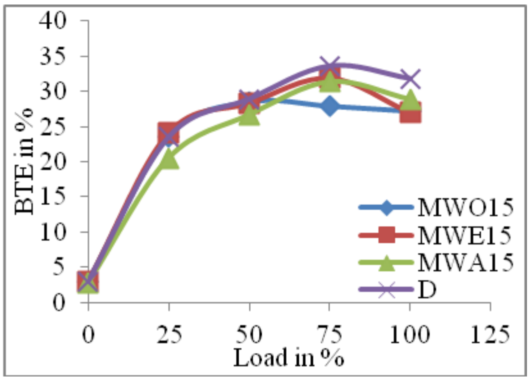

Figure 4.22 Effect of ethanol and acetone addition on the BTE of the engine with 15% blending of MWO

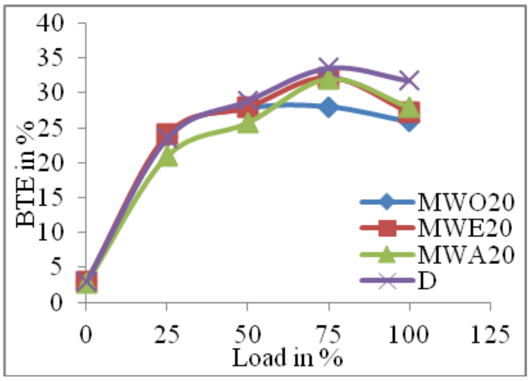

Figure 4.23 Effect of ethanol and acetone addition on the BTE of the engine with 20% blending of MWO

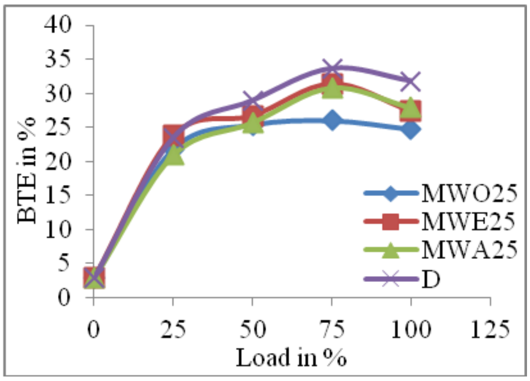

Figure 4.24 Effect of ethanol and acetone addition on the BTE of the engine with 25% blending of MWO

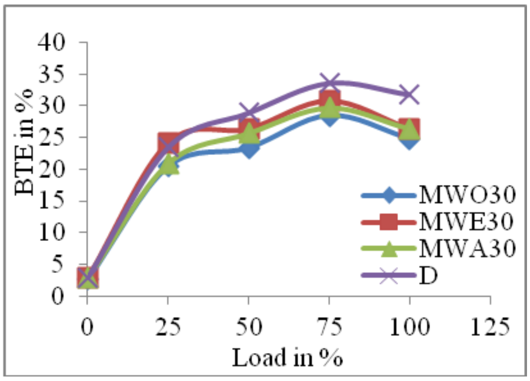

Figure 4.25 Effect of ethanol and acetone addition on the BTE of the engines with 30% blending of MWO

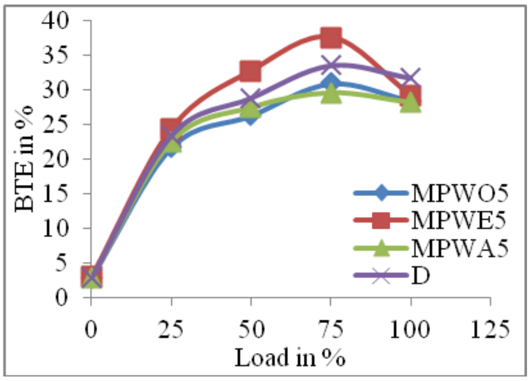

Figure 4.26 Effect of ethanol and acetone addition on the BTE of the engine with 5% blending of MPWO

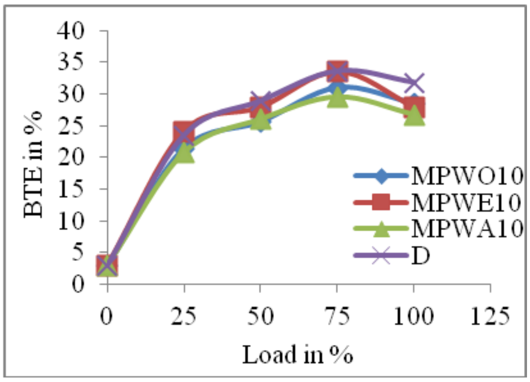

Figure 4.27 Effect of ethanol and acetone addition on the BTE of the engine with 10% blending of MPWO

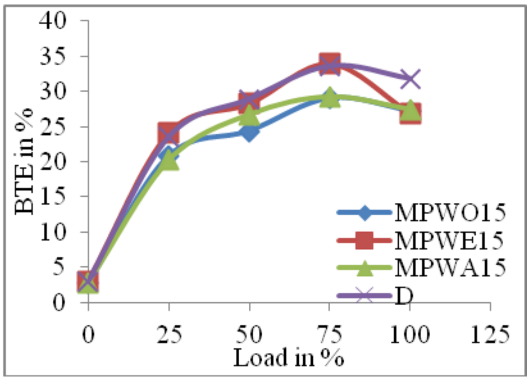

Figure 4.28 Effect of ethanol and acetone addition on the BTE of the engine with 15% blending of MPWO

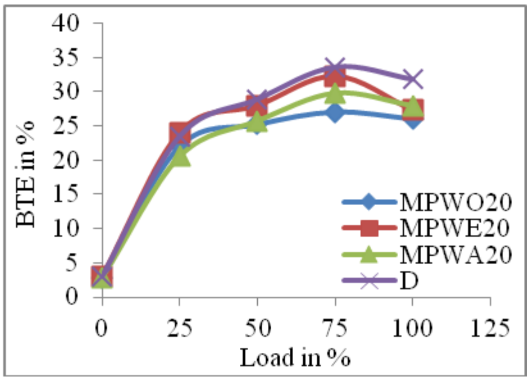

Figure 4.29 Effect of ethanol and acetone addition on the BTE of the engine with 20% blending of MPWO

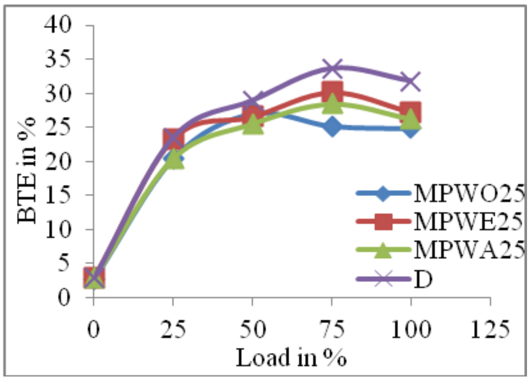

Figure 4.30 Effect of ethanol and acetone addition on the BTE of the engine with 25% blending of MPWO

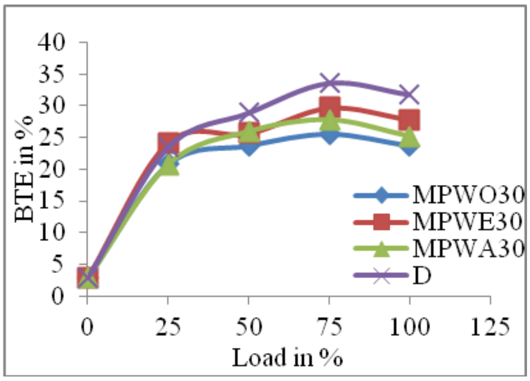

Figure 4.31 Effect of ethanol and acetone addition on the BTE of the engines with 30% blending of MPWO

It is observed that with an increase in biodiesel blends, the engine's efficiency decreases because of the lower energy content of biodiesel blends. However, the different sources possess varying energy content. However, it is observed that ethanol additions have improved the engine's efficiency (Alesawi and Qubeissi 2019). similarly, acetone additions have shown a positive effect in increasing the engine's efficiency. With the additions of ethanol (Liaquat et al. 2020) and acetone (Dhanarasu et al. 2021) to the base biodiesel blend, efficiency improvements are achieved, but they remain lesser than the efficiency of diesel.

BTE refers to the ratio of the brake power to the input power. Generally, the maximum thermal efficiency of the engine run using diesel fuel is at 75% of the loading. Efficiency increase with the increase in load percentage. However, adding biodiesel in blends decreases the engine's efficiency (Datta and Mandal 2016). The present study has also revealed similar observations.

4.1.2. Brake-specific energy consumption

BSEC refers to the energy consumed to produce a unit power output. Generally, energy consumption increases with the blend proportion of biodiesel because of the fuel's lower energy content or lower mass density.

The following figures represent load plots versus the BSEC for all prepared samples. It can be observed that with an increase in load, the BSEC decreases (Pandian 2019). Figure 4.32 illustrates the Effect of adding acetone and ethanol to diesel on the diesel engine's BSEC. The figure shows a favorable effect in reducing the specific energy consumption with ethanol and acetone additions than diesel. It may be because of the higher CV of ethanol and acetone than diesel. The variation in BSEC of the diesel engine due to ethanol and acetone additions is 2.33% and 1.99%, respectively.

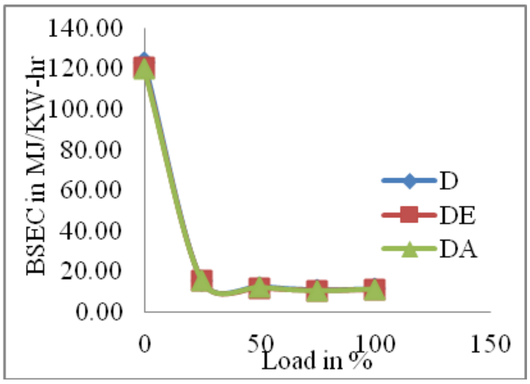

Figure 4.32 Effect of ethanol and acetone blended diesel on the BSFC of the engine

Figures 4.33- 4.38 demonstrate the significance of mixing MPO and MWO. Each combination of MPO and MWO improves the BSEC of MPO. When it comes to the BSEC, MPWO ranks higher than MPO. The average improvement of BSEC of MPO achieved as with MPWO is 3.5%.

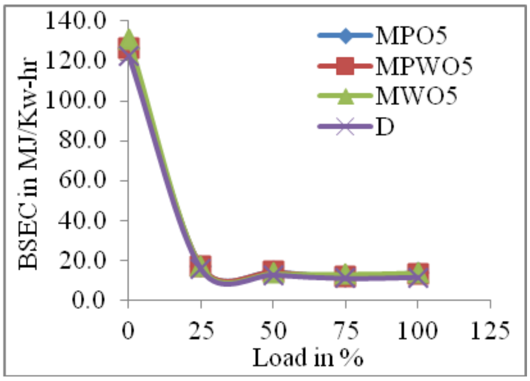

Figure 4.33 Effect of combining MPO and MWO on the BSEC of the engine at 5% blending

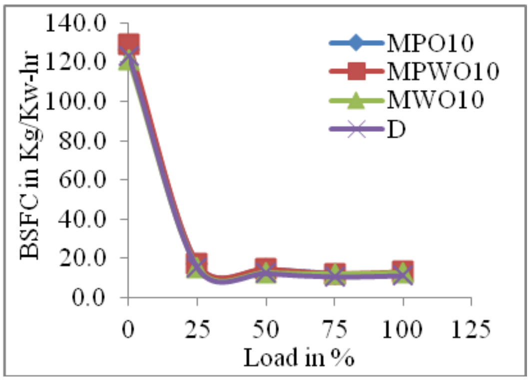

Figure 4.34 Effect of combining MPO and MWO on the BSEC of the engine at 10% blending

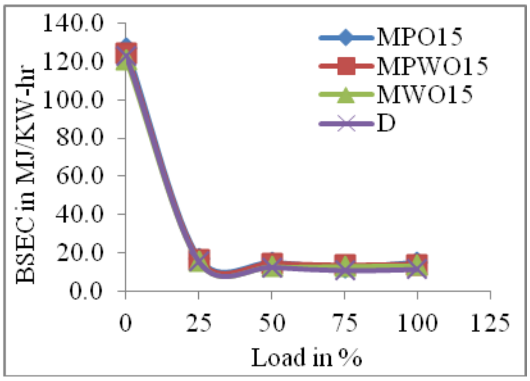

Figure 4.35 Effect of combining MPO and MWO on the BSEC of the engine at 15% blending

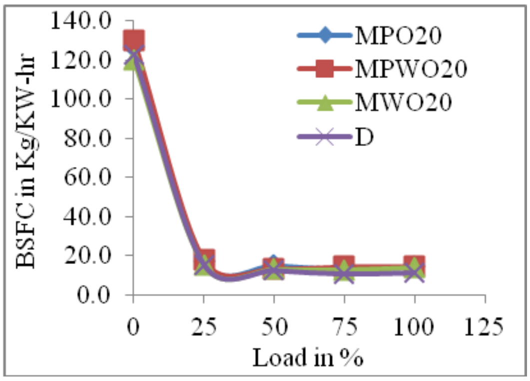

Figure 4.36 Effect of combining MPO and MWO on the BSEC of the engine at 20% blending

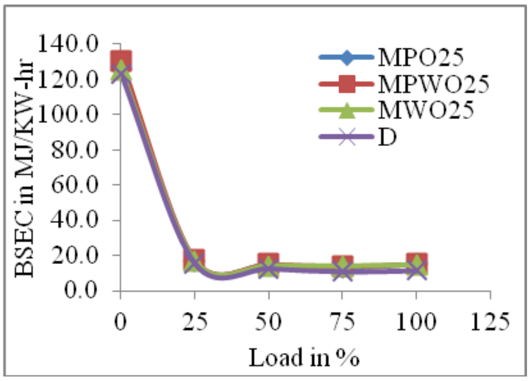

Figure 4.37 Effect of combining MPO and MWO esters on the BSEC of the engine at 25% blending

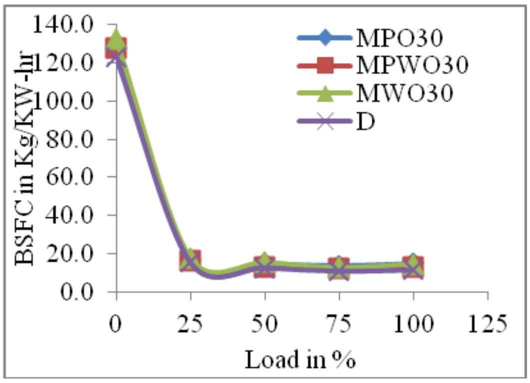

Figure 4.38 Effect of MPO and MWO on the BSEC of the engine at 30% blending

Compared to base biodiesel blends, the BSEC is better when ethanol and acetone are added to RPO blends. Figures 4.39–4.44 show the load changes concerning the BSEC for different raw biodiesel, ethanol, and acetone blends. It has been seen that adding ethanol and acetone to raw biodiesel blends makes them behave the same way in BSEC as biodiesel blends do when the engine load changes. The average increase in BSEC of RPO, RPA, and RPE compared to diesel is 41.4%, 37.69%, and 31.46%, respectively.

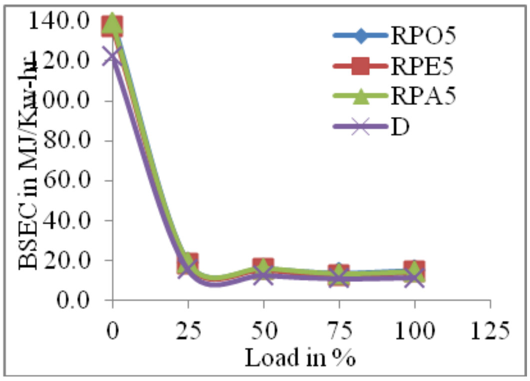

Figure 4.39 Effect of ethanol and acetone addition on the BSEC of the engine with 5% blending of RPO

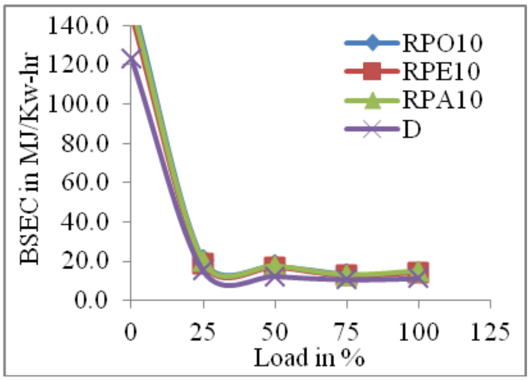

Figure 4.40 Effect of ethanol and acetone addition on the efficiency of the engine with 10% blending of RPO

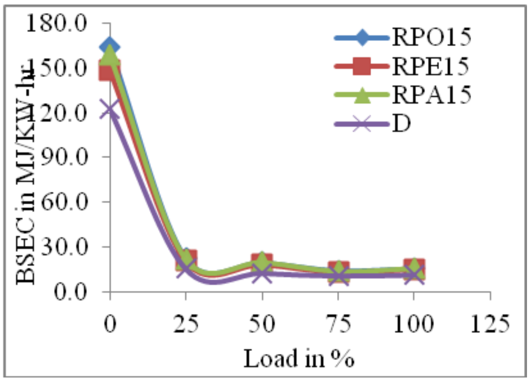

Figure 4.41 Effect of ethanol and acetone addition on the BSEC of the engine with 15% blending of RPO

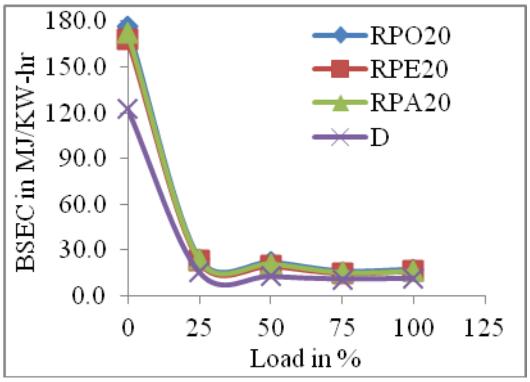

Figure 4.42 Effect of ethanol and acetone addition on the BSEC of the engine with 20% blending of RPO

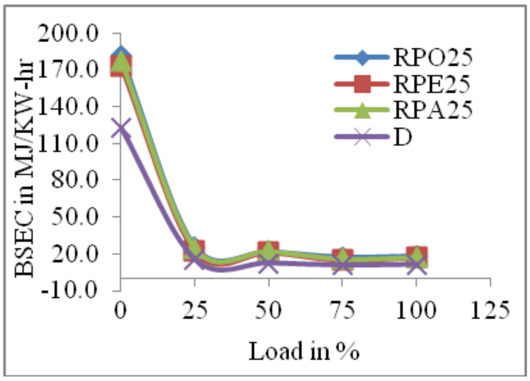

Figure 4.43 Effect of ethanol and acetone addition on the BSEC of the engine with 25% blending of RPO

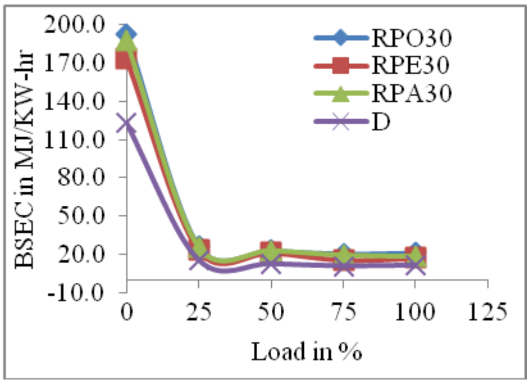

Figure 4.44 Effect of ethanol and acetone addition on the BSEC of the engine with 30% blending of RPO

Figures 4.45 to 4.50 show how the load changes with the BSEC of the engine for different mixes of raw biodiesel and additions of ethanol and acetone. Compared to MPO biodiesel blends, the BSEC is better when ethanol and acetone are added to the MPO. The engine enhancement in the BSEC of the MPO, MPA, and MPE are found at 7.66%, 7.69%, and 3.84%, respectively.

Adding ethanol and acetone to biodiesel blends of MWO has also shown that the BSEC of the engine is better than with biodiesel blends alone. Figures 4.51 to 4.56 show the relationship between load and BSEC for different blends of MWO, ethanol, and acetone added to biodiesel. At each mix of ethanol and acetone, all samples behave similarly. The BSEC average deviation for an engine that runs on MWO, MWA, and MWE is 5.13%, 5.22%, and 0.35% higher than diesel, respectively.

Adding ethanol and acetone to biodiesel blends of MPWO has also shown that the engines work better than with biodiesel blends alone. Figures 4.57 to 4.62 show the relationship between engine load and BSEC for different biodiesel blends with MPWO, ethanol, and acetone. At each mix of ethanol and acetone, all samples behave similarly. The average deviation of an engine that runs on MPWO, MPWA, and MPWE is 7.4%, 6.32 %, and 0.54% higher than diesel.

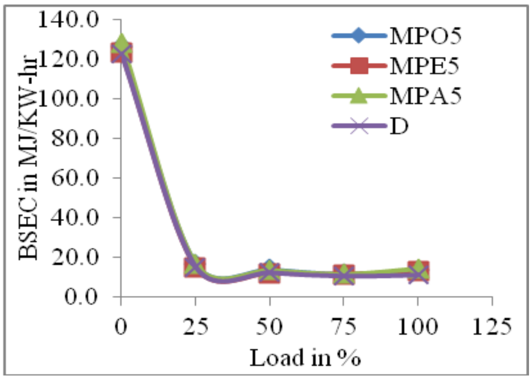

Figure 4.45 Effect of ethanol and acetone addition on the BSEC of the engine with 5% blending of MPO

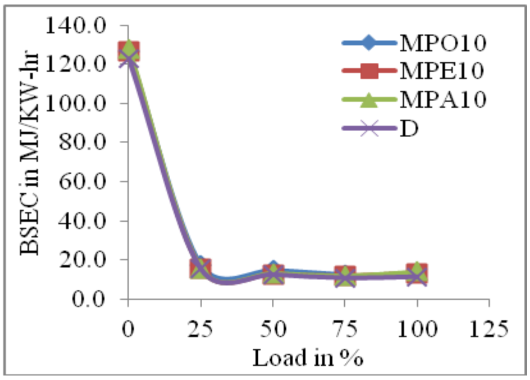

Figure 4.46 Effect of ethanol and acetone addition on the BSEC of the engine with 10% blending of MPO

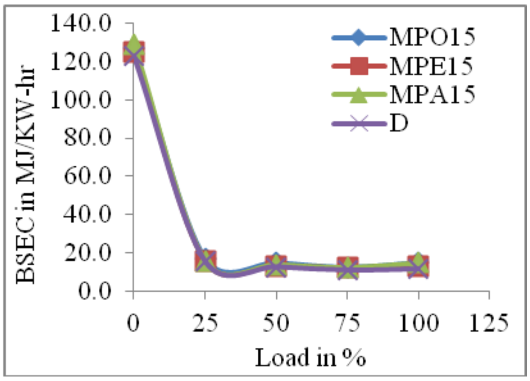

Figure 4.47 Effect of ethanol and acetone addition on the BSEC of the engine with 15% blending of MPO

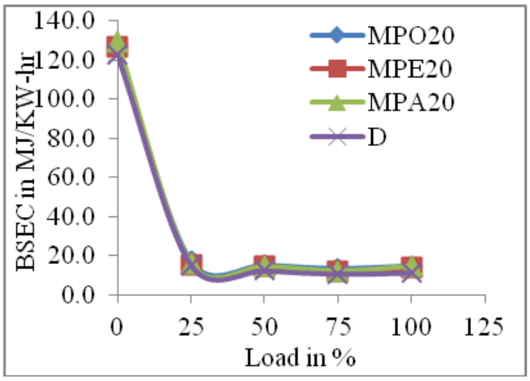

Figure 4.48 Effect of ethanol and acetone addition on the BSEC of the engine with 20% blending of MPO

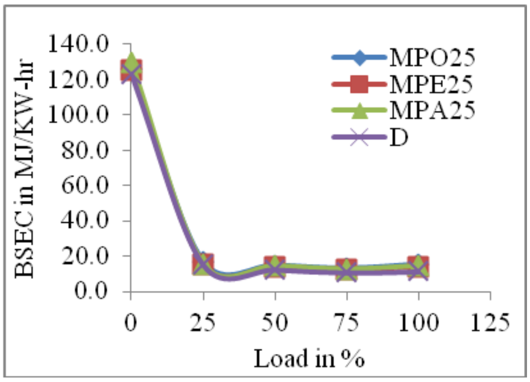

Figure 4.49 Effect of ethanol and acetone addition on the BSEC of the engine with 25% blending of MPO

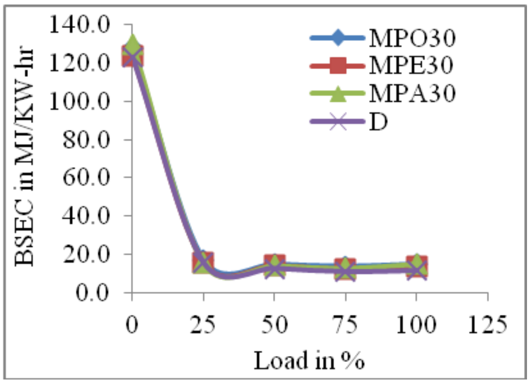

Figure 4.50 Effect of ethanol and acetone addition on the BSEC of the engine with 30% blending of MPO

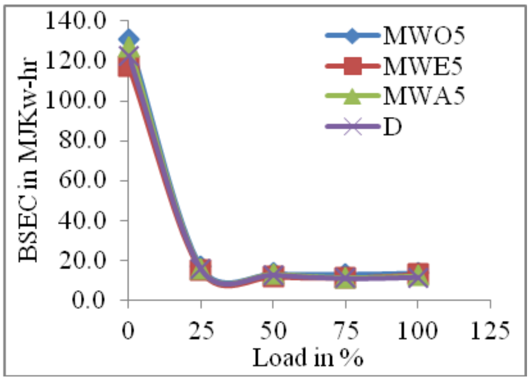

Figure 4.51 Effect of ethanol and acetone addition on the BSEC of the engine with 5% blending of MWO

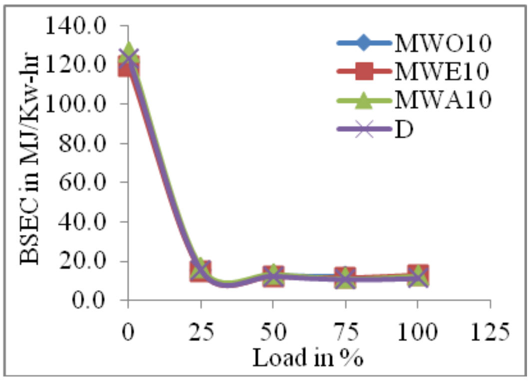

Figure 4.52 Effect of ethanol and acetone addition on the BSEC of the engine with 10% blending of MWO

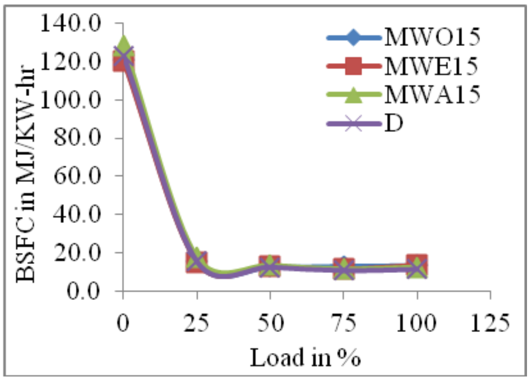

Figure 4.53 Effect of ethanol and acetone addition on the BSEC of the engine with 15% blending of MWO

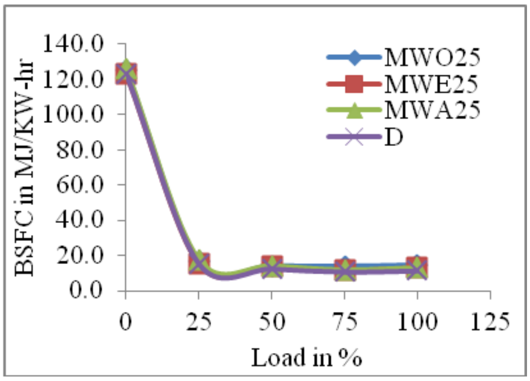

Figure 4.54 Effect of ethanol and acetone addition on the BSEC of the engine with 20% blending of MWO

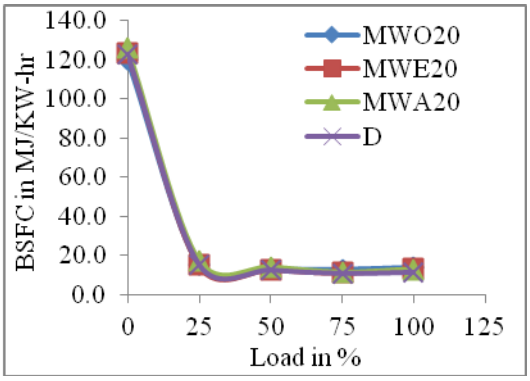

Figure 4.55 Effect of ethanol and acetone addition on the BSEC of the engine with 25% blending of MWO

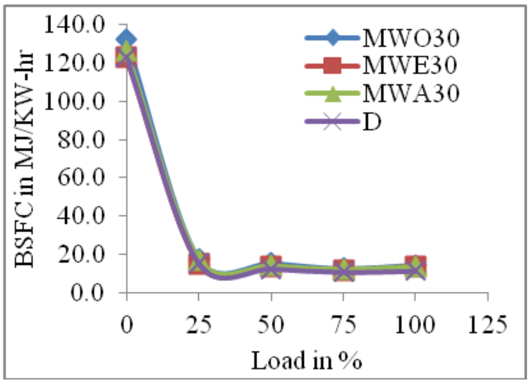

Figure 4.56 Effect of ethanol and acetone addition on the BSEC of the engines with 30% blending of MWO

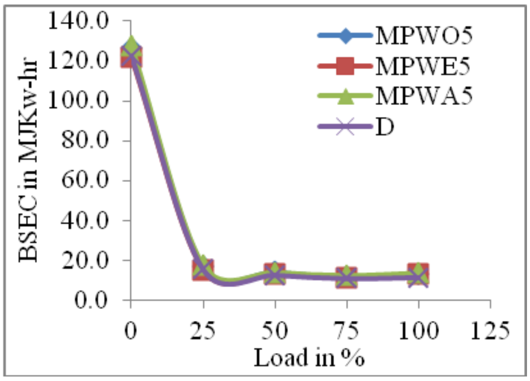

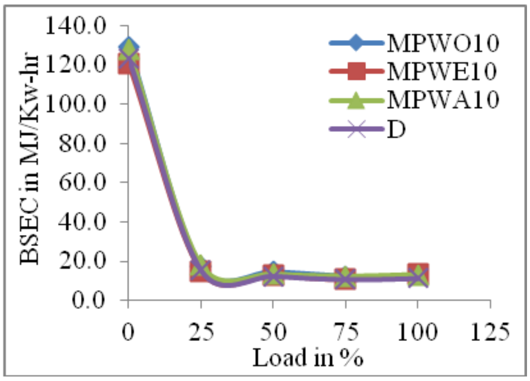

Figure 4.57 Effect of ethanol and acetone addition on the BSEC of the engine with 5% blending of MPWO

Figure 4.58 Effect of ethanol and acetone addition on the BSEC of the engine with 10% blending of MPWO

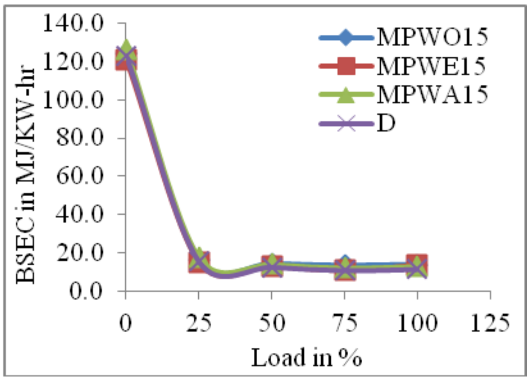

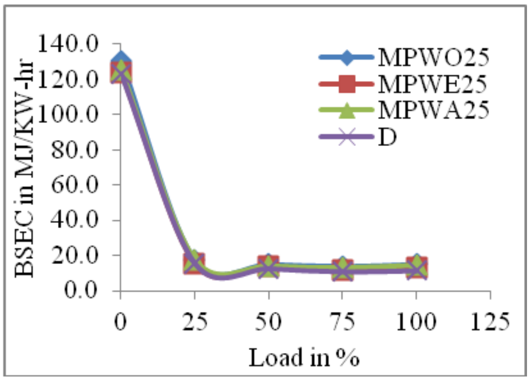

Figure 4.59 Effect of ethanol and acetone addition on the BSEC of the engine with 15% blending of MPWO

Figure 4.60 Effect of ethanol and acetone addition on the BSEC of the engine with 20% blending of MPWO

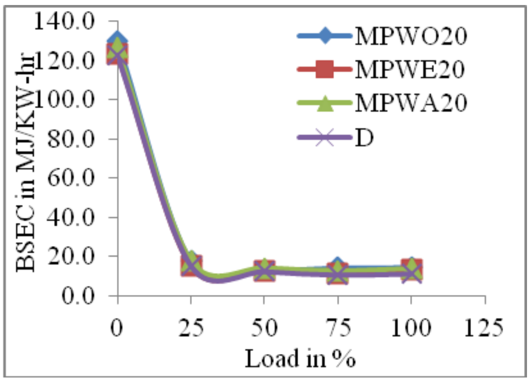

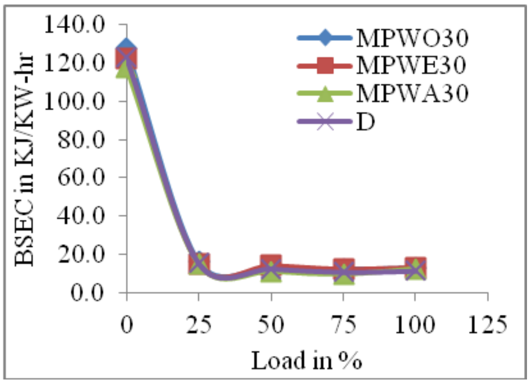

Figure 4.61 Effect of ethanol and acetone addition on the BSEC of the engine with 25% blending of MPWO

Figure 4.62 Effect of ethanol and acetone addition on the BSEC of the engines with 30% blending of MPWO

Brake-specific energy consumption increase with the increase in biodiesel blends (Wu et al. 2020). This is because biodiesel's lower calorific value and higher viscosity will harm atomization and combustion, increasing BSEC (Sianturi and Fauziyah 2020). Adding ethanol and acetone positively Effects the fuel's energy content due to lesser viscosity and higher energy content(Liaquat et al. 2020) than biodiesel blends. A similar observation is found in the present study too. With the increase in biodiesel blends, the BSEC improves upon the additions of ethanol and acetone. However, ethanol shows a better response compared to acetone.

Brake-specific energy consumption increase with the increase in biodiesel blends (Wu et al. 2020). This is because biodiesel's lower calorific value and higher viscosity will harm atomization and combustion, increasing BSEC (Sianturi and Fauziyah 2020). Adding ethanol and acetone positively affects the fuel's energy content due to lesser viscosity and higher energy content(Liaquat et al. 2020) than biodiesel blends. A similar observation is found in the present study too. With the increase in biodiesel blends, the BSEC improves upon the additions of ethanol and acetone. However, ethanol shows a better response compared to acetone.

4.2 Emission parameters

4.2.1 Carbon Monoxide

Emission CO emissions decrease with an increase in biodiesel blending. Alternatively, there is a significant increase in CO_2 and NOx emissions (Hoekman and Robbins 2012). Due to the addition of biodiesel blends. The CO emission decrease (Xue et al. 2011). The lower carbon content of the biodiesel blends that it reduces CO emissions, and the other reason is the complete combustion of the fuel, where CO is converted to CO_2 (Liaquat et al. 2020) and simultaneously increases the CO_2 emissions in the engine. However, the variation in CO and CO_2 emissions varies with different sources. Ethanol (Datta and Mandal 2016; Heydari et al. 2017) and acetone (Dhanarasu et al. 2021) addition also have shown similar behavior to biodiesel blends.

CO is considered one of the engine cylinder's harmful exhausts due to the engine cylinder's lack of oxygen. Blending biofuels with diesel has shown a positive significance in reducing CO emissions. Generally, the emissions of CO increase with an increase in engine loading. A similar trend is observed in the present study. Blending RPO, MPO, MWO, and MPWO with diesel has reduced CO emissions. The intensity of reduction is found with the increase in the blending ratio. Also, ethanol(Khalife et al.

2017) and acetone offer further reductions in the CO of the engine. Figure 4.63 shows the plot of CO versus Load for D, DE and DA. the average deviation in ethanol and acetone blended CO compared to diesel are 20.91% and 17.64%, respectively.

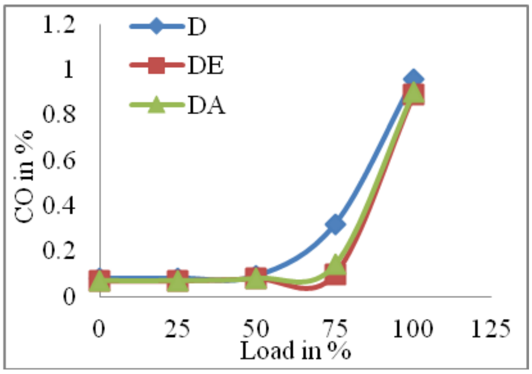

Figure 4.63 Effect of ethanol and acetone blended diesel on the CO of the engine

Figures 4.64-4.69 show the significance of combining two distinct methyl esters, MPO and MWO. The MPO-fueled engine can be improved by combining MPO and MWO at each blend. Compared to MPO, the average achievement in the CO of MPWO is 4.23%.

Adding ethanol and acetone to RPO blends improved the CO content compared to biodiesel blends. The variational plots of load vs CO for various blends of raw biodiesel, ethanol, and acetone additives are depicted in Figures 4.70 to 4.75. Adding ethanol and acetone to raw biodiesel blends has a similar CO behaviour to that of biodiesel blends under varying engine loads. The improvements in CO due to RPO, RPA, and RPE compared to diesel are 52.75%, 55.11% and 57.47%, respectively.

Figures 4.76 through 4.81 depict the variational plot of load versus the CO of the engine for various blends of raw biodiesel, ethanol, and acetone. Compared to MPO biodiesel blends, adding ethanol (Shrivastava et al. 2021) and acetone to MPO has improved the CO. In addition, adding ethanol and acetone to raw biodiesel blends is comparable to that of biodiesel blends with engine load variations. Compared to the raw biodiesel blends, the improvements in CO of MPO, MPA, and MPE are 35.59%, 33.44% and 35.59%, respectively.

The CO of the engine improved when ethanol and acetone(Dhanarasu et al. 2021) were added to MWO's biodiesel blends compared to biodiesel blends. Figures 4.82 to 4.87 demonstrate the plot of load versus CO for various biodiesel mixes of MWO, ethanol, and acetone additives. Every sample exhibits the same behaviour at every concentration of ethanol and acetone. For ethanol and acetone-fuelled biodiesel blends, the average divergence with the CO of an engine running on MWO, MWA, and MWE is 32.90%, 39.87%, and 44.57%, respectively.

The CO of the engine has improved when ethanol and acetone have been added to MPWO diesel blends compared to biodiesel blends. Figures 4.88 to 4.93 demonstrate the plot of load versus CO for various biodiesel mixes of MPWO, ethanol, and acetone additives. Every sample exhibits the same behaviour at every concentration of ethanol and acetone. For ethanol and acetone-fuelled biodiesel blends, the average divergence with the CO of an engine running on MPWO, MPWA, and MPWE is 32.90%, 37.01%, and 32.55%, respectively, compared to diesel.

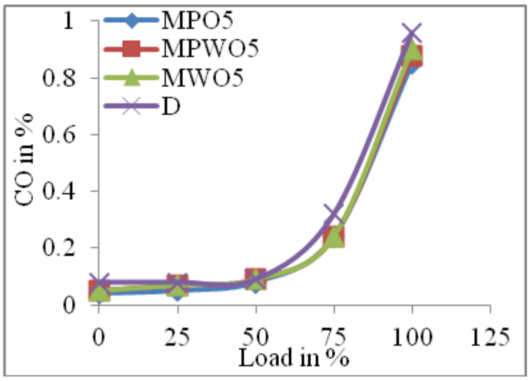

Figure 4.64 Effect of combining MPO and MWO on the CO of the engine at 5% blending

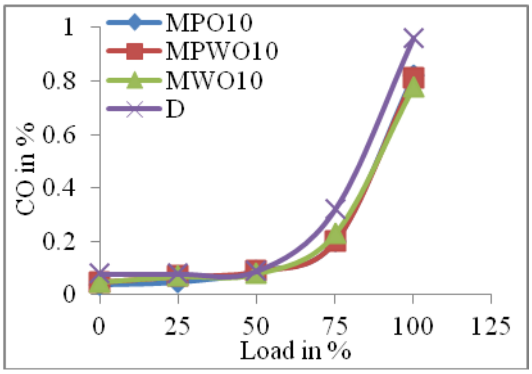

Figure 4.65 Effect of combining MPO and MWO on the CO of the engine at 10% blending

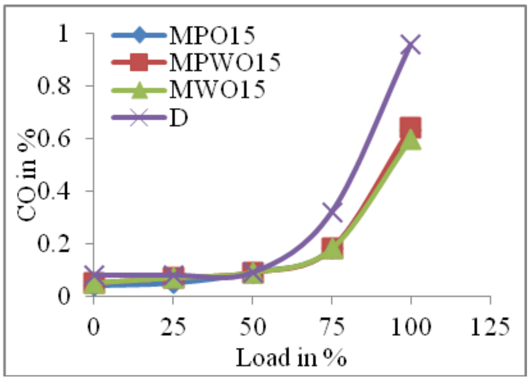

Figure 4.66 Effect of combining MPO and MWO on the CO of the engine at 15% blending

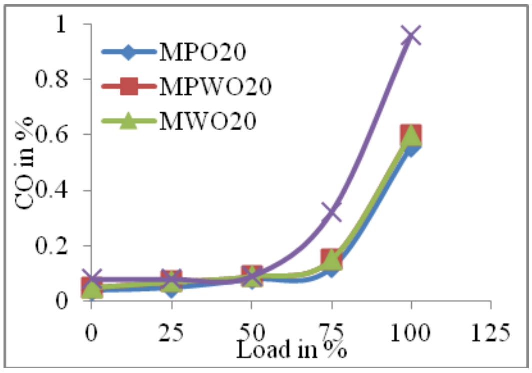

Figure 4.67 Effect of combining MPO and MWO on the CO of the engine at 20% blending

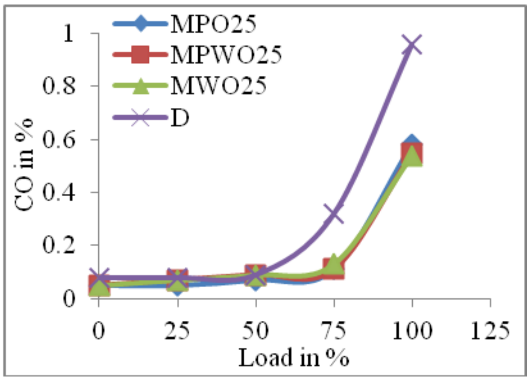

Figure 4.68 Effect of combining MPO and MWO esters on the CO of the engine at 25% blending

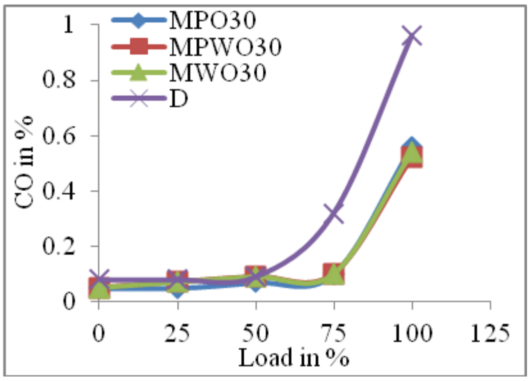

Figure 4.69 Effect of MPO and MWO on the CO of the engine at 30% blending

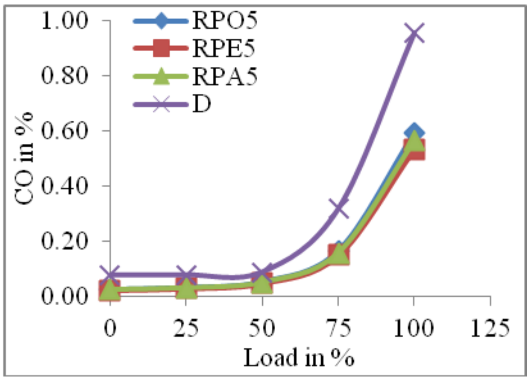

Figure 4.70 Effect of ethanol and acetone addition on the CO of the engine with 5% blending of RPO

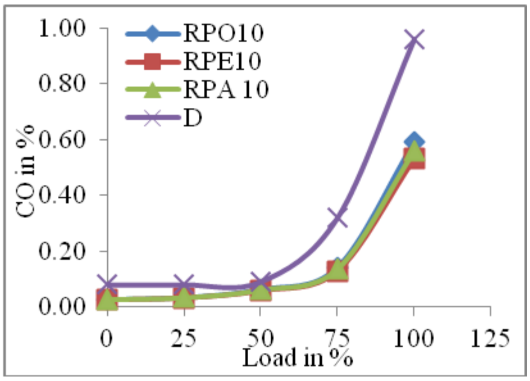

Figure 4.71 Effect of ethanol and acetone addition on the CO of the engine with 10% blending of RPO

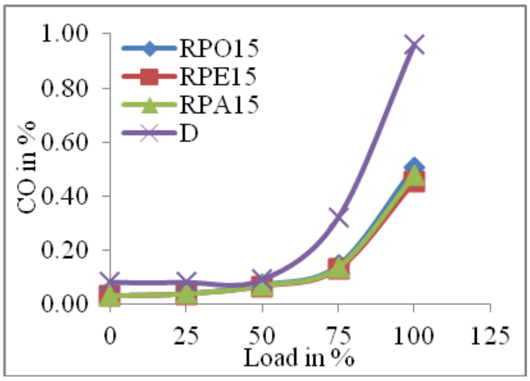

Figure 4.72 Effect of ethanol and acetone addition on the CO of the engine with 15% blending of RPO

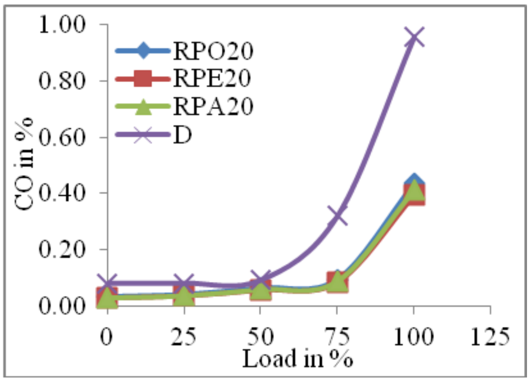

Figure 4.73 Effect of ethanol and acetone addition on the CO of the engine with 20% blending of RPO

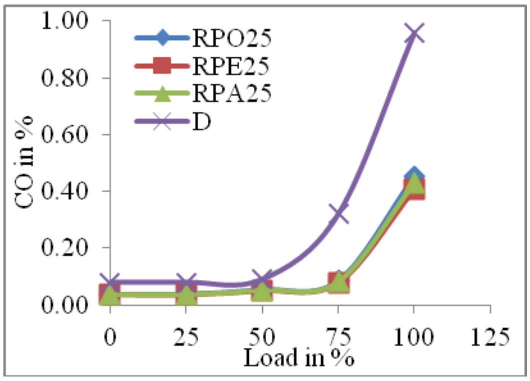

Figure 4.74 Effect of ethanol and acetone addition on the CO of the engine with 25% blending of RPO

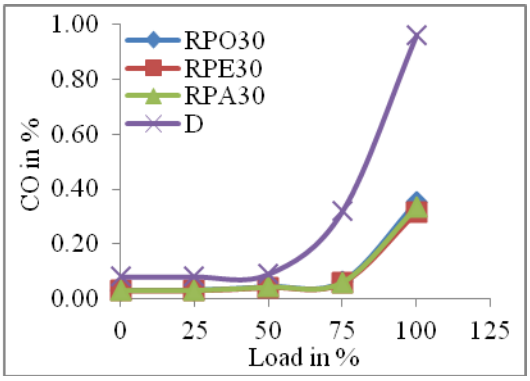

Figure 4.75 Effect of ethanol and acetone addition on the CO of the engine with 30% blending of RPO

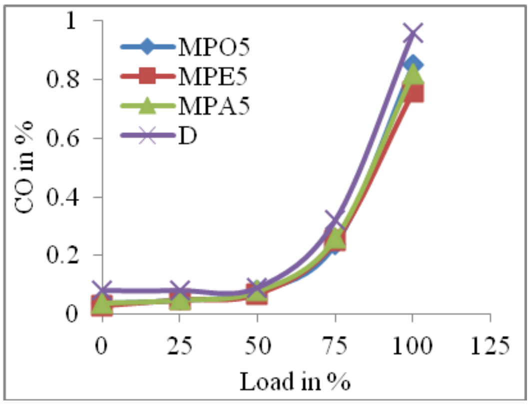

Figure 4.76 Effect of ethanol and acetone addition on the CO of the engine with 5% blending of MPO

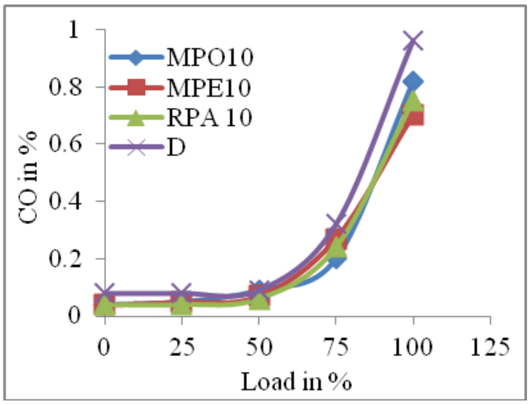

Figure 4.77 Effect of ethanol and acetone addition on the CO of the engine with 10% blending of MPO

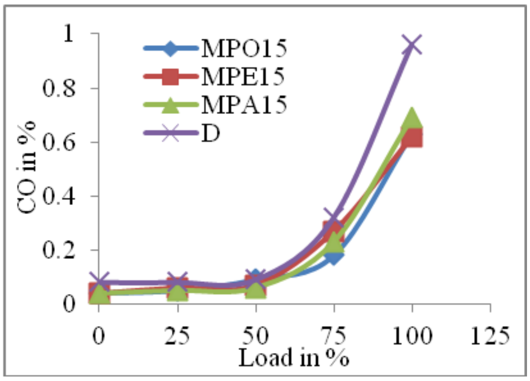

Figure 4.78 Effect of ethanol and acetone addition on the CO of the engine with 15% blending of MPO

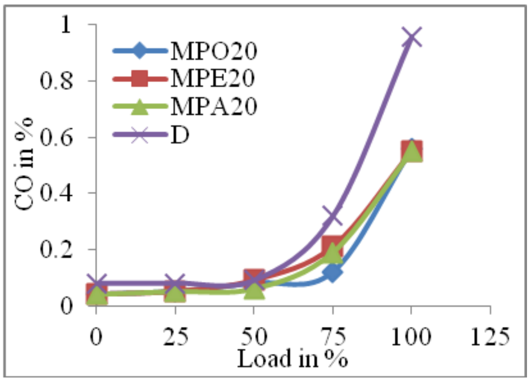

Figure 4.79 Effect of ethanol and acetone addition on the CO of the engine with 20% blending of MPO

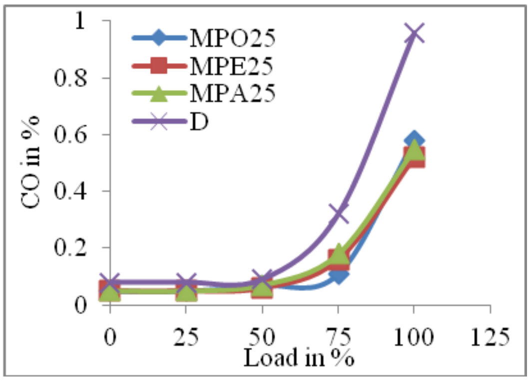

Figure 4.80 Effect of ethanol and acetone addition on the CO of the engine with 25% blending of MPO

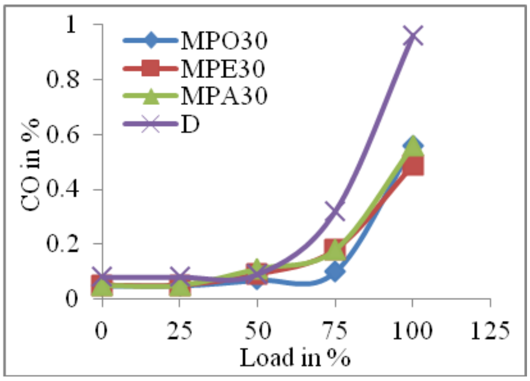

Figure 4.81 Effect of ethanol and acetone addition on the CO of the engine with 30% blending of MPO

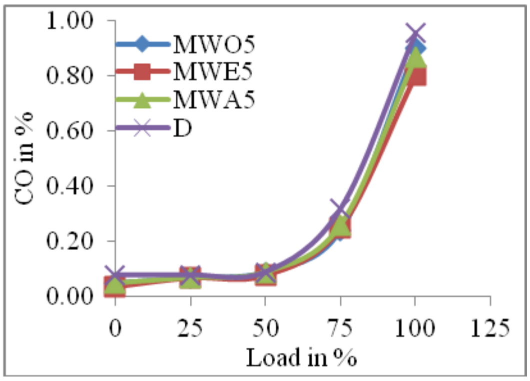

Figure 4.82 Effect of ethanol and acetone addition on the CO of the engine with 5% blending of MWO

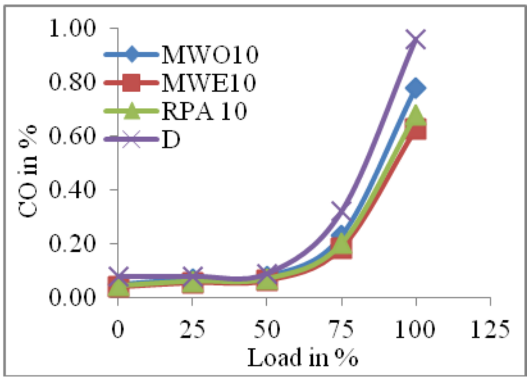

Figure 4.83 Effect of ethanol and acetone addition on the BSEC of the engine with 10% blending of MWO

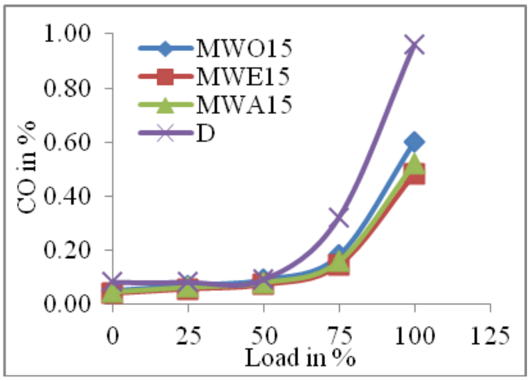

Figure 4.84 Effect of ethanol and acetone addition on the BSEC of the engine with 15% blending of MWO

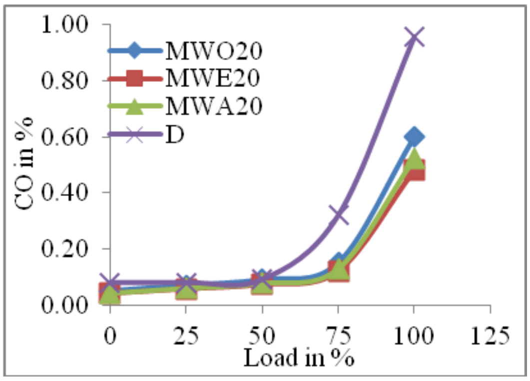

Figure 4.85 Effect of ethanol and acetone addition on the BSEC of the engine with 20% blending of MWO

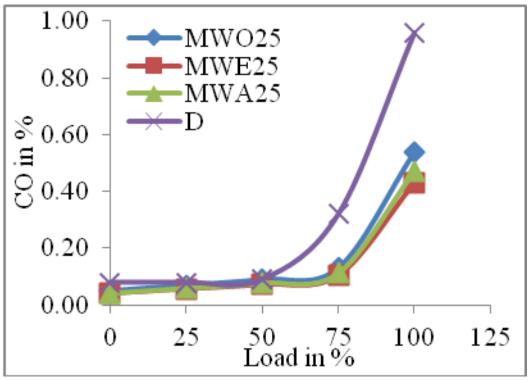

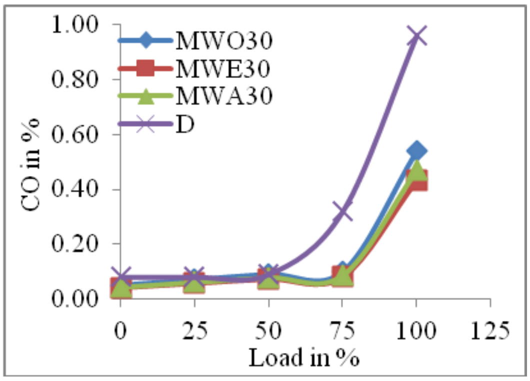

Figure 4.86 Effect of ethanol and acetone addition on the BSEC of the engine with 25% blending of MWO

Figure 4.87 Effect of ethanol and acetone addition on the BSECsss of the engines with 30% blending of MWO

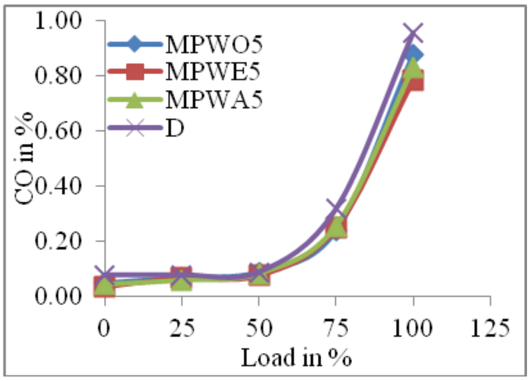

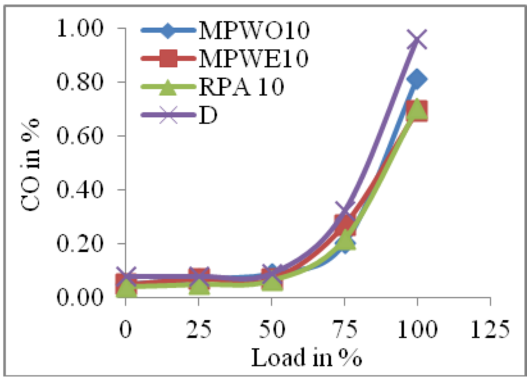

Figure 4.88 Effect of ethanol and acetone addition on the BSEC of the engine with 5% blending of MPWO

Figure 4.89 Effect of ethanol and acetone addition on the BSEC of the engine with 10% blending of MPWO

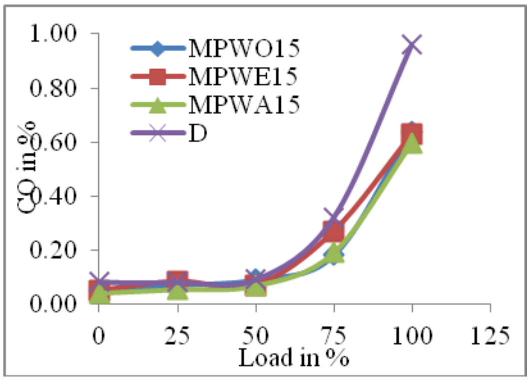

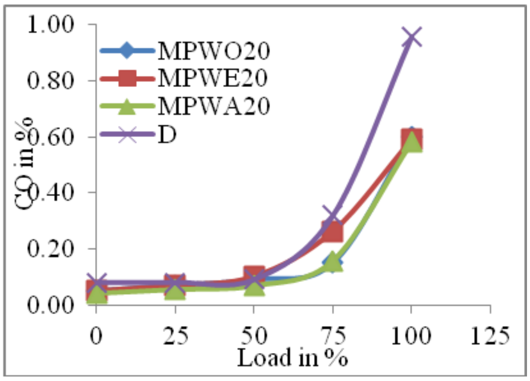

Figure 4.90 Effect of ethanol and acetone addition on the BSEC of the engine with 15% blending of MPWO

Figure 4.91 Effect of ethanol and acetone addition on the BSEC of the engine with 20% blending of MPWO

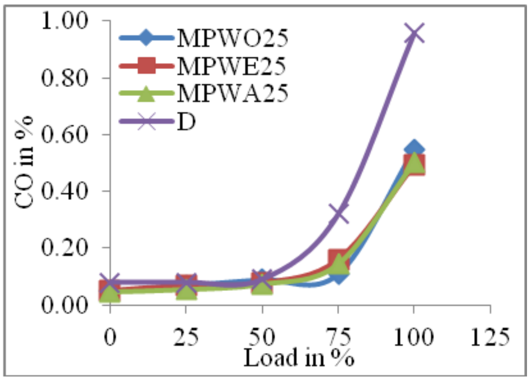

Figure 4.92 Effect of ethanol and acetone addition on the BSEC of the engine with 25% blending of MPWO

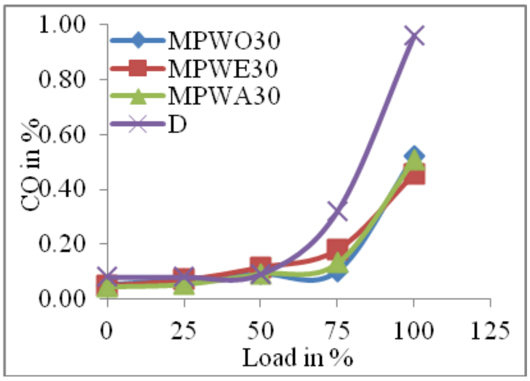

Figure 4.93 Effect of ethanol and acetone addition on the BSEC of the engines with 30% blending of MPWO

4.2.2 Carbon dioxide

CO_2 is formed due to the complete combustion of fuel in the combustion chamber. Biodiesel fuelled engines generally produce higher carbon dioxide than diesel-fueled engines due to fuel combustion inside the combustion chamber. Also, ethanol and acetone with different fuels have shown higher CO_2 emissions with additions. In the present study, the prepared alternative fuels have also demonstrated increased CO_2 emissions. A plot of Load versus CO_2 is plotted for all three specimens, namely D, DA, and DE, as shown in Figure 4.94. The average deviation in the CO_2 of ethanol and acetone compared to CO2 due to diesel is 12.77% and 18.06%, respectively.

The importance of combining the two different methyl esters, MPO and MWO, is illustrated in Figures 4.95 to 4.100. The CO_2 of MPO in each mixture is increased by combining it with MWO. Comparing MPWO to MPO, the average CO_2 accomplishment by MPWO is 1.71%.

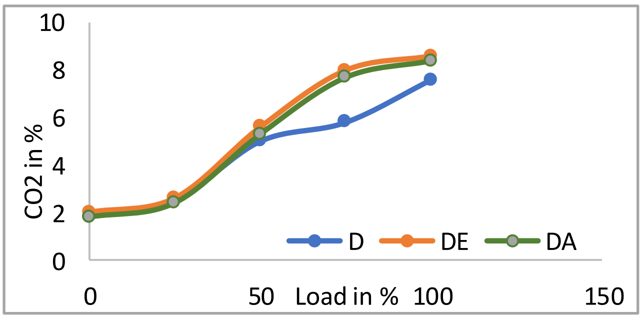

Figure 4.94 Effect of ethanol and acetone blended diesel on the CO_2 of the engine.

Compared to biodiesel blends, the CO_2 in RPO blends has improved by adding ethanol and acetone. The variational plot of load vs. CO_2 for various blends of unprocessed biodiesel, ethanol, and acetone additives is shown in Figures 4.101 to 4.106. It has shown that the CO_2 behavior of biodiesel blends with varying engine loads and adding ethanol and acetone to raw biodiesel blends are similar. The average CO_2 increments for RPO, RPA, and RPE are 33.69%, 39.62%, and 49.16%, respectively, compared to diesel.

Figures 4.107 to 4.112 show the variational plot of load vs. CO_2 for various blends of raw biodiesel and adding ethanol and acetone. Adding ethanol (Shrivastava et al. 2021)and acetone to the MPO has enhanced the CO_2 compared to MPO biodiesel blends. Additionally, adding ethanol and acetone to the raw biodiesel blends is comparable to that of the biodiesel blends with varying engine loads. The CO_2 enhancements due to MPO, MPA, and MPE are 18.20%, 22.50%%, and 28.63%, respectively, compared to diesel.

The CO_2 of the engine has improved when ethanol and acetone are added to MWO's biodiesel blends compared to biodiesel blends. Figures 4.113 to 4.118 demonstrate the plot of load versus CO_2 for various biodiesel mixes of MWO, ethanol, and acetone additives. Every sample exhibits the same behaviour at every concentration of ethanol and acetone. For MWO, acetone, and ethanol-fuelled biodiesel blends, the average divergence with the CO_2 of an engine running on diesel is 11.82%, 35.85%, and 50.10%.

Similarly, ethanol and acetone additives to MPWO's biodiesel blends have increased engine efficiency compared to biodiesel blends. For different biodiesel mixes with MPWO, ethanol, and acetone additives, the engine load is plotted against CO_2 in Figures 4.119 to 4.124. The samples exhibit the same behaviour for each ethanol and acetone mixture. For MWO, MWE and MWA blends, the average deviations with the CO2 of an engine running on MPWO are 16.79%, 27.28%, and 25.31%.

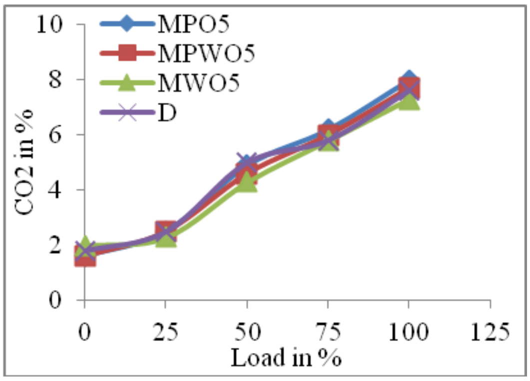

Figure 4.95 Effect of combining MPO and MWO on the CO_2 of the engine at 5% blending

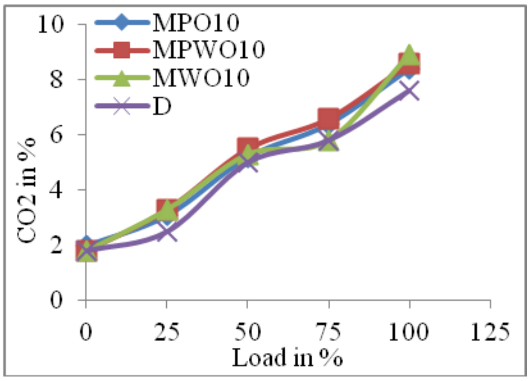

Figure 4.96 Effect of combining MPO and MWO on the CO_2 of the engine at 10% blending

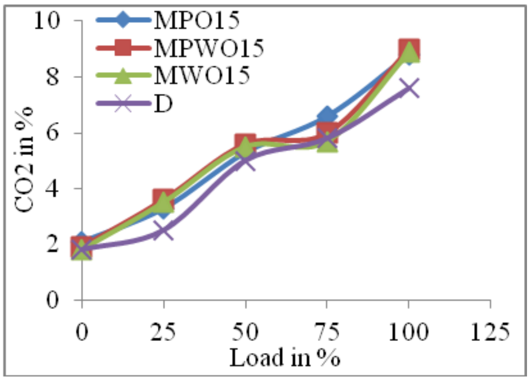

Figure 4.97 Effect of combining MPO and MWO on the CO2 of the engine at 15% blending

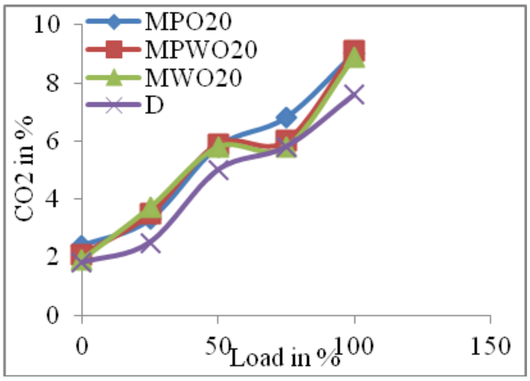

Figure 4.98 Effect of combining MPO and MWO on the CO2 of the engine at 20% blending

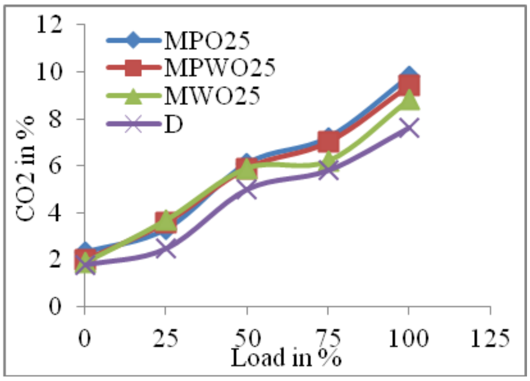

Figure 4.99 Effect of combining MPO and MWO esters on the CO_2 of the engine at 25% blending

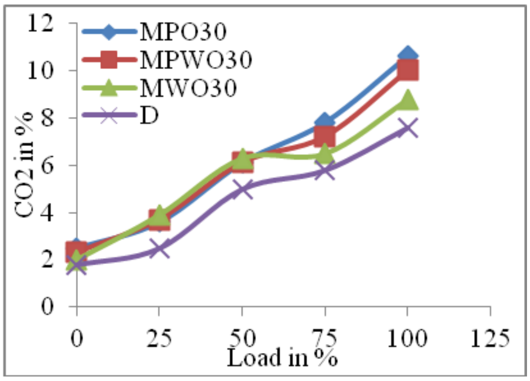

Figure 4.100 Effect of combining MPO and MWO on the CO_2 of the engine at 30% blending

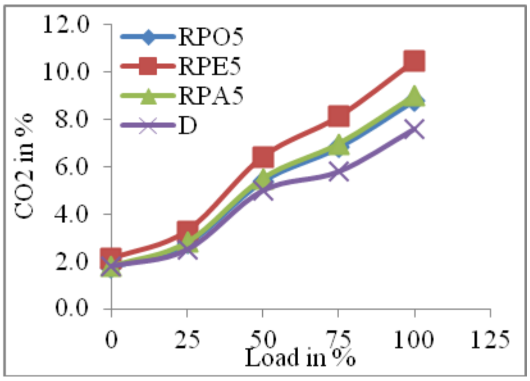

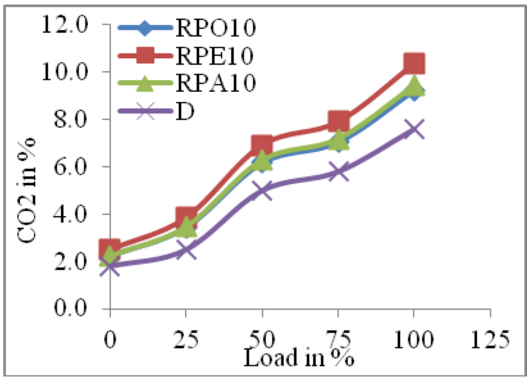

Figure 4.101 Effect of ethanol and acetone addition on the CO_2 of the engine with 5% blending of RPO

Figure 4.102 Effect of ethanol and acetone addition on the CO_2 of the engine with 10% blending of RPO

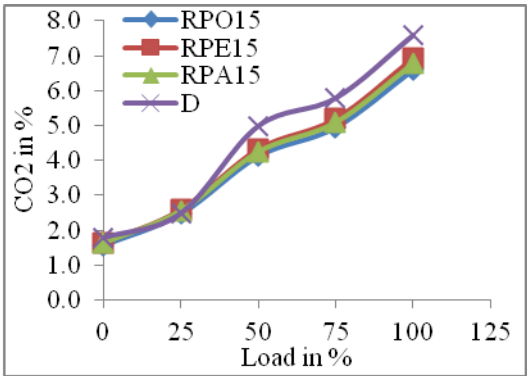

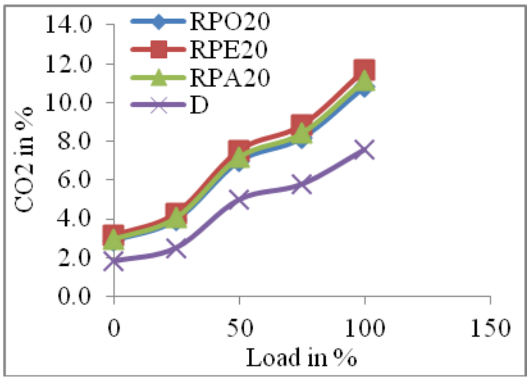

Figure 4.103 Effect of ethanol and acetone addition on the CO_2 of the engine with 15% blending of RPO

Figure 4.104 Effect of ethanol and acetone addition on the CO_2 of the engine with 20% blending of RPO

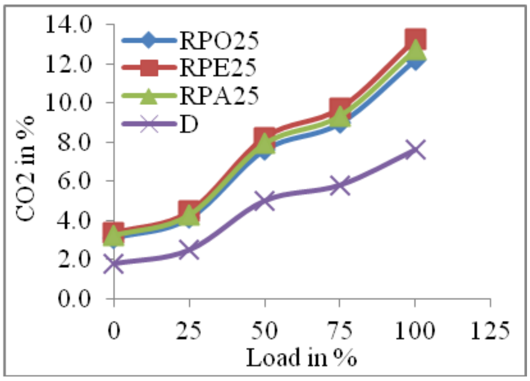

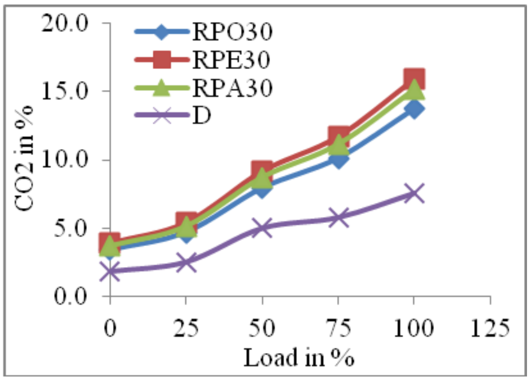

Figure 4.105 Effect of ethanol and acetone addition on the CO_2 of the engine with 25% blending of RPO

Figure 4.106 Effect of ethanol and acetone addition on the CO_2 of the engine with 30% blending of RPO

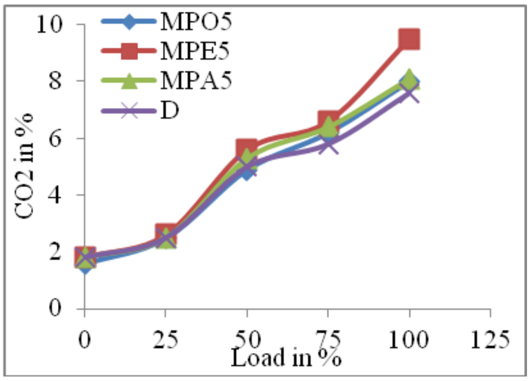

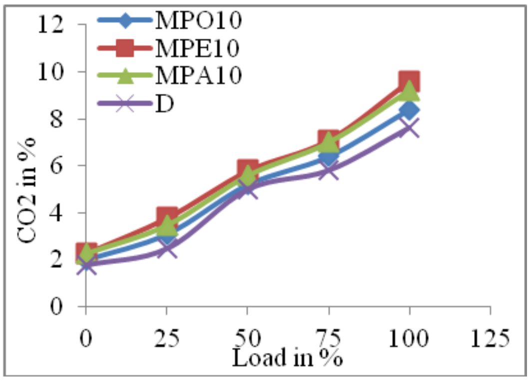

Figure 4.107 Effect of ethanol and acetone addition on the CO_2 of the engine with 5% blending of MPO

Figure 4.108 Effect of ethanol and acetone addition on the CO_2 of the engine with 10% blending of MPO

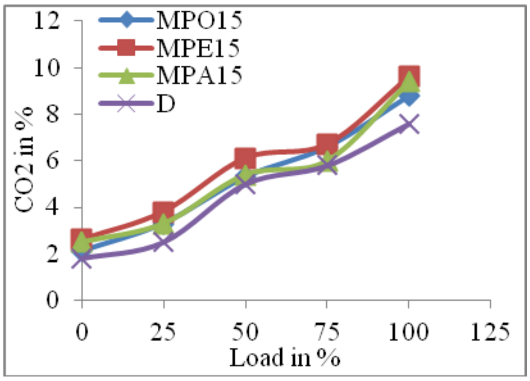

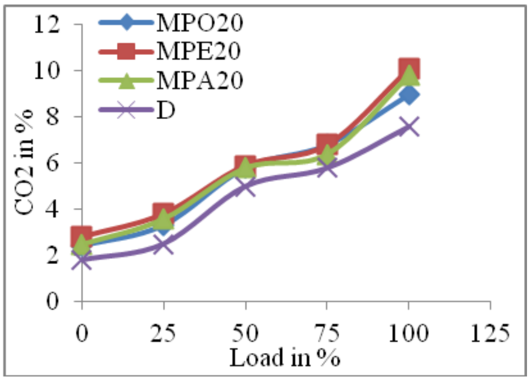

Figure 4.109 Effect of ethanol and acetone addition on the CO_2 of the engine with 15% blending of MPO

Figure 4.110 Effect of ethanol and acetone addition on the CO_2 of the engine with 20% blending of MPO

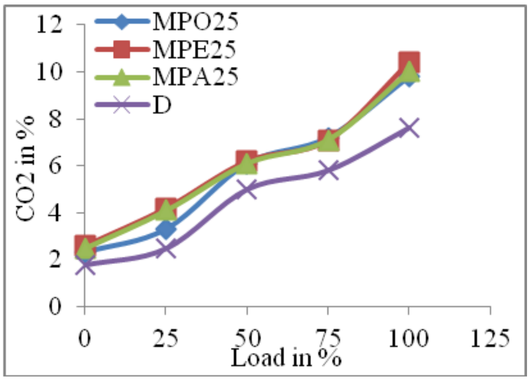

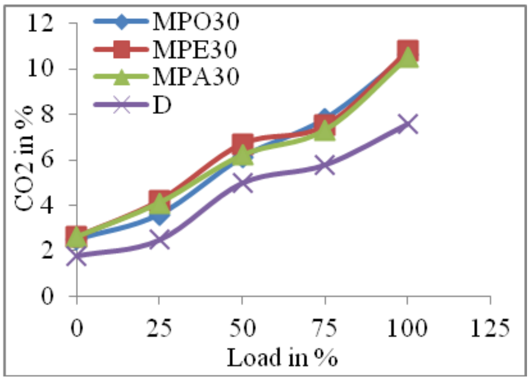

Figure 4.111 Effect of ethanol and acetone addition on the CO_2 of the engine with 25% blending of MPO

Figure 4.112 Effect of ethanol and acetone addition on the CO_2 of the engine with 30% blending of MPO

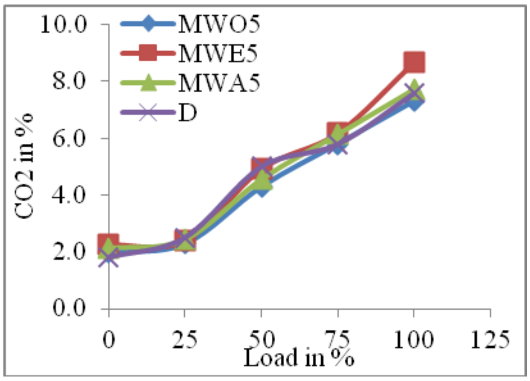

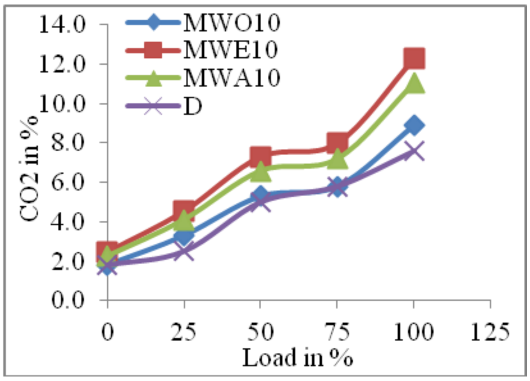

Figure 4.113 Effect of ethanol and acetone addition on the CO_2 of the engine with 5% blending of MWO

Figure 4.114 Effect of ethanol and acetone addition on the CO_2 of the engine with 10% blending of MWO

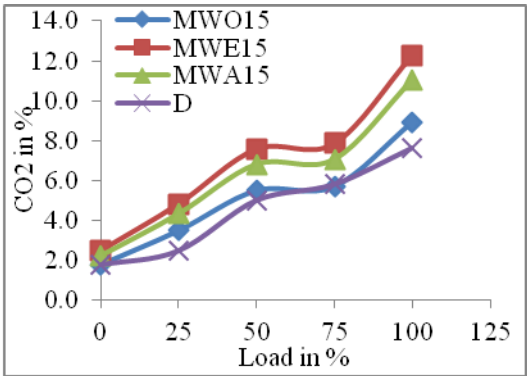

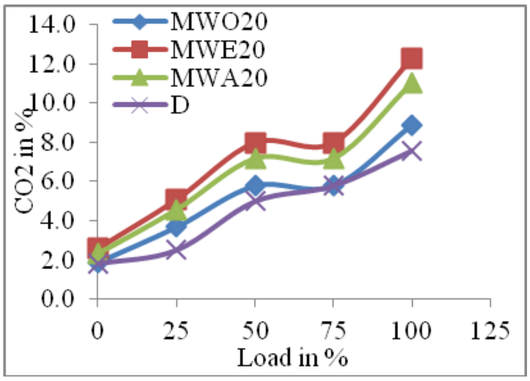

Figure 4.115 Effect of ethanol and acetone addition on the CO_2 of the engine with 15% blending of MWO

Figure 4.116 Effect of ethanol and acetone addition on the CO2 of the engine with 20% blending of MWO

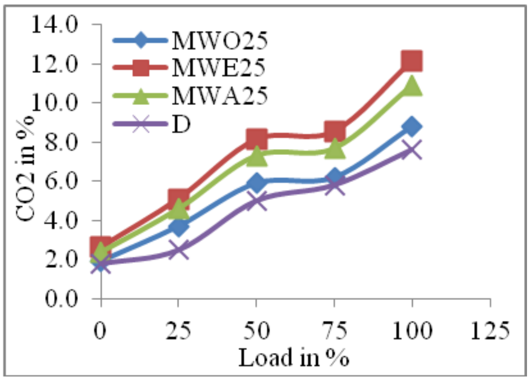

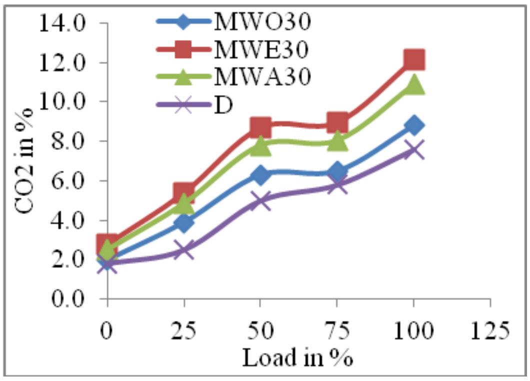

Figure 4.117 Effect of ethanol and acetone addition on the CO_2 of the engine with 25% blending of MWO

Figure 4.118 Effect of ethanol and acetone addition on the CO_2 of the engines with 30% blending of MWO

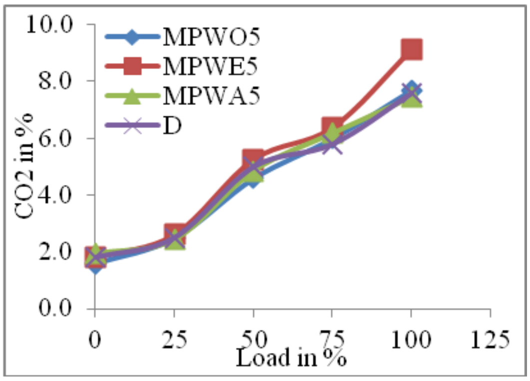

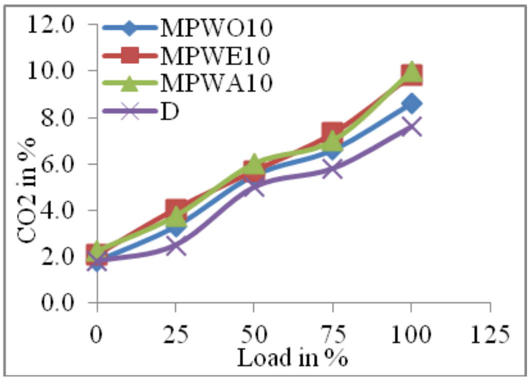

Figure 4.119 Effect of ethanol and acetone addition on the CO_2 of the engine with 5% blending of MPWO

Figure 4.120 Effect of ethanol and acetone addition on the CO_2 of the engine with 10% blending of MPWO

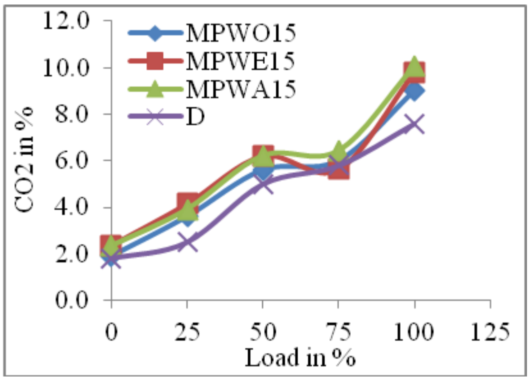

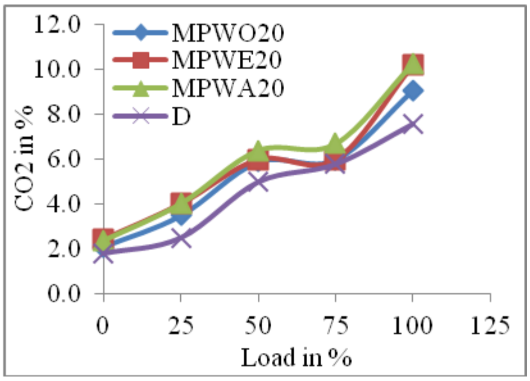

Figure 4.121 Effect of ethanol and acetone addition on the CO_2 of the engine with 15% blending of MPWO

Figure 4.122 Effect of ethanol and acetone addition on the CO_2 of the engine with 20% blending of MPWO

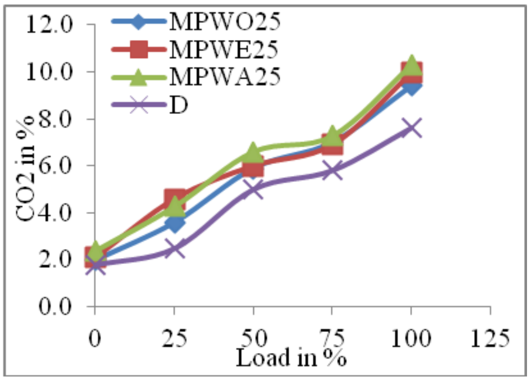

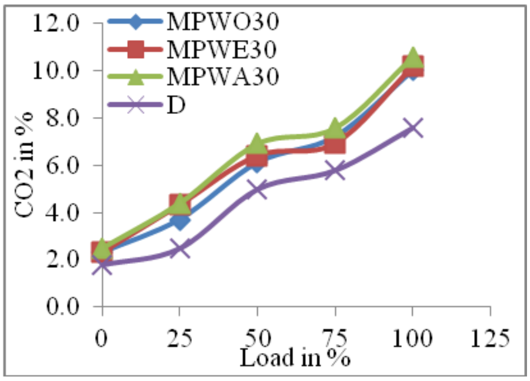

Figure 4.123 Effect of ethanol and acetone addition on the CO_2 of the engine with 25% blending of MPWO

Figure 4.124 Effect of ethanol and acetone addition on the CO_2 of the engines with 30% blending of MPWO

4.2.3 Unburnt hydrocarbon

Figure 4.125 shows the graph of load versus UHC for D, DA, and DE samples. The average reductions in UHC of DA and DE compared to D are 7.69% and 11.53%, respectively.

Figures 4.126 to 4.131 demonstrate the importance of combining two different methyl esters, MPO and MWO. Combining MWO's UHC in each blend can be improved with MPO. When MPWO and MPO are compared, the average increase in UHC of MPWO is 5.3%. When ethanol and acetone are added to RPO blends, they reduce UHC compared to biodiesel blends. Figures 4.132–4.137 depict a variational plot of load versus UHC for various blends of raw biodiesel, ethanol, and acetone. When ethanol and acetone are added to raw biodiesel blends, the UHC behavior is similar to that of biodiesel blends with variable engine load. Compared to diesel blends, the average UHC reductions of RPO, RPA, and RPE are 45.56%, 48.22%, and 51.10%, respectively.

Figures 4.138–4.143 depict a variational plot of load versus UHC for various biodiesel blends with and without ethanol and acetone additions. When ethanol (Shrivastava et al. 2021) and acetone are added to MPO biodiesel, UHC levels improve compared to MPO biodiesel blends. Furthermore, adding ethanol and acetone to raw biodiesel blends is analogous to adding ethanol and acetone to biodiesel blends with engine load variations. When compared to diesel, UHC reductions are 30.86%, 33.51%, and 39.37%

Compared to biodiesel blends, ethanol, and acetone (Dhanarasu et al. 2021), additions to MWO biodiesel improved engine UHC. Figures 4.144- 4.149 show plots of load versus UHC for various biodiesel blends containing MWO, ethanol, and acetone additions to MWO. All of the samples behave similarly at each ethanol/acetone blend. The average UHC deviation of an MWO, MWA, and MWE compared to diesel are 24.81%, 34.09%, and 39.85%, respectively.

Similarly, adding ethanol and acetone to MPWO biodiesel increased engine efficiency compared to biodiesel blends. Figures 4.150-4.155 show the engine's load versus UHC plot for various MPWO, ethanol, and acetone biodiesel blends. At each ethanol/acetone blend, all of the samples behave similarly. For ethanol and acetone-fueled biodiesel blends, the average deviation with UHC of an MPWO-fueled engine is 27.17%, 38.65%, and 37.71%, respectively.

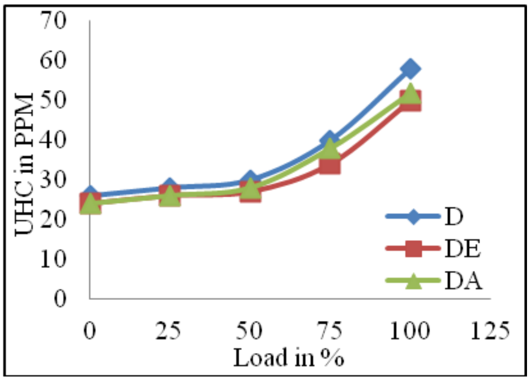

Figure 4.125 Inflence of ethanol and acetone blended diesel on the UHC of the engine

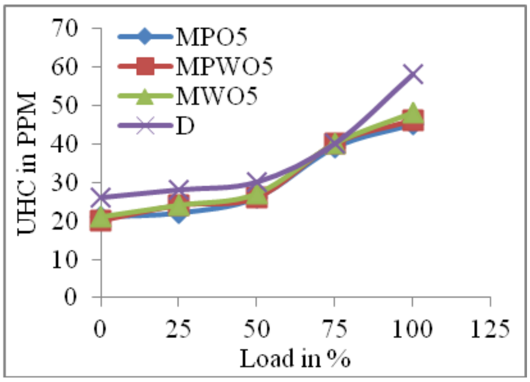

Figure 4.126 Effect of combining MPO and MWO on the UHC of the engine at 5% blending

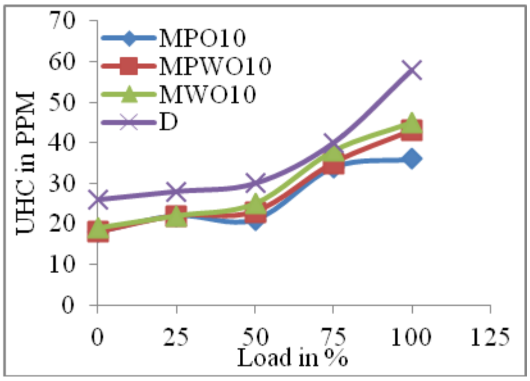

Figure 4.127 Effect of combining MPO and MWO on the UHC of the engine at 10% blending

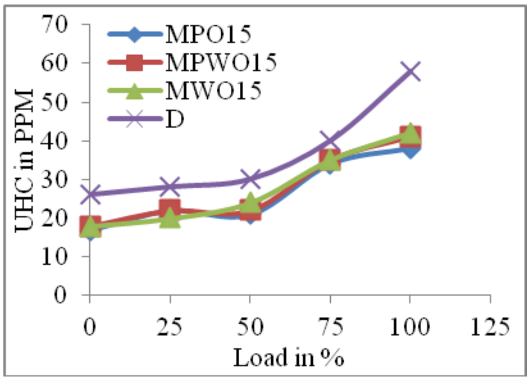

Figure 4.128 Effect of combining MPO and MWO on the UHC of the engine at 15% blending

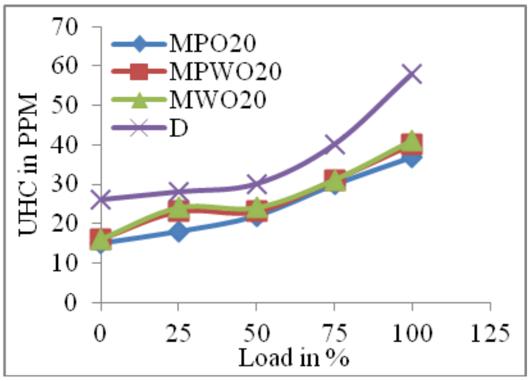

Figure 4.129 Effect of combining MPO and MWO on the UHC of the engine at 20% blending

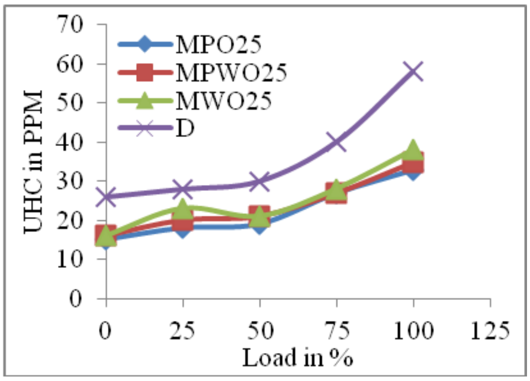

Figure 4.130 Effect of combining MPO and MWO esters on the UHC of the engine at 25% blending

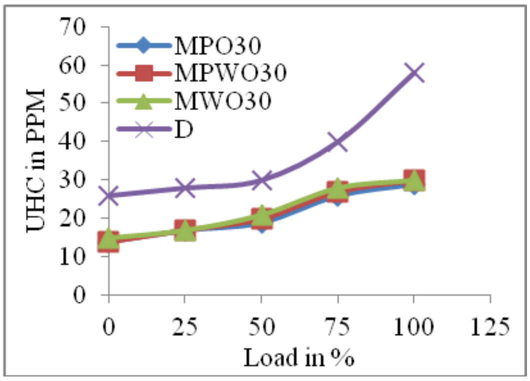

Figure 4.131 Effect of combining MPO and MWO on the UHC of the engine at 30% blending

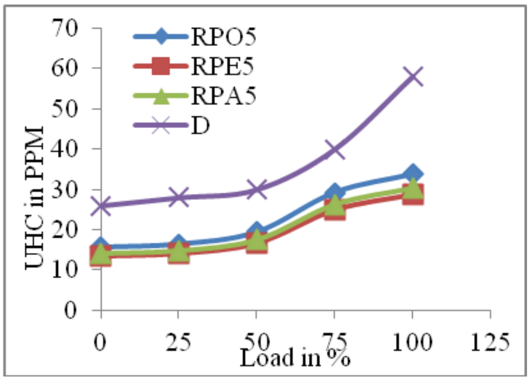

Figure 4.132 Effect of ethanol and acetone addition on the UHC of the engine with 5% blending of RPO

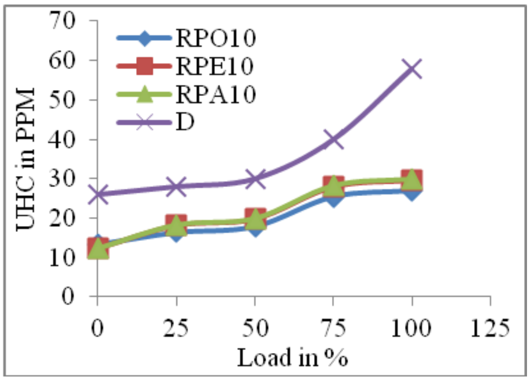

Figure 4.133 Effect of ethanol and acetone addition on the UHC of the engine with 10% blending of RPO

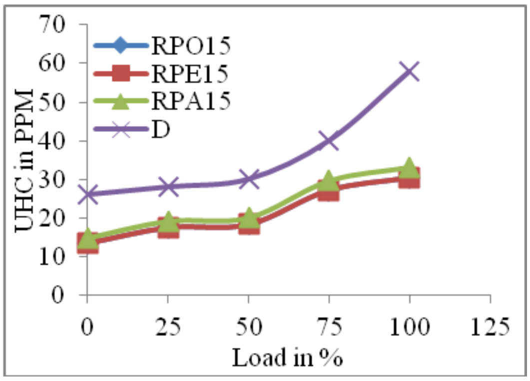

Figure 4.134 Effect of ethanol and acetone addition on the UHC of the engine with 15% blending of RPO

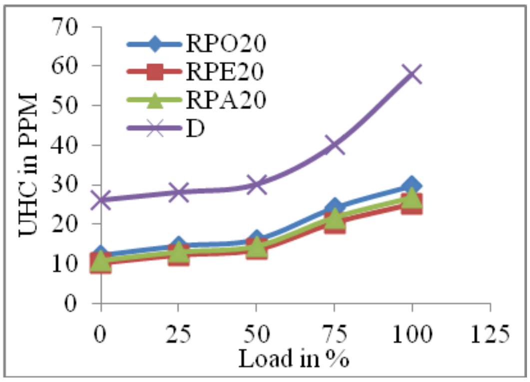

Figure 4.135 Effect of ethanol and acetone addition on the UHC of the engine with 20% blending of RPO

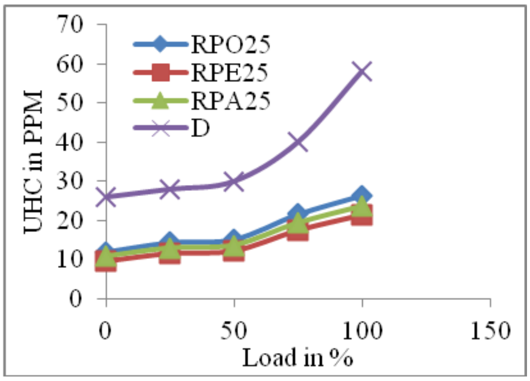

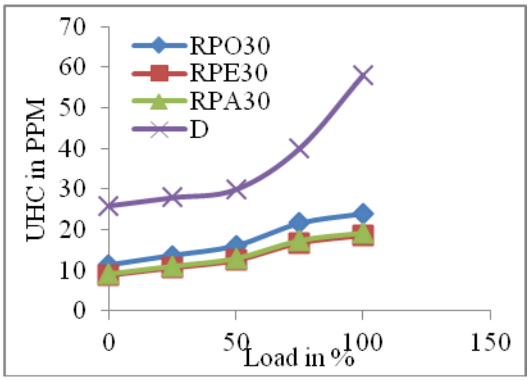

Figure 4.136 Effect of ethanol and acetone addition on the UHC of the engine with 25% blending of RPO

Figure 4.137 Effect of ethanol and acetone addition on the UHC of the engine with 30% blending of RPO

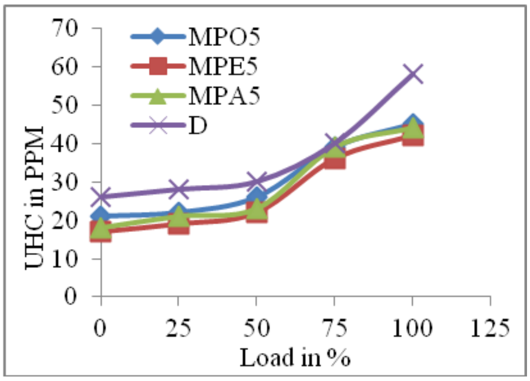

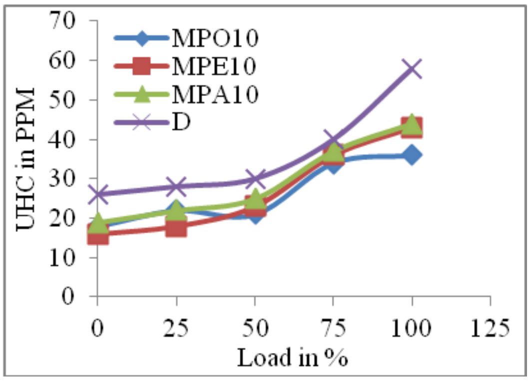

Figure 4.138 Effect of ethanol and acetone addition on the UHC of the engine with 5% blending of MPO

Figure 4.139 Effect of ethanol and acetone addition on the UHC of the engine with 10% blending of MPO

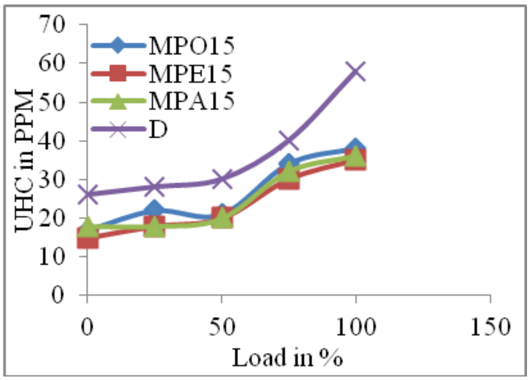

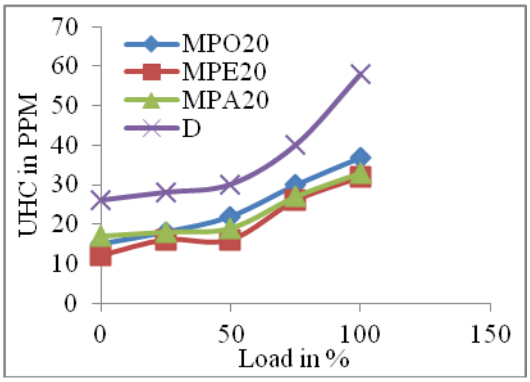

Figure 4.140 Effect of ethanol and acetone addition on the UHC of the engine with 15% blending of MPO

Figure 4.141 Effect of ethanol and acetone addition on the UHC of the engine with 20% blending of MPO

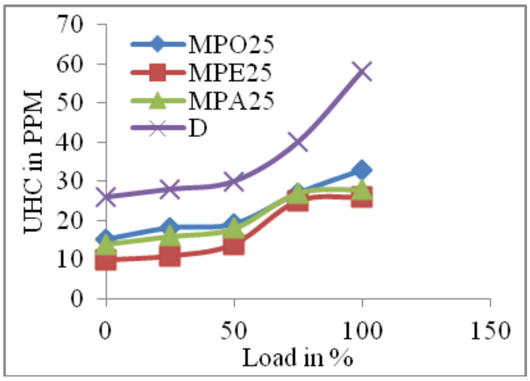

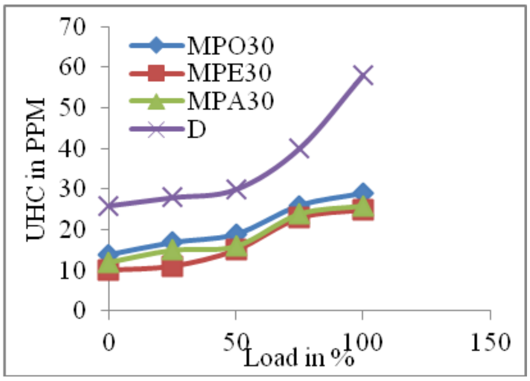

Figure 4.142 Effect of ethanol and acetone addition on the UHC of the engine with 25% blending of MPO

Figure 4.143 Effect of ethanol and acetone addition on the UHC of the engine with 30% blending of MPO

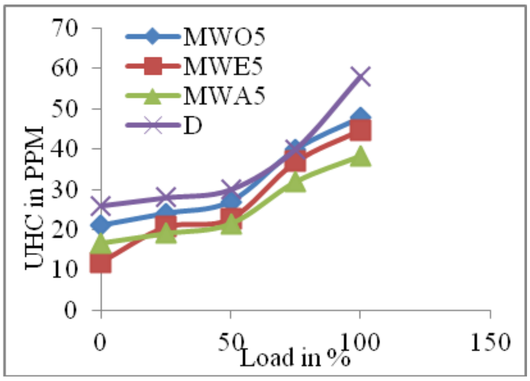

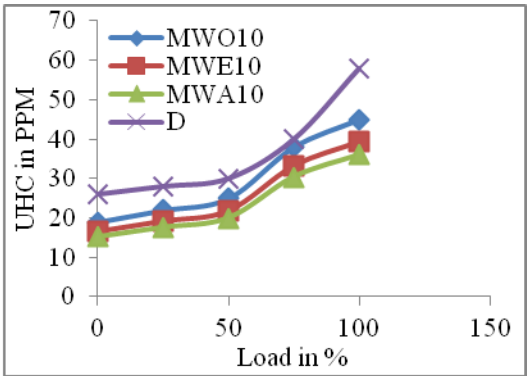

Figure 4.144 Effect of ethanol and acetone addition on the UHC of the engine with 5% blending of MWO

Figure 4.145 Effect of ethanol and acetone addition on the UHC of the engine with 10% blending of MWO

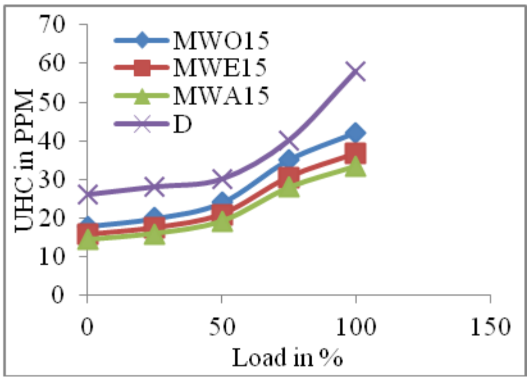

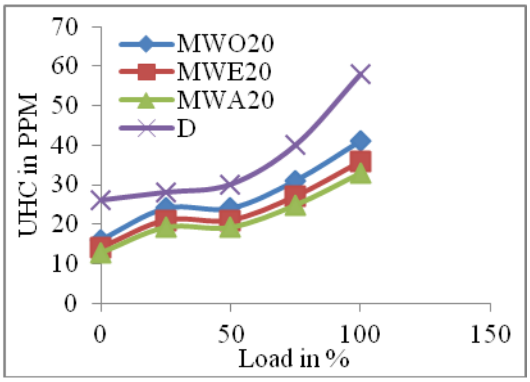

Figure 4.146 Effect of ethanol and acetone addition on the UHC of the engine with 15% blending of MWO

Figure 4.147 Effect of ethanol and acetone addition on the UHC of the engine with 20% blending of MWO

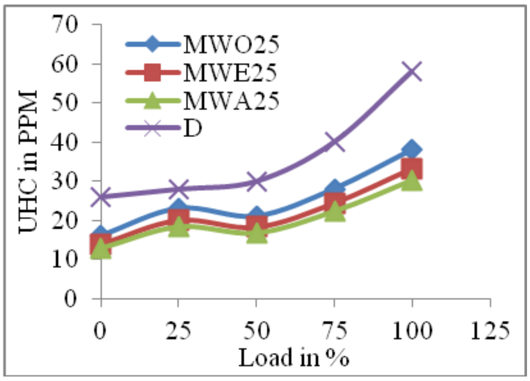

Figure 4.148 Effect of ethanol and acetone addition on the UHC of the engine with 25% blending of MWO

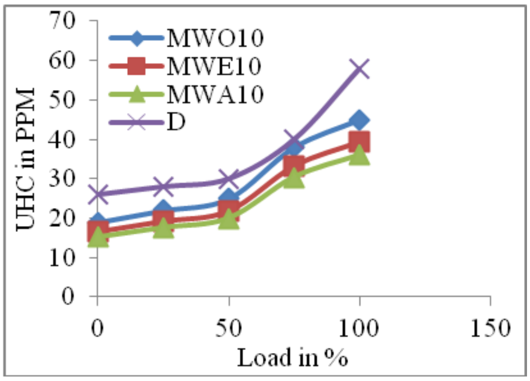

Figure 4.149 Effect of ethanol and acetone addition on the UHC of the engines with 30% blending of MWO

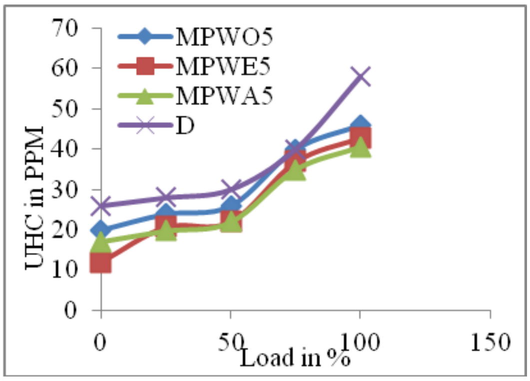

Figure 4.150 Effect of ethanol and acetone addition on the UHC of the engine with 5% blending of MPWO

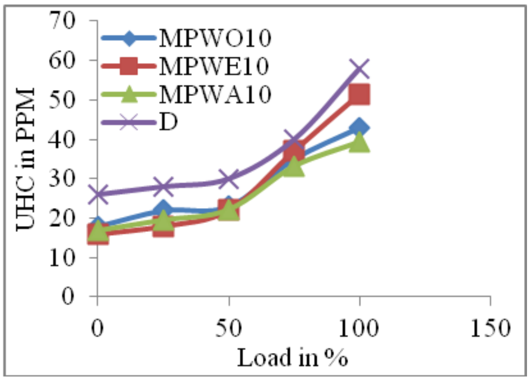

Figure 4.151 Effect of ethanol and acetone addition on the UHC of the engine with 10% blending of MPWO

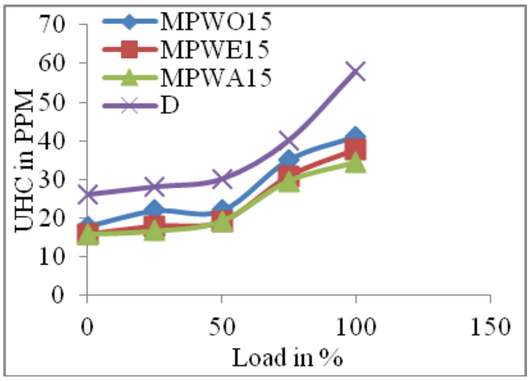

Figure 4.152 Effect of ethanol and acetone addition on the UHC of the engine with 15% blending of MPWO

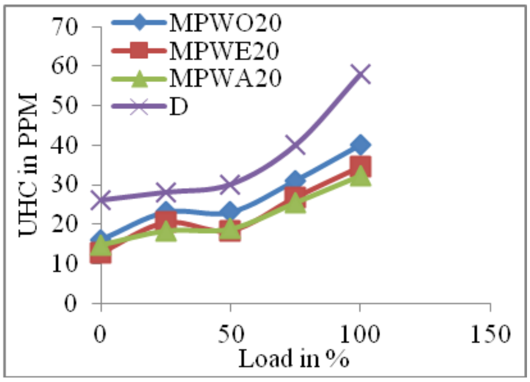

Figure 4.153 Effect of ethanol and acetone addition on the UHC of the engine with 20% blending of MPWO

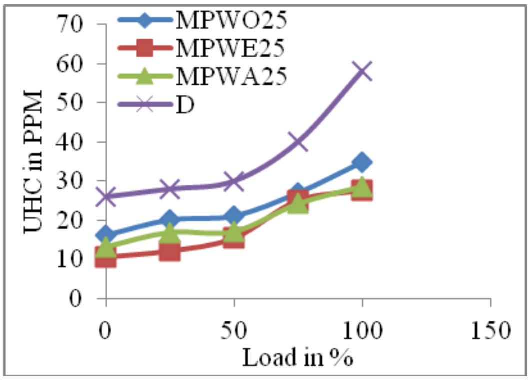

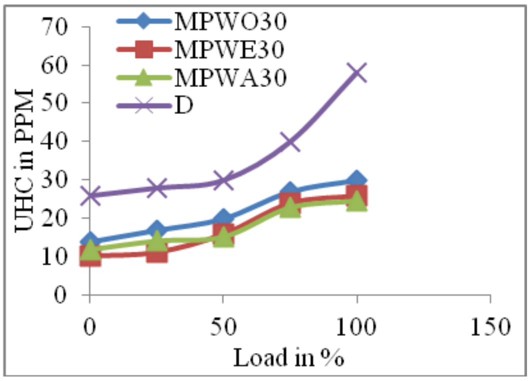

Figure 4.154 Effect of ethanol and acetone addition on the UHC of the engine with 25% blending of MPWO

Figure 4.155 Effect of ethanol and acetone addition on the UHC of the engines with 30% blending of MPWO

UHC emissions decrease with increased biodiesel blending (Petersen et al. 2018). A sample can emit less UHC only if a complete combustion process exists. Due to excess oxygen in the blended samples compared to diesel, the combustion process emits less UHC (Ogunkunle and Ahmed 2021). Similar observations in the trend are also found with the base biodiesel blends. The addition of ethanol and acetone (Dhanarasu et al. 2021) has also contributed to the reduction in the UHC; the reason behind this is the oxygen supply during combustion. However, ethanol can reduce UHC emissions better as compared to acetone.

Gaseous hydrocarbons are found in the relatively thick low-temperature boundary layer along the cylinder wall, and the apertures are the leading cause of hydrocarbon emissions. Generally, the addition of biodiesel reduces UHC emissions. Further addition of acetone and ethanol (Khalife et al. 2017) reduces UHC emissions.

4.2.4 Nitrous oxide

Figure 4.156 shows the graph of load versus NOx for D, DA, and DE samples. The average reductions in NOx of DA and DE (Khalife et al. 2017) compared to D are 35.34% and 43.75%, respectively.

Figures 4.157-4.162 demonstrate the importance of combining two different methyl esters, MPO and MWO. NOx of MPO in each blend can be improved by combining it with MWO. When MPWO and MPO are compared, the average NOX achievement is 9.74%.

When ethanol and acetone are added to RPO blends, they reduce NO_X compared to biodiesel blends. Figures 4.163–4.168 depict a variational plot of load versus NO_X for various raw biodiesel, ethanol, and acetone blends. When ethanol and acetone are added to raw biodiesel blends, the NO_X behaviour is similar to that of biodiesel blends with variable engine load. Compared to raw biodiesel blends, NO_X reductions are 144.05%, 163.97%, and 172.68%, respectively.

Figures 4.169–4.174 depict a variational plot of NOx for various raw biodiesel blends with and without ethanol and acetone additions. When ethanol (Nair et al. 2021) and acetone are added to MPO biodiesel, NOx levels improve compared to MPO biodiesel blends. Furthermore, adding ethanol and acetone to raw biodiesel blends is analogous to adding ethanol and acetone to biodiesel blends with engine load variations. Unlike diesel blends, NOX reductions of MPO, MPA, and MPE are 107.90%, 117.39%, and 122.45%, respectively. Compared to biodiesel blends, ethanol, and acetone.

Compared to biodiesel blends, ethanol and acetone additions to MWO biodiesel improved engine NO_X. Figures 4.175-4.180 show load versus NO_X plots for various biodiesel blends containing MWO, ethanol, and acetone. All of the samples behave similarly at each ethanol/acetone blend. The average NO_X deviation of an MWO, MWA, and MWE-powered engine compared to diesel is 77.4%, 86.27%, and 98.21%, respectively.

Similarly, adding ethanol and acetone to MPWO biodiesel increased engine efficiency compared to biodiesel blends. Figures 4.181-4.186 show the engine's load versus NO_X plot for various MPWO, ethanol, and acetone biodiesel blends. At each ethanol/acetone blend, all of the samples behave similarly. The average deviation with NOX compared to diesel for MPWO, MPWA, and MPWE-powered engines is 93.03%, 98.45%, and 99.25%, respectively.

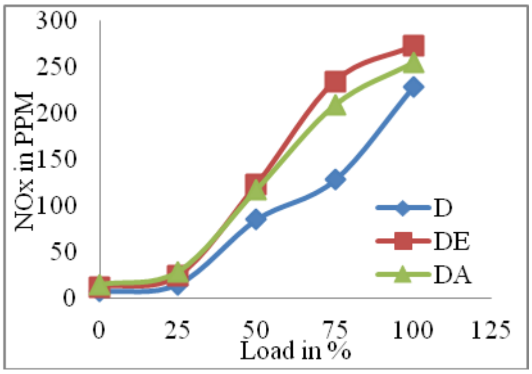

Figure 4.156 Effect of ethanol and acetone blended diesel on the NOx of the engine

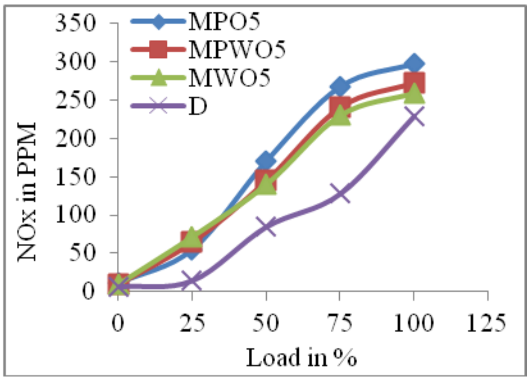

Figure 4.157 Effect of combining MPO and MWO on the NOx of the engine at 5% blending

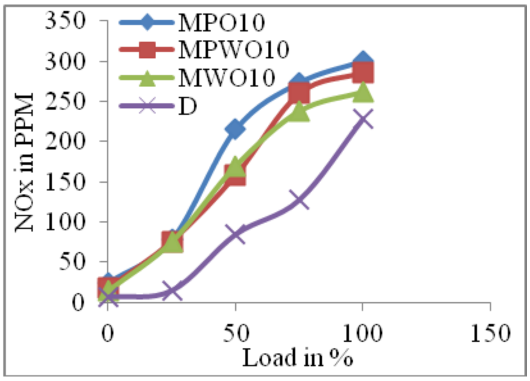

Figure 4.158 Effect of combining MPO and MWO on the NOx of the engine at 10% blending

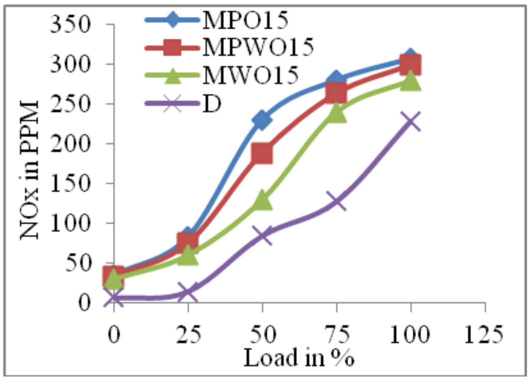

Figure 4.159 Effect of combining MPO and MWO on the NOx of the engine at 15% blending

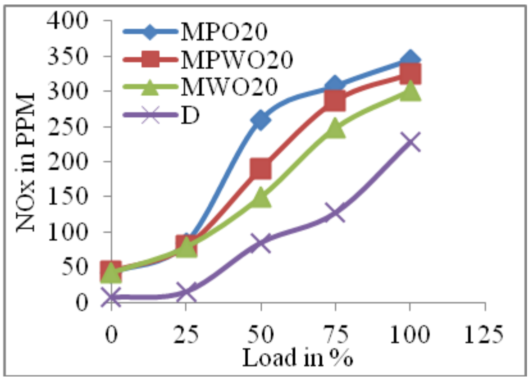

Figure 4.160 Effect of combining MPO and MWO on the NOx of the engine at 20% blending

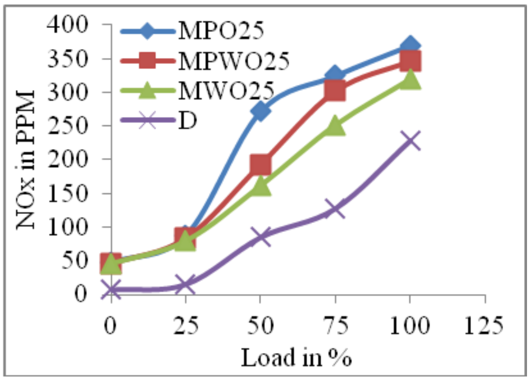

Figure 4.161 Effect of combining MPO and MWO esters on the NOx of the engine at 25% blending

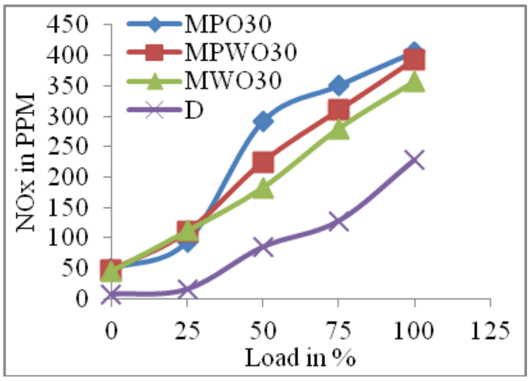

Figure 4.162 Effect of combining MPO and MWO on the NOx of the engine at 30% blending

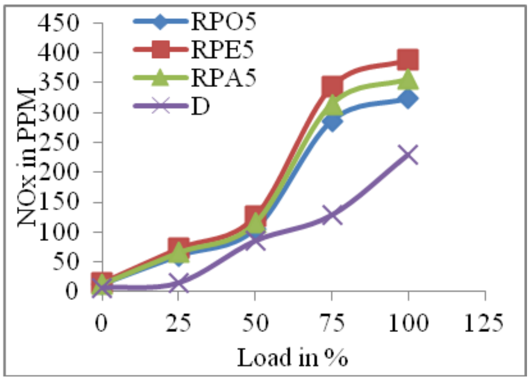

Figure 4.163 Effect of ethanol and acetone addition on the NOx of the engine with 5% blending of RPO

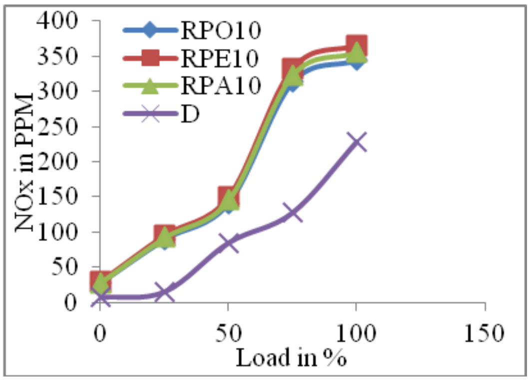

Figure 4.164 Effect of ethanol and acetone addition on the NOx of the engine with 10% blending of RPO

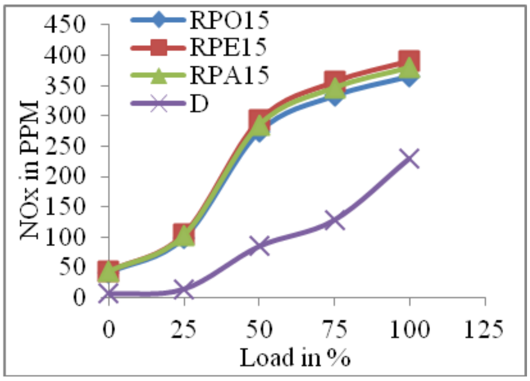

Figure 4.165 Effect of ethanol and acetone addition on the NOx of the engine with 15% blending of RPO

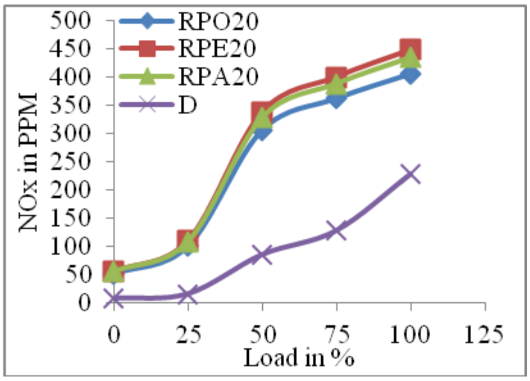

Figure 4.166 Effect of ethanol and acetone addition on the NOx of the engine with 20% blending of RPO

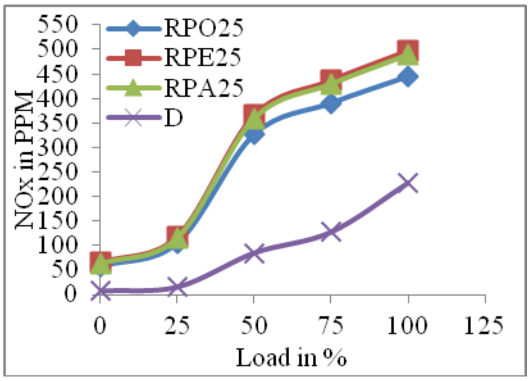

Figure 4.167 Effect of ethanol and acetone addition on the NOx of the engine with 25% blending of RPO

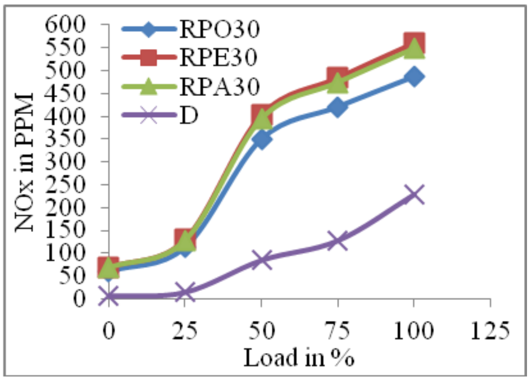

Figure 4.168 Effect of ethanol and acetone addition on the NOx of the engine with 30% blending of RPO

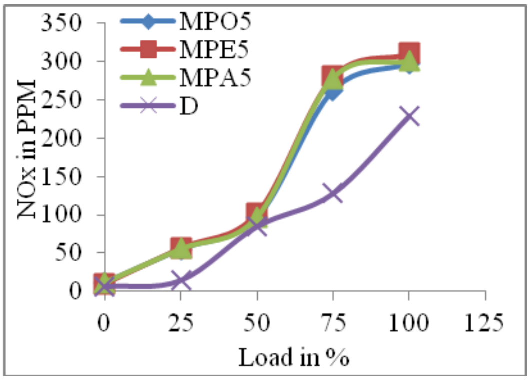

Figure 4.169 Effect of ethanol and acetone addition on the NOx of the engine with 5% blending of MPO

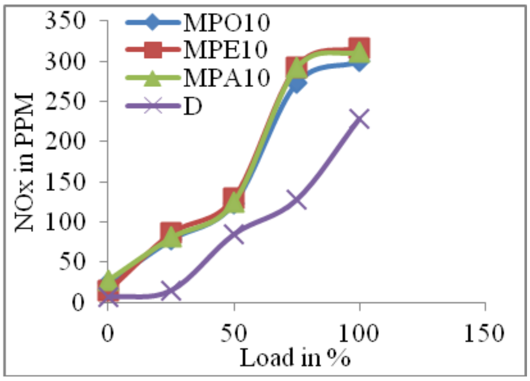

Figure 4.170 Effect of ethanol and acetone addition on the NOx of the engine with 10% blending of MPO

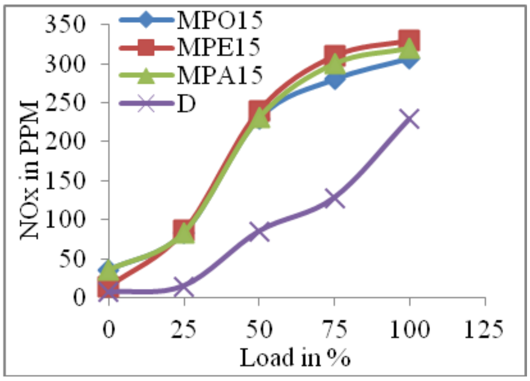

Figure 4.171 Effect of ethanol and acetone addition on the NOx of the engine with 15% blending of MPO

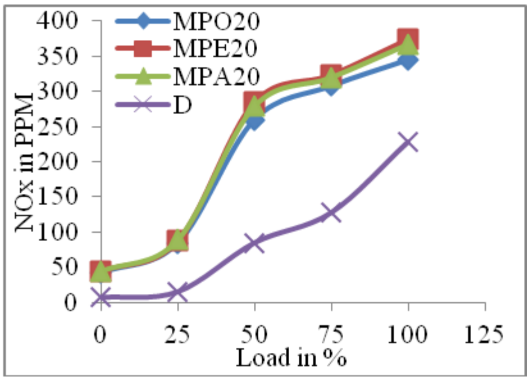

Figure 4.172 Effect of ethanol and acetone addition on the NOx of the engine with 20% blending of MPO

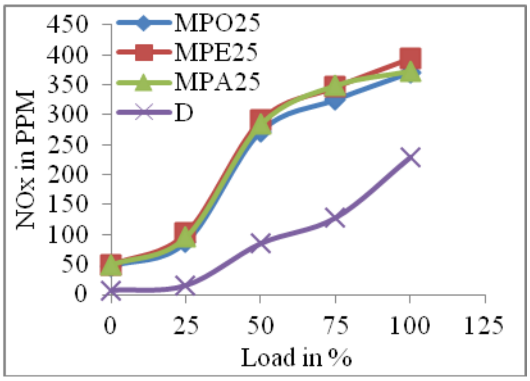

Figure 4.173 Effect of ethanol and acetone addition on the NOx of the engine with 25% blending of MPO

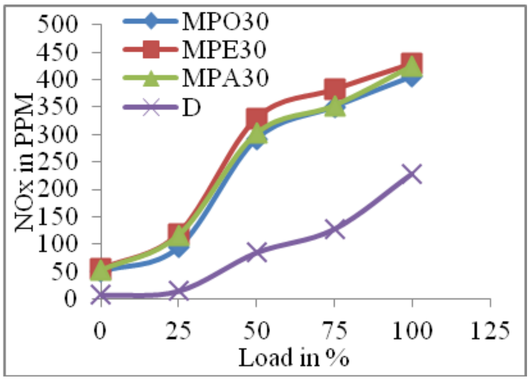

Figure 4.174 Effect of ethanol and acetone addition on the NOx of the engine with 30% blending of MPO

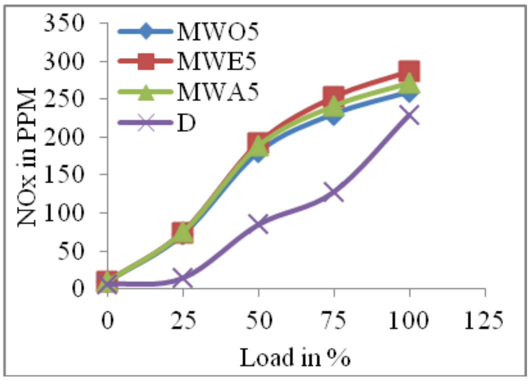

Figure 4.175 Effect of ethanol and acetone addition on the NOx of the engine with 5% blending of MWO

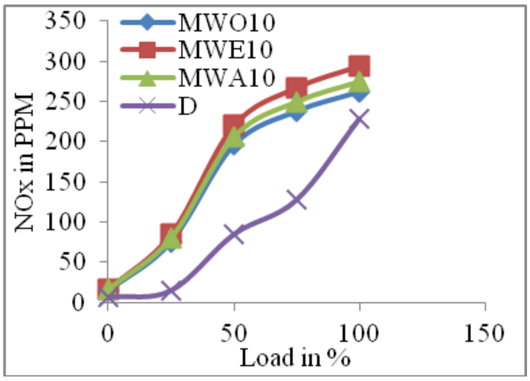

Figure 4.176 Effect of ethanol and acetone addition on the NOx of the engine with 10% blending of MWO

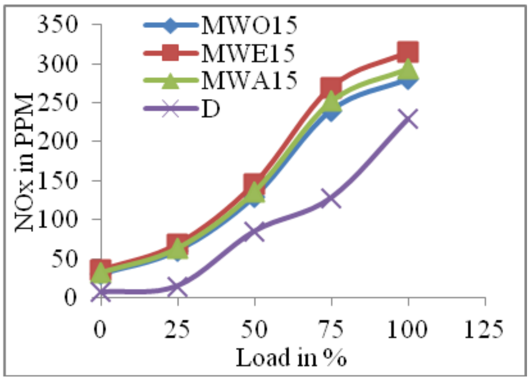

Figure 4.177 Effect of ethanol and acetone addition on the NOx of the engine with 15% blending of MWO

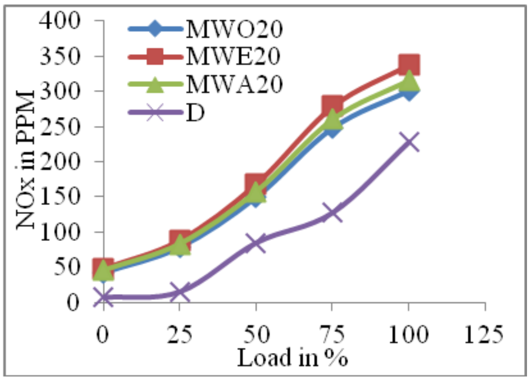

Figure 4.178 Effect of ethanol and acetone addition on the NOx of the engine with 20% blending of MWO

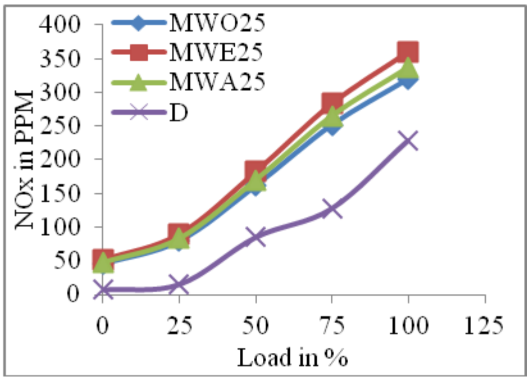

Figure 4.179 Effect of ethanol and acetone addition on the NOx of the engine with 25% blending of MWO

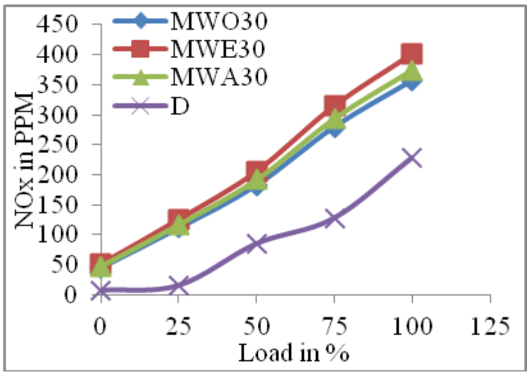

Figure 4.180 Effect of ethanol and acetone addition on the NOx of the engines with 30% blending of MWO

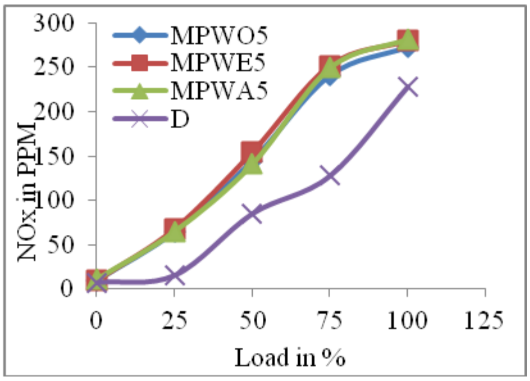

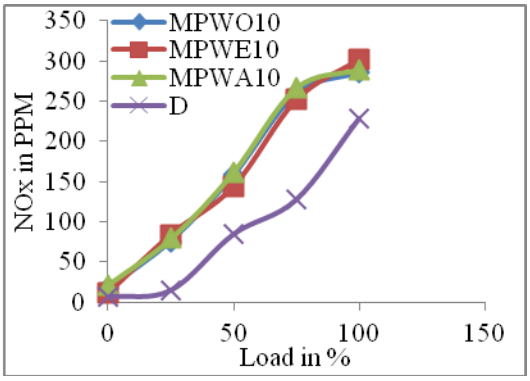

Figure 4.181 Effect of ethanol and acetone addition on the NOx of the engine with 5% blending of MPWO

Figure 4.182 Effect of ethanol and acetone addition on the NOx of the engine with 10% blending of MPWO

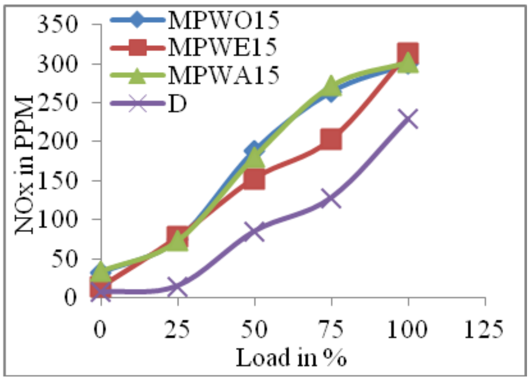

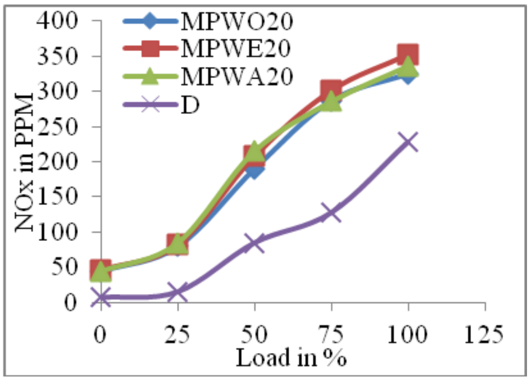

Figure 4.183 Effect of ethanol and acetone addition on the NOx of the engine with 15% blending of MPWO

Figure 4.184 Effect of ethanol and acetone addition on the NOx of the engine with 20% blending of MPWO

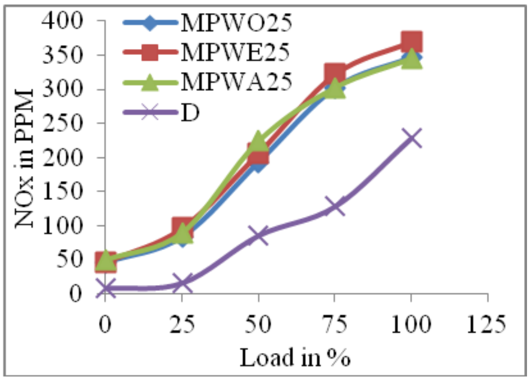

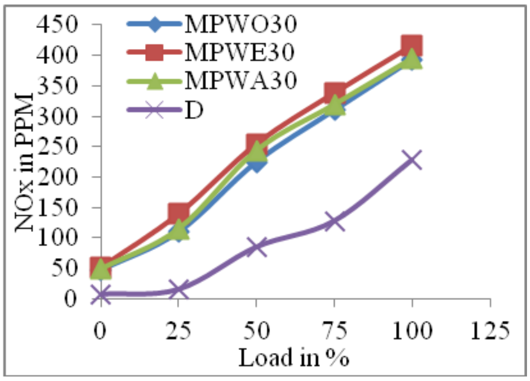

Figure 4.185 Effect of ethanol and acetone addition on the NOx of the engine with 25% blending of MPWO

Figure 4.186 Effect of ethanol and acetone addition on the NOx of the engines with 30% blending of MPWO

NOx emissions increase with an increase in the blend percentage of biodiesel. Oxygen in biodiesel fuel results in increased heat release during combustion, which significantly contributes to increased NOx emissions (Palash et al. 2013). incremental ethanol additions have also shown NOx increments (Datta and Mandal 2016; Maleney et al. 2017). The increment is because it adds oxygen content to the fuel, increasing the combustion temperature and resulting in higher NOx. The addition of acetone shows similar behaviour (Dhanarasu et al. 2021).

CHAPTER 5

STATISTICAL ANALYSIS OF PERFORMANCE AND EMISSIONS OF THE ENGINE

5.1 Analysis of variance (ANOVA) analysis and Multi Linear Regression Modelling

An ANOVA test is a way to find out if survey or experiment results are significant. In other words, they help you to figure out if you need to reject the null hypothesis or accept the alternate hypothesis .

ANOVA and MLRM are carried out to predict the engine's performance and emission parameters. The input parameters considered for this study are blend percentage (B), load (L), the mass of fuel consumed (MF), density (D), kinematic viscosity (KV) and calorific value (CV) of the fuel. A higher order model is developed to improve the model's accuracy. The cross-products considered are load- mass of fuel consumed and blend-mass of fuel consumed. The prediction models are developed at a confidence interval of 95%. Minitab V19 is used to carry out ANOVA analysis and MLR modelling.

The models that are developed performance is rated based on their R- square values. It is found that the R-squared values in predicting all the parameters are above 70%. The Most significant parameter contributing to the output variable's variation is decided based on the P- Values (≤ 0.05). ANOVA analysis is tabulated, and the significant parameters are identified based on the P-Values. The contribution of each parameter in the development of the model is also represented in the form of a pie chart.

A regression equation and performance and the effect of each parameter are described under the regression analysis. The T-value signifies the Effect of the parameter. The performance of the model is described based on the R-squared value. A graph of Predicted versus experimental is drawn for each output. A regression model is also developed to predict the predicted value based on the experimental value.

5.1.1 ANOVA analysis for the BTE of the Engine

Table 5.1 represents the results of the ANOVA analysis for BTE. All the input parameters are significant, with P-values less than 0.05, except for KV. Figure 5.1

shows that the most influential parameter for BTE is load, followed by the mass of fuel consumed, whose contributions are 61.22% and 25%.

Table 5.1 ANOVA analysis for predicting the BTE of the engine

Source	DF	Adj SS	Adj MS	F-Value	P-Value
Regression	8	33631.4	4203.9	739.15	0.000
B in %	1	234.1	234.1	41.16	0.000
L in %	1	17125.3	17125.3	3011.03	0.000
D in g/cc	1	141.7	141.7	24.91	0.000
KV in Cst	1	8.3	8.3	1.45	0.229
CV in MJ/Kg	1	44.3	44.3	7.79	0.006
MF in Kg/s	1	771.5	771.5	135.65	0.000
B in %*MF in Kg/s	1	424.9	424.9	74.70	0.000
L in %*MF in Kg/s	1	334.6	334.6	58.83	0.000
Error	366	2081.6	5.7		
Total	374				

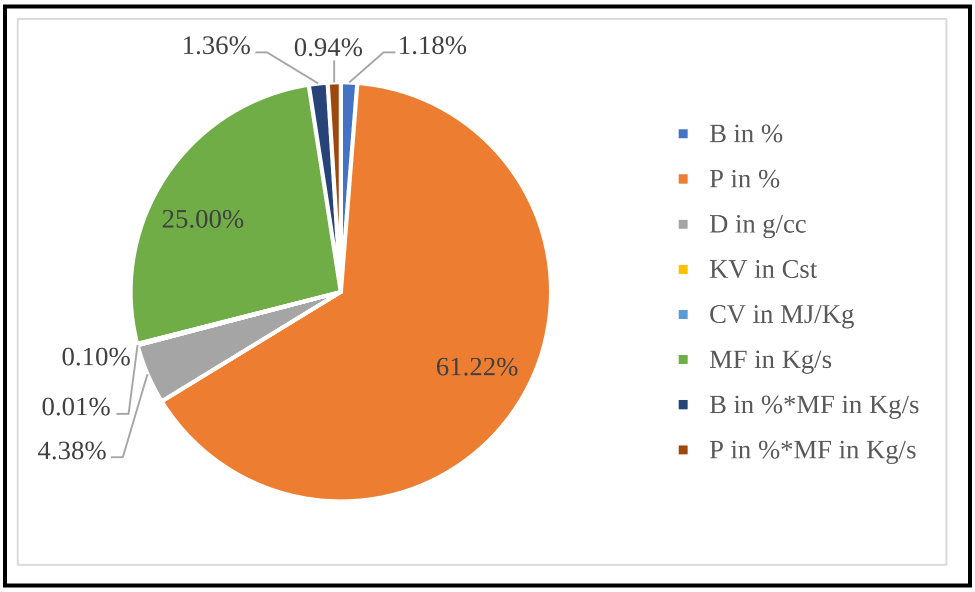

Figure 5.1 Percentage contribution of input variables on the BTE of the engine

5.1.2 ANOVA analysis for the BSEC of the Engine

Table 5.2 represents the results of the ANOVA analysis for BSEC. All the input parameters are significant, with P-values less than 0.05, except for KV and CV.

From Figure 5.2, the most influential parameter for BTE is load, followed by the mass of fuel consumed, whose contributions are 50.98% and 17.65%.

Table 5.2 ANOVA analysis for predicting the BSEC of the engine

Source	DF	Adj SS	Adj MS	F-Value	P-Value
Regression	8	658942	82368	131.42	0.000
B in %	1	8077	8077	12.89	0.000
L in %	1	324191	324191	517.27	0.000
D in g/cc	1	3260	3260	5.20	0.023
KV in Cst	1	24	24	0.04	0.846
CV in MJ/Kg	1	1601	1601	2.55	0.111
MF in Kg/s	1	7074	7074	11.29	0.001
B in %*MF in Kg/s	1	17802	17802	28.40	0.000
L in %*MF in Kg/s	1	18121	18121	28.91	0.000
Error	366	229387	627		
Total	374				

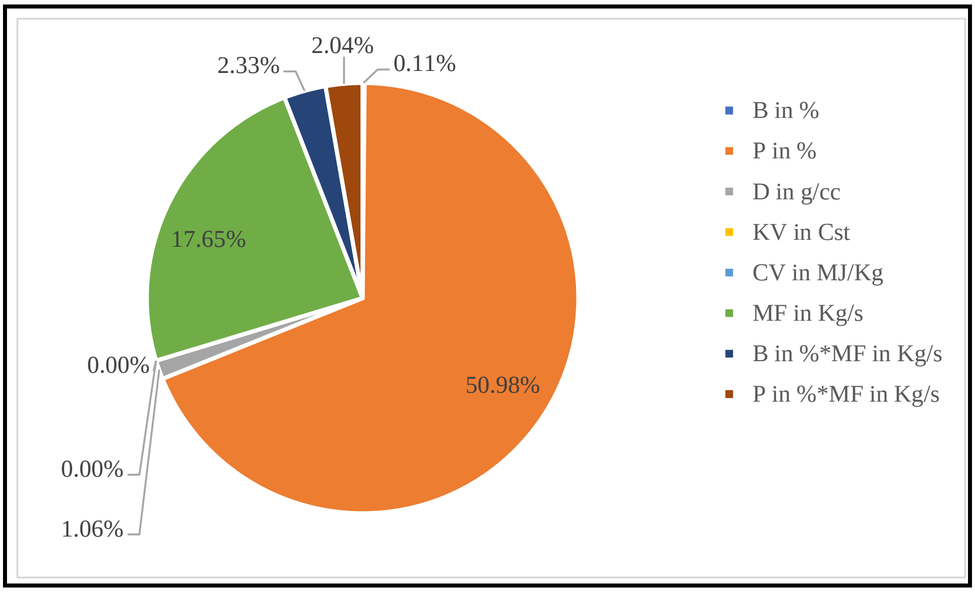

Figure 5.2 Percentage contribution of input variables on the BSEC of the engine

5.1.3 ANOVA analysis for the CO of the Engine

Table 5.3 represents the results of the ANOVA analysis for CO. All the input parameters are significant, with P-values less than 0.05 except for CV and D.

From Figure 5.3, The most influential parameter for CO is load, followed by the Product of load and mass of fuel consumed, and the mass of fuel consumed, whose contributions are 60.37%, 9.80%, and 8.3%, respectively.

Table 5.3 ANOVA analysis for predicting the CO of the engine

Source	**DF**	**Adj SS**	**Adj MS**	**F-Value**	**P-Value**
Regression	8	16.4152	2.05191	357.48	0.000
B in %	1	0.1267	0.12670	22.07	0.000
L in %	1	0.1180	0.11804	20.57	0.000
D in g/cc	1	0.0197	0.01973	3.44	0.065
KV in Cst	1	0.0857	0.08571	14.93	0.000
CV in MJ/Kg	1	0.0076	0.00761	1.33	0.250
MF in Kg/s	1	0.0847	0.08470	14.76	0.000
B in %*MF in Kg/s	1	1.1138	1.11383	194.05	0.000
L in %*MF in Kg/s	1	1.8140	1.81400	316.03	0.000
Error	366	2.1008	0.00574		
Total	374				

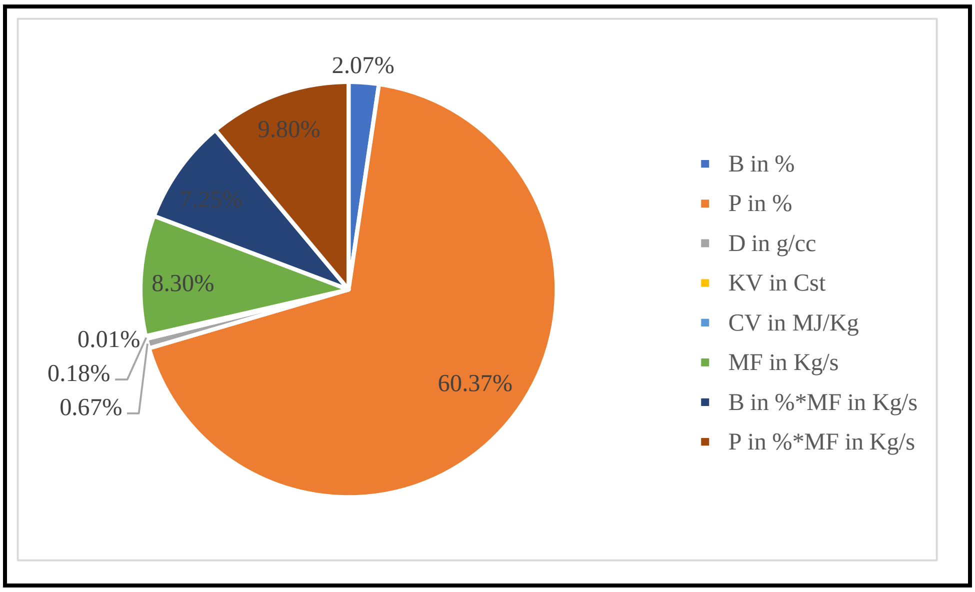

Figure 5.3 Percentage contribution of input variables on the CO of the engine

5.1.4 ANOVA analysis for the CO_2 of the Engine

Table 5.3 represents the results of the ANOVA analysis for CO_2. All the input parameters are significant, with P-values less than 0.05 except for KV, MF, and P*MF. From Figure 5.4, the most influential parameter for CO_2 is load, followed by the blend, whose contributions are 82.42% and 4.83%, respectively.

Table 5.4 ANOVA analysis for predicting the CO_2 of the engine

Source	DF	Adj SS	Adj MS	F-Value	P-Value
Regression	8	2879.78	359.973	423.66	0.000
B in %	1	6.15	6.146	7.23	0.007
L in %	1	105.64	105.644	124.33	0.000
D in g/cc	1	5.95	5.947	7.00	0.009
KV in Cst	1	2.64	2.643	3.11	0.079
CV in MJ/Kg	1	4.86	4.856	5.72	0.017
MF in Kg/s	1	0.05	0.047	0.06	0.814
B in %*MF in Kg/s	1	15.17	15.172	17.86	0.000
L in %*MF in Kg/s	1	0.42	0.420	0.49	0.482
Error	366	310.98	0.850		
Total	374				

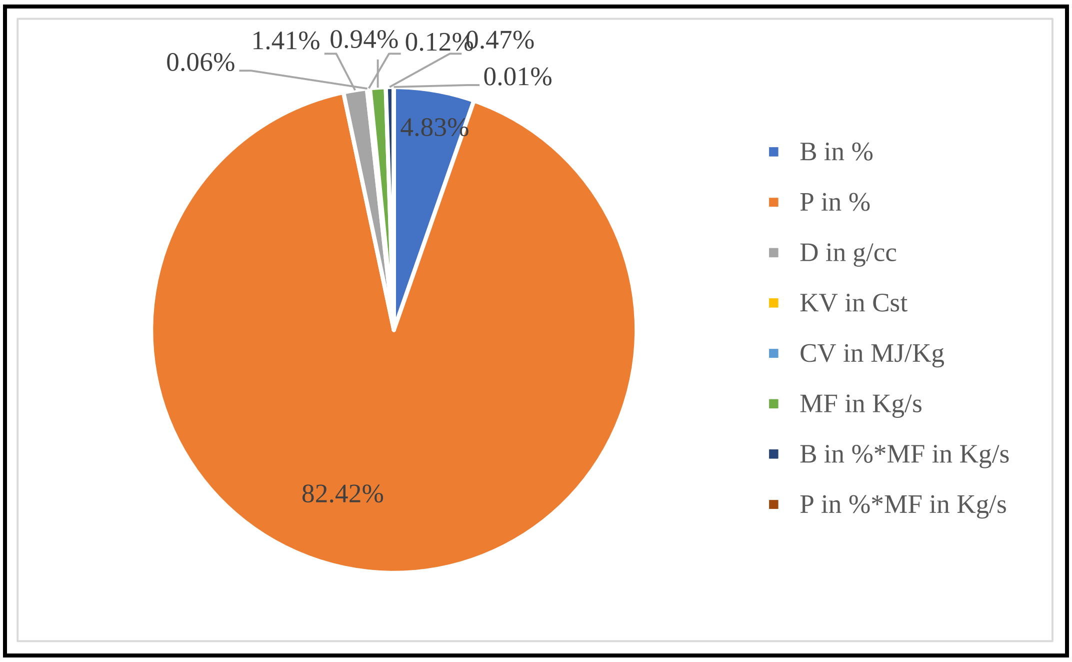

Figure 5.4 Percentage contribution of input variables on the CO_2 of the engine

5.1.5 ANOVA analysis for the UHC of the Engine

Table 5.3 represents the results of the ANOVA analysis for UHC. All the input parameters are significant, with P-values less than 0.05, except for D and CV. From Figure 5.4, the most influential parameter for UHC is load, followed by blend, whose contributions are 61.48% and 15.05%, respectively.

Table 5.5 ANOVA analysis for predicting the UHC of the engine

Source	DF	Adj SS	Adj MS	F-Value	P-Value
Regression	8	25013.0	3126.62	237.00	0.000
B in %	1	238.4	238.42	18.07	0.000
L in %	1	1332.2	1332.22	100.98	0.000
D in g/cc	1	45.9	45.91	3.48	0.063
KV in Cst	1	144.0	143.97	10.91	0.001
CV in MJ/Kg	1	40.8	40.76	3.09	0.080
MF in Kg/s	1	254.9	254.87	19.32	0.000
B in %*MF in Kg/s	1	355.4	355.42	26.94	0.000
P in %*MF in Kg/s	1	689.6	689.59	52.27	0.000
Error	366	4828.5	13.19		
Total	374				

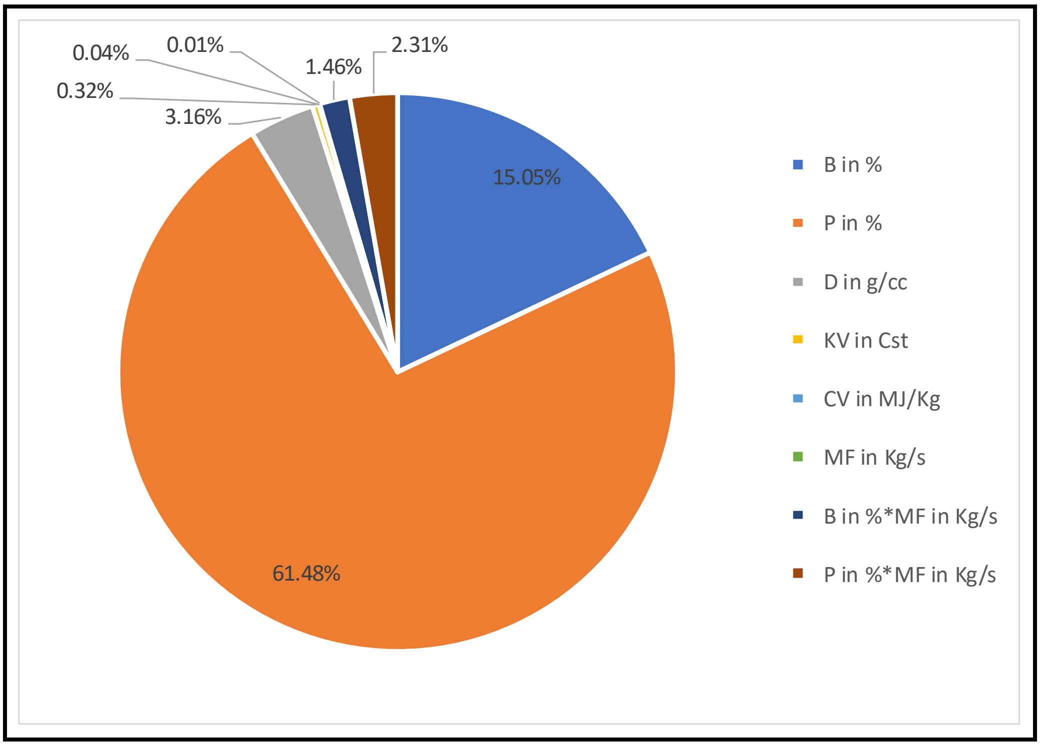

Figure 5.5 Percentage contribution of input variables on the UHC of the engine

5.1.6 ANOVA analysis for the NOx of the Engine

Table 5.6 represents the results of the ANOVA analysis for NOx. All the input parameters are significant, with P-values less than 0.05, except for CV.

From Figure 5.3, The most influential parameter for NOx is load, followed by the Product of load and blend, whose contributions are 80.96% and 6.63%, respectively.

Table 5.6 ANOVA analysis for predicting the NOx of the engine

Source	DF	Adj SS	Adj MS	F-Value	P-Value
Regression	8	6147178	768397	633.03	0.000
B in %	1	14767	14767	12.17	0.001
L in %	1	260724	260724	214.79	0.000
D in g/cc	1	5924	5924	4.88	0.028
KV in Cst	1	11992	11992	9.88	0.002
CV in MJ/Kg	1	3822	3822	3.15	0.077
MF in Kg/s	1	56013	56013	46.15	0.000
B in %*MF in Kg/s	1	28939	28939	23.84	0.000
L in %*MF in Kg/s	1	79393	79393	65.41	0.000
Error	366	444265	1214		
Total	374				

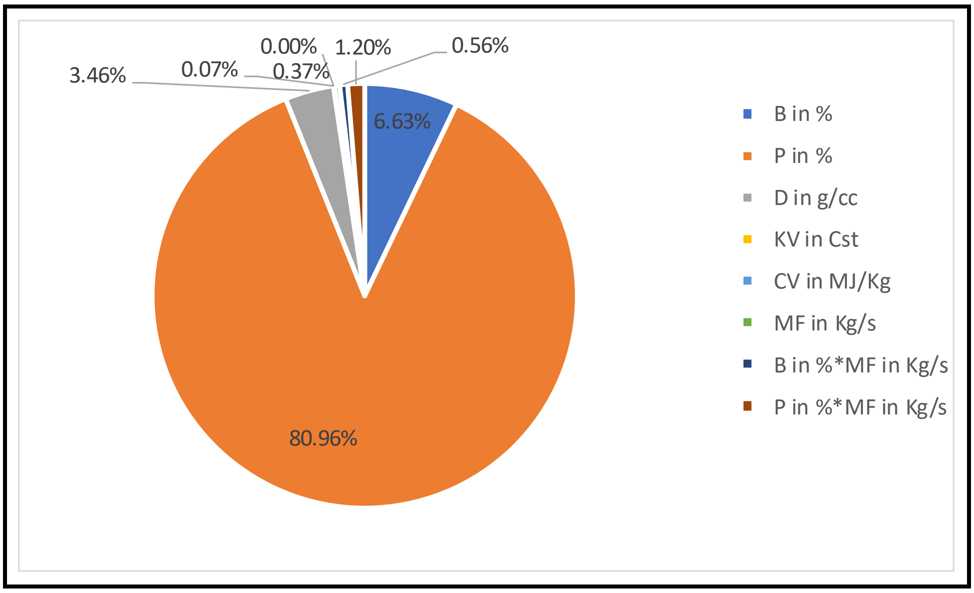

Figure 5.6 Percentage contribution of input variables on the NOX of the engine

5.1.7 Development of regression model to predict the BTE of engine

A regression equation and performance and the Effect of each parameter are described under the regression analysis. The T-value signifies the Effect of the parameter. The performance of the model is described based on the R-squared value. A graph of Predicted versus experimental is drawn for each output. A Regression model is also developed to predict the predicted value based on the experimental value and shown in Figures 5.7 to 5.12.

The regression model is developed to predict the BTE of the engine and is represented as Equation 5.1.

BTE (%) = 10.6-0.2786B + 0.6907L +36.16D +1.34 KV -0.619CV -100784MF +969B in % *MF -399L*MF ………………………… (5.1)

Where, BTE is Brake thermal efficiency in % B is blending in %, L is Load in %, D is Density in g/cc, KV is kinematic viscosity in Cst, CV is calorific value in MJ/Kg, MF is mass of fuel consumed in Kg/s

Table 5.7 shows the performance of the regression model developed. The model's performance is around 94.17% in predicting the BTE of the engine. From Table 5.8, it is clear that the T-values of B, CV, and MF have negative correlations in the development of the model. The other parameters, P, D, and KV correlate positively. Figure 5.7 illustrates the plots of predicted BTE versus experimental BTE.

Table 5.7 Model summary for predicting the BTE of the engine

S	R-sq	R-sq(adj)	R-sq(pred)
2.38486	94.17%	94.04%	93.74%

Table 5.8 Regression analysis results for predicting the BTE of the engine

Term	Coef	SE Coef	T-Value	P-Value
Constant	10.6	11.5	0.92	0.358
B in %	-0.2786	0.0434	-6.42	0.000
L in %	0.6907	0.0126	54.87	0.000
D in g/cc	36.16	7.24	4.99	0.000
KV in Cst	1.34	1.11	1.21	0.229
CV in MJ/Kg	-0.619	0.222	-2.79	0.006
MF in Kg/s	-100784	8653	-11.65	0.000
B in %*MF in Kg/s	969	112	8.64	0.000
L in %*MF in Kg/s	-399.0	52.0	-7.67	0.000

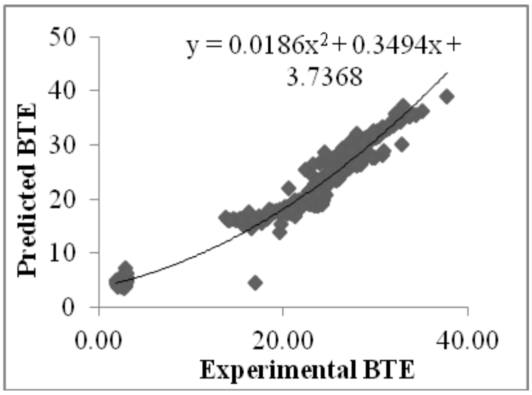

Figure 5.7 Relationship between experimental and prediction values of BTE

A Regression equation with performance is also plotted. The regression equation in the graph can be used to predict output BTE based on experimental BTE.

5.1.8 Development of regression model to predict the BSEC of engine

The regression model is developed to predict the BSEC of the engine and is represented as equation 5.2.

BSEC (MJ/KW-hr) = 52+1.636 B - 3.005L -173.4 D -2.3 KV +3.72CV +305177MF - 6271B*MF +2937 L *MF …………………(5.2)

Where, BSEC is specific energy consumption in MJ/KW-hr B is blending in %, L is Load in %, D is Density in g/cc, KV is kinematic viscosity in Cst, CV is calorific value in MJ/Kg, MF is mass of fuel consumed in Kg/s.

Table 5.9 shows the performance of the regression model developed. The model's performance is around 73.94% in predicting the BSEC of the engine. From Table 5.10, it is clear that the T-values of D, CV, and KV have negative correlations in the development of the model. The other parameters, B, P, and MF correlate positively.

Table 5.9 Model summary for predicting the BSEC of the engine

S	R-sq	R-sq(adj)	R-sq(pred)
25.0348	74.18%	73.61%	72.57%

Table 5.10 Regression analysis results for predicting the BSEC of the engine

Term	Coef	SE Coef	T-Value	P-Value
Constant	52	121	0.43	0.668
B in %	1.636	0.456	3.59	0.000
P in %	-3.005	0.132	-22.74	0.000
D in g/cc	-173.4	76.0	-2.28	0.023
KV in Cst	-2.3	11.6	-0.19	0.846
CV in MJ/Kg	3.72	2.33	1.60	0.111
MF in Kg/s	305177	90838	3.36	0.001
B in %*MF in Kg/s	-6271	1177	-5.33	0.000
L in %*MF in Kg/s	2937	546	5.38	0.000

Figure 5.8 illustrates the plots of predicted BSEC versus experimental BSEC. A Regression equation with performance is also plotted.

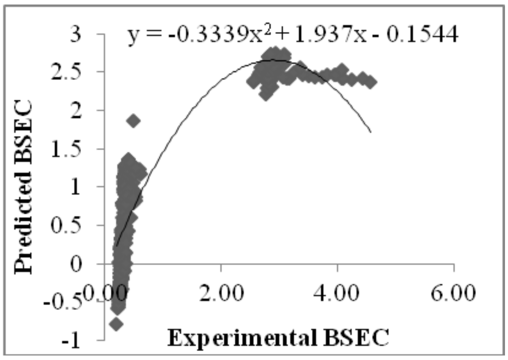

Figure 5.8 Relationship between experimental and prediction values of BSEC

5.1.9 Development of regression model to predict the CO of engine

The regression model is developed to predict the CO of the engine and is represented as equation 5.3.

CO (%) = -0.411+0.00648B - 0.001813L -0.427 D +0.1326 KV +0.00811CV -1056MF -49.61B *MF +29.38 L*MF……………(5.3)

Where, CO is Carbon monoxide in %, B is blending in %, L is Load in %, D is Density in g/cc, KV is kinematic viscosity in Cst, CV is calorific value in MJ/Kg, MF is mass of fuel consumed in Kg/s.

Table 5.11 shows the performance of the regression model developed. The model's performance is around 88.65% in predicting the CO of the engine. From Table 5.12, it is clear that the T-values of D, CV, and KV have negative correlations in the development of the model. The other parameters, B, P, and MF correlate positively. Figure 5.9 illustrates the plots of predicted CO versus experimental CO.

Table 5.11 Model summary for predicting the CO of the engine

S	R-sq	R-sq(adj)	R-sq(pred)
0.0757623	88.65%	88.41%	87.79%

Table 5.12 Regression analysis results for predicting the CO of the engine

Term	Coef	SE Coef	T-Value	P-Value
Constant	-0.411	0.367	-1.12	0.264
B in %	0.00648	0.00138	4.70	0.000
P in %	-0.001813	0.000400	-4.53	0.000
D in g/cc	-0.427	0.230	-1.85	0.065
KV in Cst	0.1362	0.0352	3.86	0.000
CV in MJ/Kg	0.00811	0.00705	1.15	0.250
MF in Kg/s	-1056	275	-3.84	0.000
B in %*MF in Kg/s	-49.61	3.56	-13.93	0.000
L in %*MF in Kg/s	29.38	1.65	17.78	0.000

A Regression equation with performance is also plotted. The regression equation in the graph can be used to predict output CO based on experimental CO.

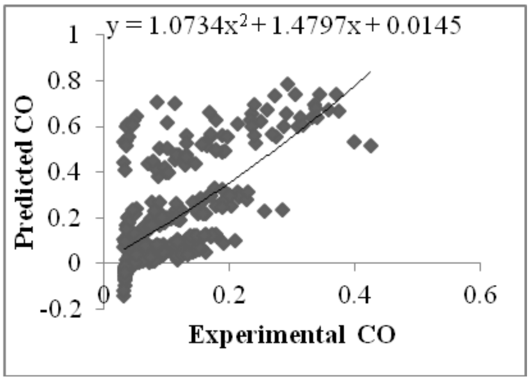

Figure 5.9 Relationship between experimental and prediction values of CO

5.1.10 Development of regression model to predict the CO_2 of engine

The regression model is developed to predict the CO_2 of the engine and is represented as equation 5.4.

CO2 (%) = -11+0.0451B - 0.05425L +7.41 D -0.756 KV +0.2049 CV +789MF +183B in % *MF +14.1 L*MF …………………………..(5.4)

Where, CO_2 is Carbon dioxide in %, B is blending in %, L is Load in %, D is Density in g/cc, KV is kinematic viscosity in Cst, CV is calorific value in MJ/Kg, MF is mass of fuel consumed in Kg/s.

Table 5.13 shows the performance of the regression model developed. The model's performance is around 90.25% in predicting the CO_2 of the engine. From Table 5.14, it is clear that the T-values of D, CV, and KV have negative correlations in the development of the model. The other parameters, B, P, and MF correlate positively. Figure 5.10 illustrates the plots of predicted CO_2 versus experimental CO_2. A Regression equation with performance is also plotted. The regression equation in the graph can be used to predict output CO_2 based on experimental CO_2.

Table 5.13 Model summary for predicting the CO_2 of the engine

S	R-sq	R-sq(adj)	R-sq(pred)
0.921779	90.25%	90.04%	89.67%

Table 5.14 Regression analysis results for predicting the CO_2 of the engine

Term	Coef	SE Coef	T-Value	P-Value
Constant	-11.00	4.46	-2.46	0.014
B in %	0.0451	0.0168	2.69	0.007
L in %	0.05425	0.00487	11.15	0.000
D in g/cc	7.41	2.80	2.65	0.009
KV in Cst	-0.756	0.429	-1.76	0.079
CV in MJ/Kg	0.2049	0.0857	2.39	0.017
MF in Kg/s	789	3345	0.24	0.814
B in %*MF in Kg/s	183.1	43.3	4.23	0.000
L in %*MF in Kg/s	14.1	20.1	0.70	0.482

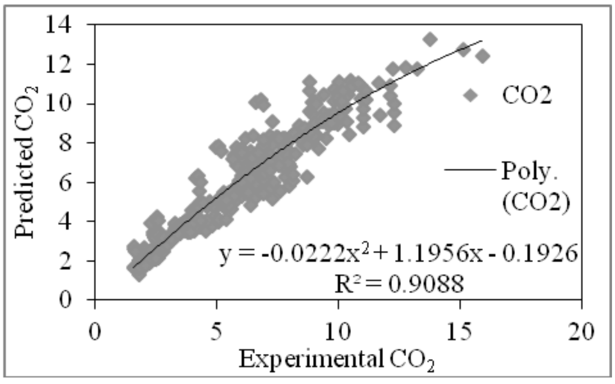

Figure 5.10 Relationship between experimental and prediction values of CO_2

5.1.11 Development of regression model to predict the UHC of engine

The regression model is developed to predict the UHC of the engine and is represented as equation 5.5.

UHC (PPM) = 47.5-0.2812B+ 0.1927L -20.6 D+5.58 KV-0.594CV-57927MF-886B*MF +572.9 L*MF ………………………..(5.5)

Where, UHC is Unburnt hydro carbon consumption in PPM, B is blending in %, L is Load in %, D is Density in g/cc, KV is kinematic viscosity in Cst, CV is calorific value in MJ/Kg, MF is mass of fuel consumed in Kg/s.

Table 5.13 shows the performance of the regression model developed. The model's performance is around 83.64% in predicting the CO_2 of the engine. From Table 5.14, it is clear that the T-values of D, CV, and KV have negative correlations in the development of the model. The other parameters, B, P, and MF correlate positively. Figure 5.10 illustrates the plots of predicted CO_2 versus experimental CO_2. A Regression equation with performance is also plotted. The regression equation in the graph can be used to predict output CO_2 based on experimental CO_2.

Table 5.15 Model summary for predicting the UHC of the engine

S	R-sq	R-sq(adj)	R-sq(pred)
3.63216	83.82%	83.47%	82.82%

Table 5.16 Regression analysis results for predicting the UHC of the engine

Term	Coef	SE Coef	T-Value	P-Value
Constant	47.5	17.6	2.70	0.007
B in %	-0.2812	0.0661	-4.25	0.000
P in %	0.1927	0.0192	10.05	0.000
D in g/cc	-20.6	11.0	-1.87	0.063
KV in Cst	5.58	1.69	3.30	0.001
CV in MJ/Kg	-0.594	0.338	-1.76	0.080
MF in Kg/s	-57927	13179	-4.40	0.000
B in %*MF in Kg/s	-886	171	-5.19	0.000
P in %*MF in Kg/s	572.9	79.2	7.23	0.000

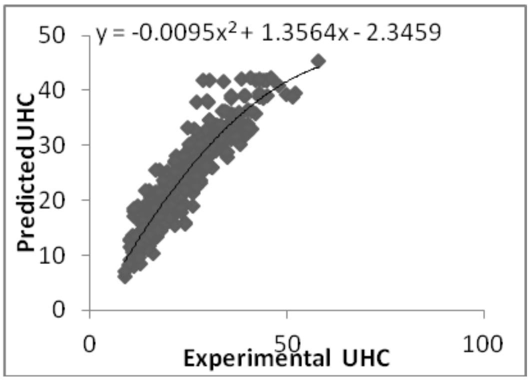

Figure 5.11 Relationship between experimental and prediction values of UHC

5.1.12 Development of regression model to predict the NOx of engine

The regression model is developed to predict the CO_2 of the engine and is represented as equation 5.6.

NOx (PPM) = -366+2.213B-2.695L+234D-50.9KV+5.75CV+858751MF +7996B *MF – 6147L*MF …………………….(5.6)

Where, NOx oxides of Nitrogen in PPM, B is blending in %, L is Load in %, D is Density in g/cc, KV is kinematic viscosity in Cst, CV is calorific value in MJ/Kg, MF is mass of fuel consumed in Kg/s.

Table 5.13 shows the performance of the regression model developed. The model's performance is around 93.15% in predicting the CO_2 of the engine. From Table 5.14, it is clear that the T-values of D, CV, and KV have negative correlations in the development of the model. The other parameters, B, L, and MF, correlate positively. Figure 5.10 illustrates the plots of predicted CO_2 versus experimental CO_2. A regression equation with performance is also plotted. The regression equation in the graph can be used to predict output CO_2 based on experimental CO_2.

Table 5.17 Model summary for predicting the NOx of the engine

S	R-sq	R-sq(adj)	R-sq(pred)
34.8402	93.26%	93.11%	92.89%

Table 5.18 ANOVA analysis for predicting the NOx of the engine

Term	Coef	SE Coef	T-Value	P-Value
Constant	-366	169	-2.17	0.031
B in %	2.213	0.634	3.49	0.001
P in %	2.695	0.184	14.66	0.000
D in g/cc	234	106	2.21	0.028
KV in Cst	-50.9	16.2	-3.14	0.002
CV in MJ/Kg	5.75	3.24	1.77	0.077
MF in Kg/s	858751	126417	6.79	0.000
B in %*MF in Kg/s	7996	1638	4.88	0.000
P in %*MF in Kg/s	-6147	760	-8.09	0.000

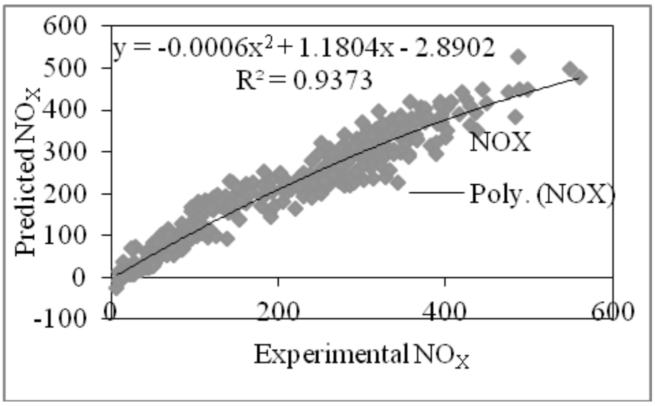

Figure 5.12 Relationship between experimental and prediction values of NOx

CHAPTER 6

ANN ANALYSIS OF THE PERFORMANCE AND EMISSIONS OF THE ENGINE

6.1 Introduction

A deep learning method, the Artificial Neural Network (ANN), arose from the concept of biological neural networks in human brains. ANN is developed due to an effort to replicate the workings of the human brain. Biological neural networks have many similarities to ANNs. However, ANNs operate somewhat differently. ANN has three layers: the input layer, the output layer, and the hidden layer or layers. The nodes in the input layer must be connected to the nodes in the hidden layer. Each node in the hidden layer must be connected to the nodes in the output layer. The Learning and training methods are used to compute the ANN model's operations, including data collection and analysis, network structure design, number of hidden layers, network simulation, and trade-offs between weights and bias.

6.2 Multi-Layer Perceptron Neural Network (MLPNN)

In this study, an MLPNN model, a feed-forward-back propagation artificial neural network, is used to predict the performance and emission parameters of the engine. The structure of the model consists of three layers an input layer (M_i), an output layer (O_i), and a hidden layer (H_i).

As shown in Figure 6.1, the (M_i) enters the feed-forward neural network where each M_i is connected with a weight(W_i) as a product in the training process. The product is then summed into a junction with a bias(B_j) represented as Eq.. 6.1. The present investigation's input parameters are a blend, load, density, kinematic viscosity, and calorific value. The output parameters include BTE, BSEC, CO, CO_2, UHC, and NOX (Hosamani et al. 2021).

$$X= \sum_{I=I}^{n}(WijMi) + bj\ldots\ldots\ldots\ldots\ldots\ldots \quad (6.1)$$

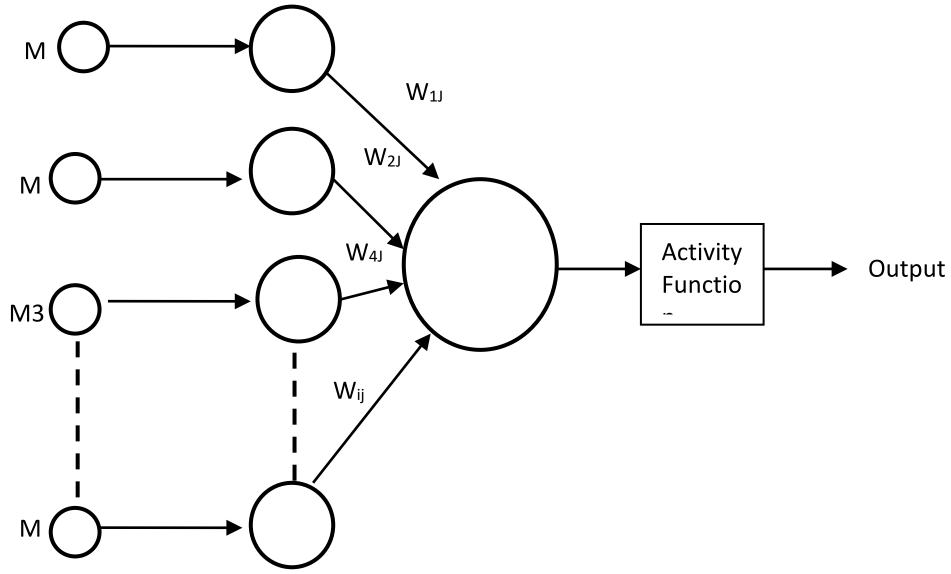

Figure 6.1: Generalized structure of artificial neurons

Two transfer functions are used, one LOGSIG and the other TRANSIG. TRANSIG is the most commonly used function. The activation function used is the sigmoid function and is represented as shown in Eq.. 6.2

$$F(X) = 1/(1+ e^{-x}) \quad (6.2)$$

During the training and testing period, the input and the target data enter into the network. The inputted data are trained by learning algorithms, which most commonly used is the Levenberg-Marquardt (LM) (Hagan and Menhaj 1994), which is faster than other algorithms. For performing the analysis, MatLab 2019a is used.

6.3 Development of ANN models for predicting the performance and emissions of the engine

A total of 375 samples are used to carry out the analysis. An MLPNN model is chosen, including six input and six output parameters. Input parameters include blend, engine load, the mass of fuel consumed, density, kinematic viscosity, and calorific value. The output parameters are BTE, BSEC, CO, CO_2, UHC, and NO_X.

Of 375 data sets, 263 are used for training the model, and the remaining 112 are used for testing and validating the model. 50% of 112 data is shared equally for each testing and validation. A feed-forward backpropagation algorithm is used as a learning algorithm. Based on the trial and error techniques, the neurons are chosen from 4-10 (Kannan 2013). The TRANSIG transfer function is used as a sigmoid function.

The output and the error involved in the development of the model are recorded. The root mean square error is then computed for each neuron. The best model is the neuron corresponding to the least RMSE value (Kumar 2020). The equation to compute RMSE is represented as Eq.. 6.3. The RMSE is calculated for each neuron, varying from 4 to 10 in increments of one. It is found that the optimized model for predicting BTE, BSEC, CO, and NOx is the one with 6-neurons. The best model for predicting the UHC and CO_2 is the one with 5 neurons. The details of the RMSE values for the output parameters with different neurons are given in Table 6.1

Table 6.1 RMSE of the output parameters for various neurons

Neurons	RMSE					
	BTE	BSEC	CO	CO2	UHC	NOX
4	10.6712	0.65102	0.29439	8.89302	6.39242	29.162
5	4.71505	0.53651	0.46011	1.06747	3.84756	25.1842
6	3.61402	0.4749	0.26433	1.44179	3.8746	5.01839
7	4.03607	0.55427	0.42545	1.21049	4.02336	23.0194
8	18.4185	1.13339	0.77433	3.36957	4.25555	28.8222
9	4.25471	1.21866	0.4881	1.6492	4.17979	26.2116
10	3.69299	0.51741	0.27585	1.07327	4.14955	24.8236

The performance model and regression fittings for both 5 and 6 neurons are shown in Figures 6.2 to 6.9. Figures 6.2 and 6.6 represent the MLPNN model's architecture with several 6 and 5 neurons inputs. A screenshot of the training state can be visualised in Figures 6.3 and 6.10, where the number of validations checks and the epoch shall be noted. Once the network is trained, the performance check is carried out. Figures 6.4 and 6.11 show the validation performance for 6 and 5 neurons. The best validation is represented at epoch 5, which is 110.7545 for a 5-neuron model.

Similarly, a validation at an epoch which is 992.4 is found for a 6- neuron model. The regression model in Figures 13 and 17 shows the pattern of data fitting for the model in terms of R-Square. The R-squared value for the model developed is 0.99 for both 6 and 5 neurons ANN models. The performance of the regression models is shown in Figures 40 and 44.

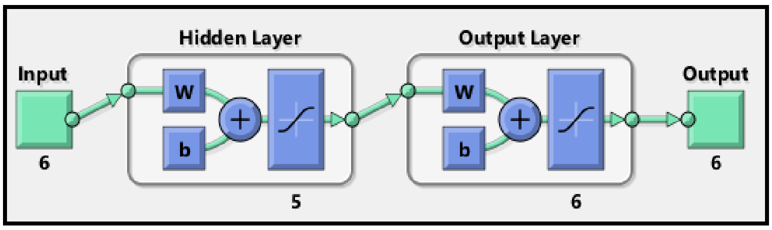

Figure 6.2 Network architecture of MLPNN with 5 neurons

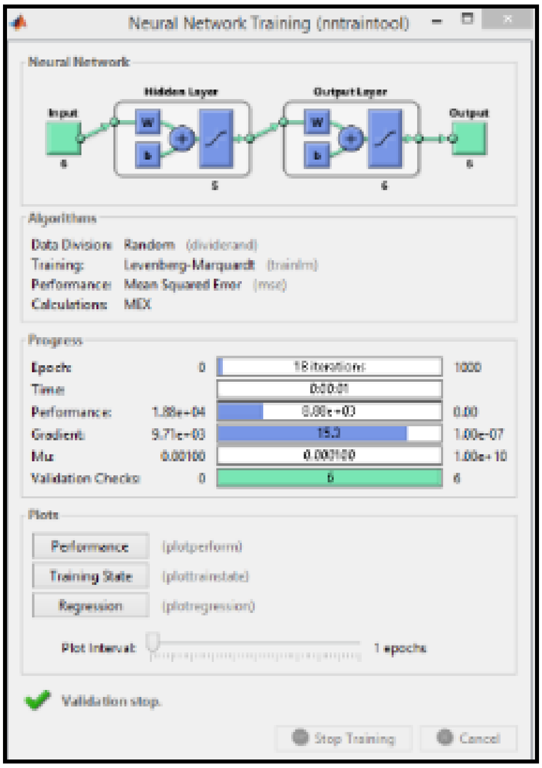

Figure 6.3 Pictorial view of the training state with 6 neurons

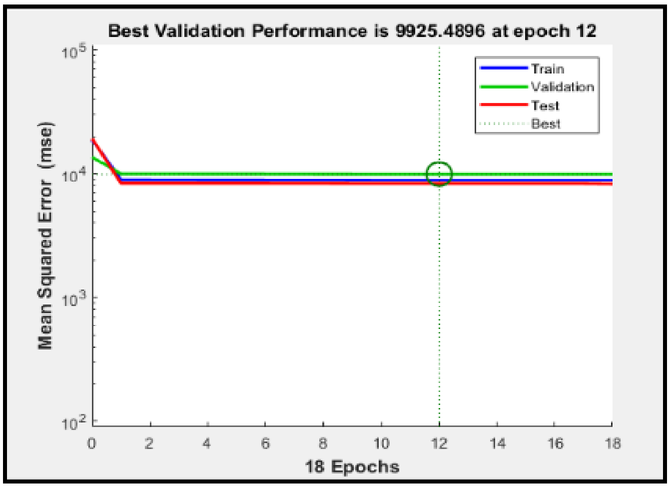

Figure 6.4 Performance of ANN training and testing with 6 neurons

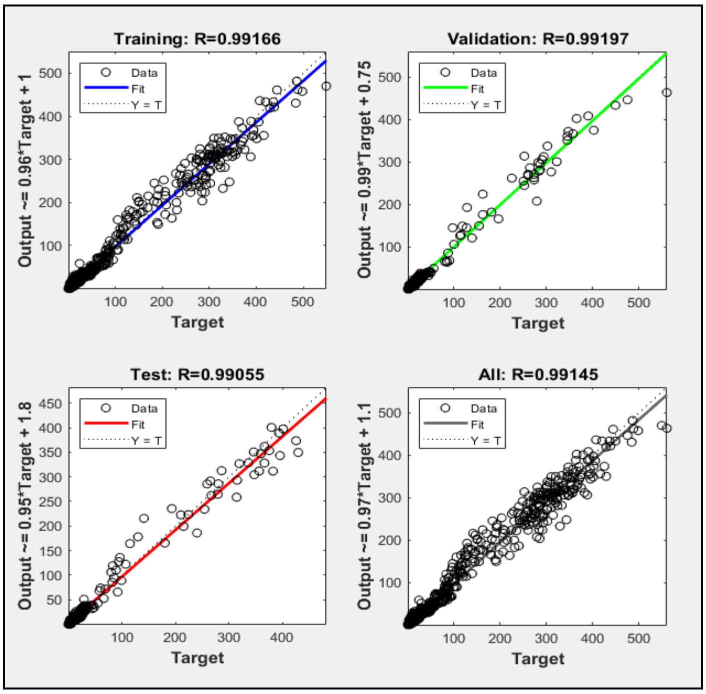

Figure 6.5 Regression Model of MLPNN with 6 neurons

Figure 6.10 shows the architecture of the MLPNN model with a number of inputs of 6 and the number of neurons of 6. The output variables are also 6. A screenshot of the training state can be visualized in Figure 6.11, where the number of validation checks and the epoch shall be noted. Once the network is trained, the performance check is carried out. Figure 6.12 shows the validation performance for 6 neurons. The best validation is represented at epoch 19, which is 142.8933. the regression model, as shown in Figure 6.13, shows the pattern of data fitting for the model in terms of R-Square. The R-squared value for the model developed is 0.99344, 0.99113, 0.99022, and 0.9926 for training, validation testing, and overall fitting with 6 input neurons.

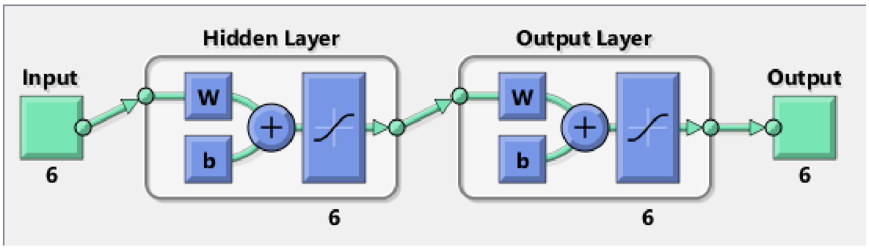

Figure 6.6 Network architecture of MLPNN with 5 neurons

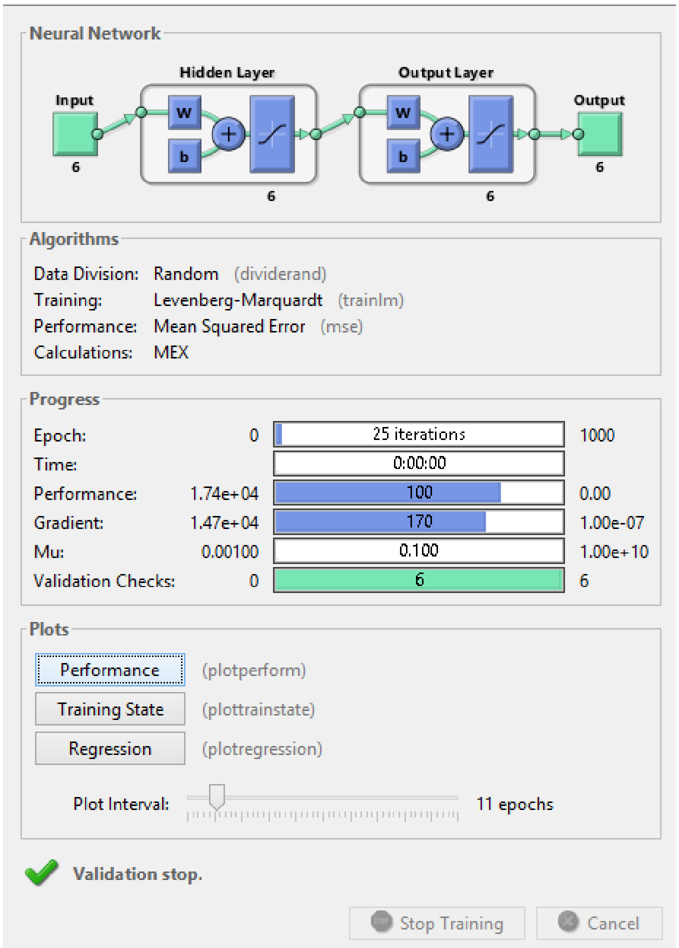

Figure 6.7 Pictorial view of the training state with 6 neurons

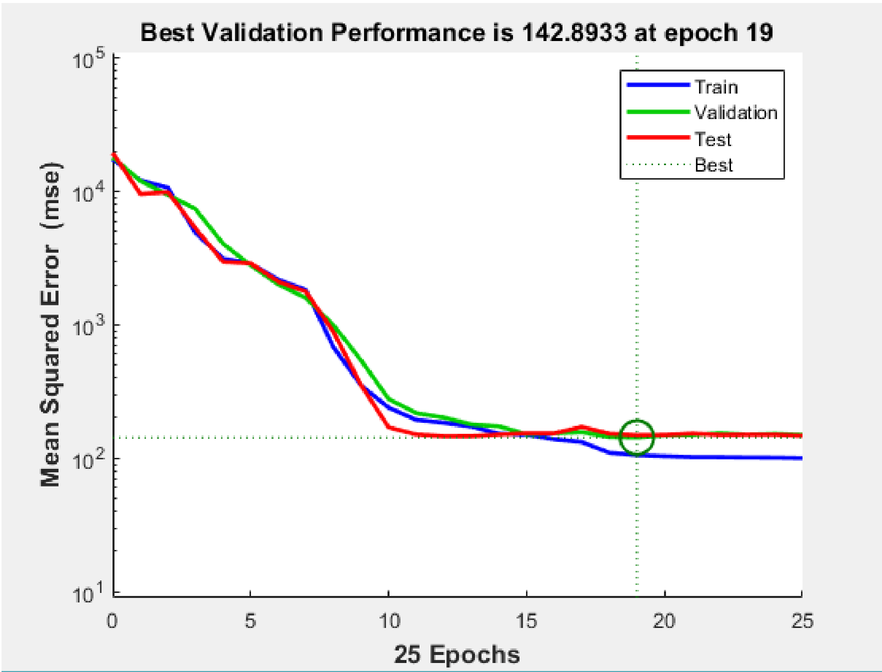

Figure 6.8: Performance of ANN training and testing with 6 neurons

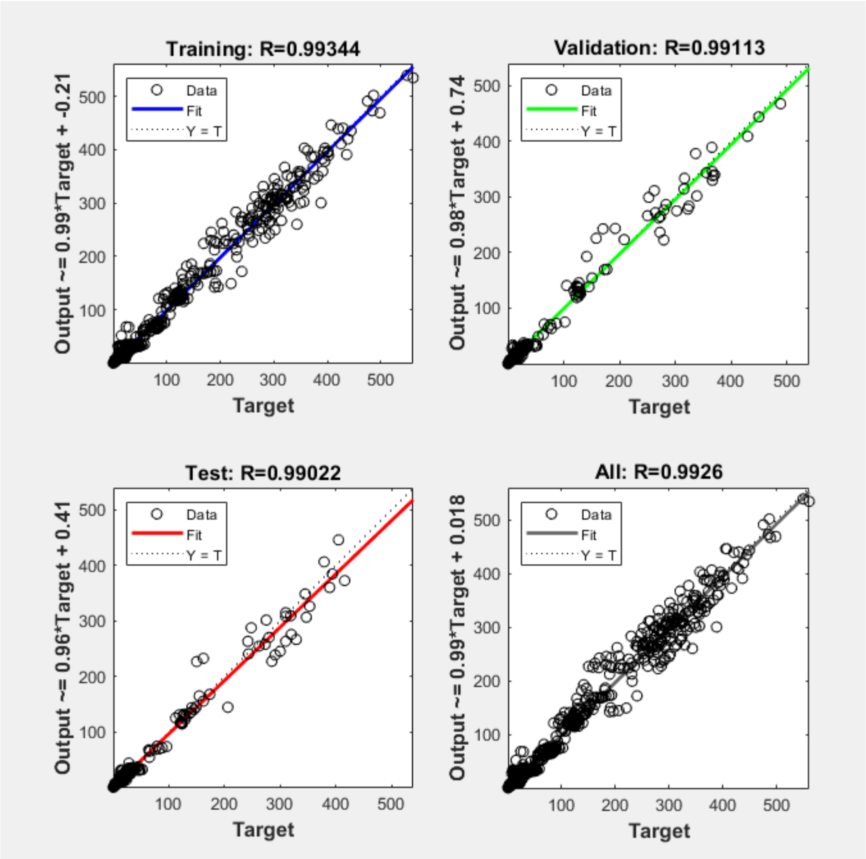

Figure 6.9 Regression Model of MLPNN with 6 neurons

Plotting an error analysis is a standard mode of validating the model's performance. A similar thing is achieved in this study. Errors are measured as the difference between the experimental and predicted values. These errors are represented in the form of a bar graph. A random distribution of the bars on either side of the zero line indicated the best validations of the model. Figure 6.10 to 6.15 shows the Error plot for BTE, BSEC, CO, CO_2, UHC, and NO_X. The error bars show a random distribution of the data on either side of the zero line. Hence the model can be considered to be validated.

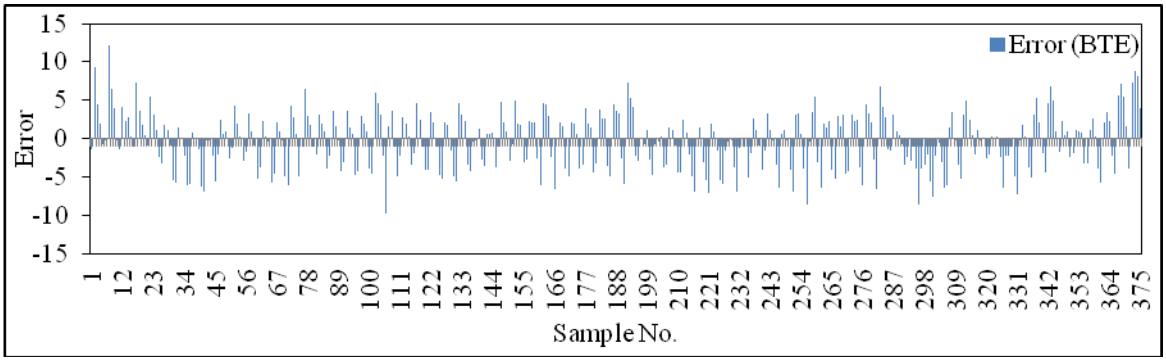

Figure 6.10 Error graph of BTE

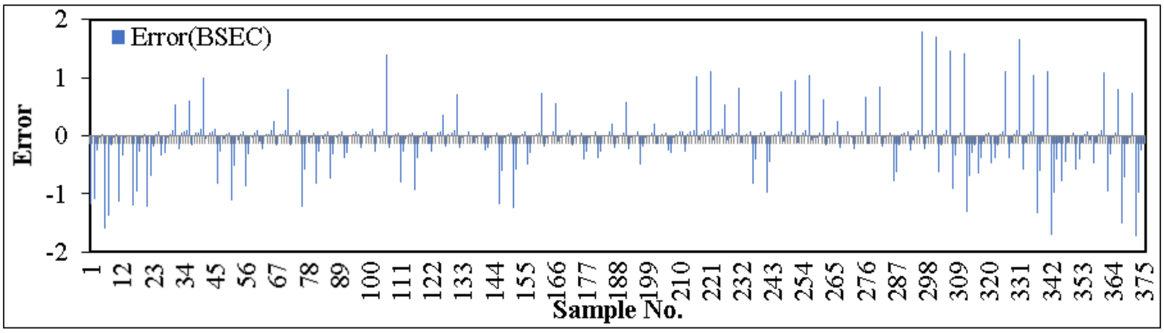

Figure 6.11 Error graph of BSEC

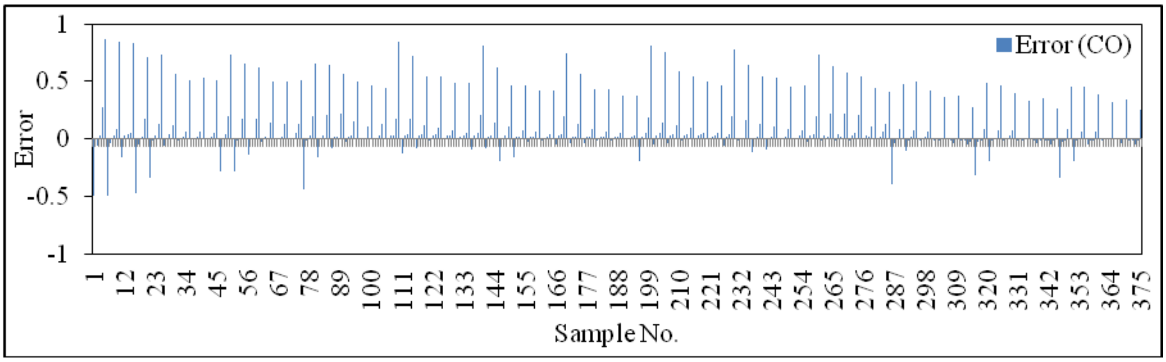

Figure 6.12 Error graph of CO

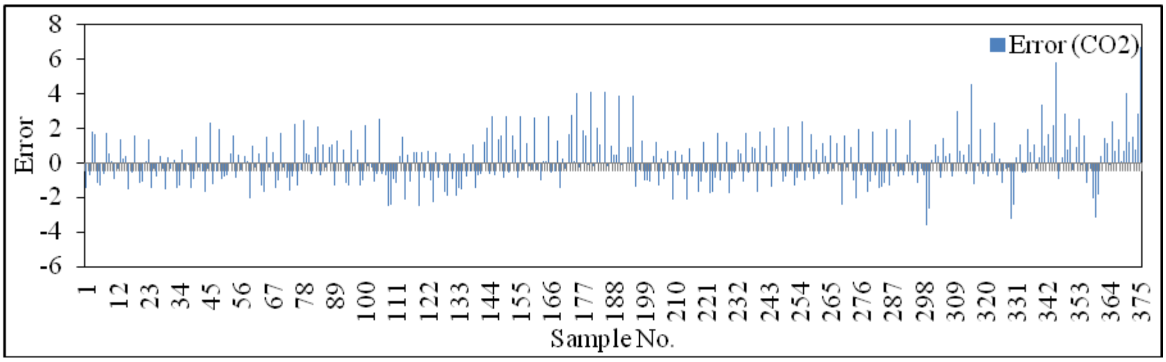

Figure 6.13 Error graph of CO_2

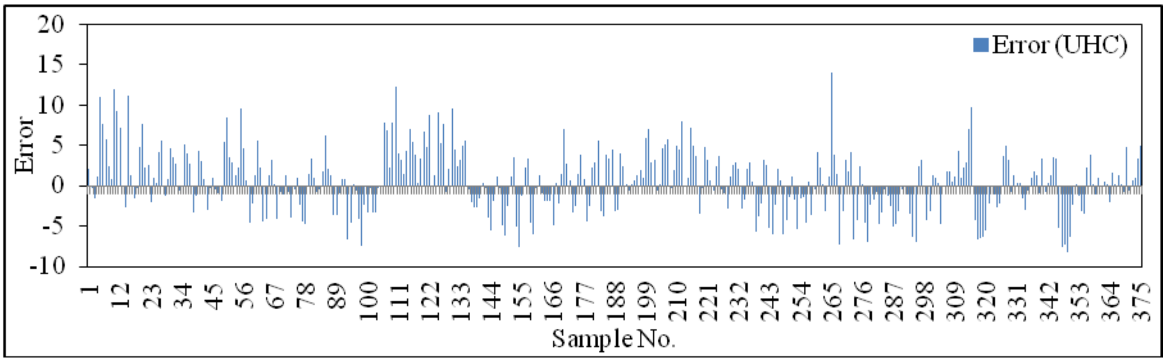

Figure 6.14 Error graph of UHC

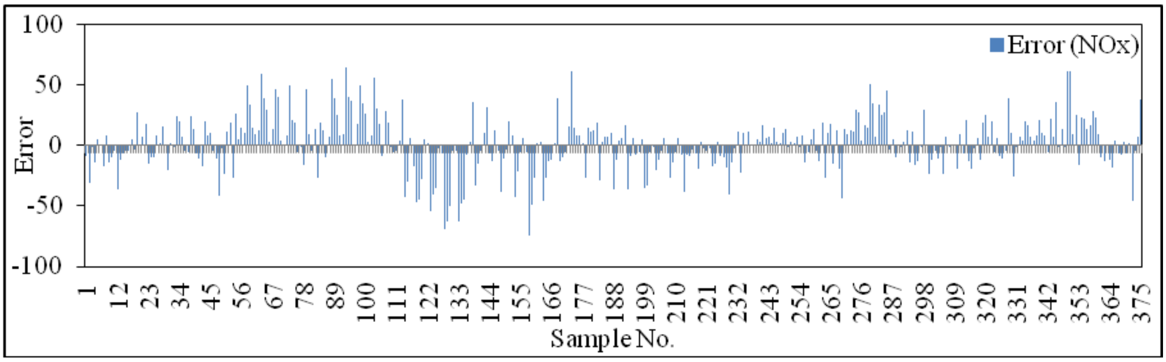

Figure 6.15 Error graph of NOx

CHAPTER 7

FIELD STUDY USING ALTERNATIVE FUELS

7.1 Introduction

In the present study, attention is given that the study is not limited to only experimentations on the lab scale. Hence, the same application is also extended to the case study. Mine environment plays a vital role in the sustainability of every mine, as per the web report “clean cities,” June 2009. It is reported that using biodiesel in underground mines reduces the particulate matter and hence be implemented. The case study is carried out in one of southern India's esteemed underground metal mines.

7.2 About the case study mine

Hutti Gold Mines Ltd. (HGML) is the only producer of primary gold in the nation, a Government of Karnataka undertaking founded in 1947 as Hyderabad Gold Mines. Gold reserves in Karnataka have been actively explored, developed, and exploited by HGML. The company has its corporate headquarters in Bangalore. It runs two mining operations: the Hutti Gold Unit (HGU) in Raichur district and the Chitradurga Gold Unit (CGU) in Chitradurga district, both of which have active mines in Ajjanahalli (Tumkur District). HGU is a fully integrated facility with an annual production capacity of 5,50,000 tonnes.

7.3 Application of alternative fuels on the equipment used in underground mines

The Indian regulation for blending biodiesel guides the application of alternative fuels. As per the Indian biofuel policy regulations, it must blend 20% of biodiesel with diesel. The study also intends to implement a 20% blending of the basic biodiesel fuels with diesel, i.e., MPO, MWO, and MWCO. However, ethanol and acetone blendings are not covered because of the challenges faced with fuel line systems. Hence a 20% blending of RPO, MPO, MWO, and MPWO is tested on the underground mine equipment. The equipment provided by the mining authority was a TATA make tipper of BS-III engine purchased in 2007 by the mine. The same vehicle was used to test all the samples. The vehicle was used to shift the OB from the mine.

The measurement included four gases: CO, Nitric oxide (NO), nitrogen dioxide (NO_2), and NOx oxides of nitrogen. The emission equipment used for the study is Drager EM

200 E. The pictorial representation of the same is shown in Figure 7.1. The specifications of the equipment are listed in Table 7.1.

Figure 7.1 Pictorial representation of Drager EM 200 emission measuring equipment (Courtesy of Drager)

Table 7.1 Specifications of the Drager EM 200 exhaust analyser

<table>
<tr><td colspan="3">Display</td><td colspan="2">Liquid crystal graphic display,
backlit, manual</td></tr>
<tr><td colspan="3">Interface</td><td colspan="2">USB for PC interface, infrared
for printer, no multifunction
jack for additional instruments</td></tr>
<tr><td colspan="3">Operating temperature</td><td colspan="2">+5 °C … +40 °C</td></tr>
<tr><td colspan="3">Power supply</td><td colspan="2">Internal: high power battery, 4.8 V 2,000 mAh, an indication of the state of charge, external charger</td></tr>
<tr><td colspan="3">Operating capacity</td><td colspan="2">Typically 10 hours</td></tr>
<tr><td colspan="3">Gas extraction</td><td colspan="2">Membrane pump for gas sampling</td></tr>
<tr><td colspan="3">Weighting</td><td colspan="2">1,100 g</td></tr>
<tr><td colspan="3">Dimensions</td><td colspan="2">195 mm x 165 mm x 75 mm (H x W x D)</td></tr>
<tr><td>Display</td><td>Principle of measurement</td><td>Measuring range (PPM)</td><td>Resolution Accuracy (PPM)</td><td>Accuracy (PPM)</td></tr>
<tr><td>CO</td><td rowspan="4">EI chem Sensor</td><td>0-8000</td><td rowspan="4">1</td><td>Up to±100PPM</td></tr>
<tr><td>NO</td><td>0-2000</td><td>Up to±10PPM</td></tr>
<tr><td>NO_2</td><td>0-200</td><td>Up to±5PPM</td></tr>
<tr><td>NOX</td><td>0-2000</td><td>Up to±10PPM</td></tr>
</table>

Experimental trials are conducted using the base biodiesel samples of 20% blendings, i.e., the blends of MPO, MPWO, MWO, and RPO 20% and 80% of diesel by volume. The experiments are conducted on a TATA tipper truck which is a 2007 make BSIII engine. It is observed that CO can be reduced with the implementation of biodiesel. Alternatively, the number of NO_X increased.

7.4 Emission Testing for the Use of alternative fuels

The fuel samples are subjected to combustion in the tipper, and the emission values, namely CO, NO, NO_2, and NOx, are recorded. Following Table 7.2 illustrate the representation of the emission values at empty load conditions and full load conditions:

Table 7.2 Results of the emissions of various fuels used at empty load condition and full load conditions

Type of Emissions	Empty load condition				
	Diesel	MPO	MWO	MPWO	RPO
CO (PPM)	61	58	51	55	43
NO (PPM)	267	296	287	291	320
NO_2 (PPM)	26	33	24	28	36
NOx (PPM)	293	329	311	299	356
Full load condition					
CO (PPM)	601	318	300	308	296
NO (PPM)	67	89	75	82	96
NO_2 (PPM)	36	37	31	35	41
NOx (PPM)	103	126	106	117	137

The deviation measures in CO, NO, NO2, and NOx compared to diesel are estimated for both idle and high idle conditions. Table 7.3 illustrates the MPO, MWO, MPWO, and RPO deviations. The largest deviation is found in the RPO blend for CO and NOx emissions. RPO is considered a good carbon reducer. Alternatively, increasing the nitrogen oxide emissions.

Table 7.3 Estimation of deviations of emissions of biodiesel blend from diesel.

	Deviations with respect to diesel			
Type of Emissions	Empty load condition			
	MPO	MWO	MPWO	RPO
CO (PPM)	4.918033	16.39344	9.836066	29.5082
NO (PPM)	-10.8614	-7.49064	-8.98876	-19.8502
NO_2 (PPM)	-26.9231	-7.69231	-11.5385	-38.4615
NOx (PPM)	4.918033	16.39344	9.836066	29.5082
	Full load condition			
CO (PPM)	47.08819	50.08319	48.75208	50.74875
NO (PPM)	-32.8358	-11.9403	-22.3881	-43.2836
NO_2 (PPM)	-2.77778	13.88889	2.777778	-13.8889
NOx (PPM)	-22.3301	-2.91262	-13.5922	-33.0097

CHAPTER 8

CONCLUSIONS

8.1 Summary of the study

In the present study, different forms of alternative fuels are developed, with Pongamia pinnata as a basic resource. These include raw form, esterification form, and combinational with other methyl esters. Further, the significance of adding ethanol and acetone to the samples is also studied. The samples are subjected to combustion in an IC engine at the laboratory. The performance and emission parameters are evaluated. The Effect of loading and blending are studied. Statistical analysis is carried out, and ANN models are developed to predict the performance and emission parameters of the engine. A field study on the air quality parameters of mine equipment is carried out by implementing the base biodiesel blends as per Indian biofuel regulations(20% blending). The conclusions and observations are as follows

8.1.1 Properties of the samples

- Mixing methyl esters of waste cooking oil (MWO) with methyl esters of Pongamia pinnata oil (MPO) improved the properties of MPO.
- A 10% blending of ethanol and acetone to MPO, MWO, MPWO, and Raw Pongamia Oil (RPO) along with diesel improved the Calorific value (CV), kinematic viscosity (KV), and density.
- The properties of all studied samples are found to be much closer to the properties of diesel. However, ethanol tends to improve higher as compared to acetone. DE is considered the best alternative with properties.
- The maximum deviation in the properties with emulsifications for density, kinematic viscosity, and calorific value is with RPO, which is 1.66% higher, 13.24% higher, and 1.81% lower at the highest blend of 30%, respectively. Hence, RPO is considered the poorest fuel source as far as the properties are concerned.

8.1.2 Engine test

- The engine test reveals that mixing two methyl esters, namely, MPO and MWO, improves the quality in terms of engine performance and emissions compared to individual sources.

- A 10% addition of acetone and ethanol has shown positive improvements in the efficiencies and emissions. However, the performance and emission deteriorate with increased biodiesel blends.
- There is a decrease in the efficiency of the engine fuelled with RPO. RPO is the poorest source compared to diesel, with an efficiency deviation of 32.73% at a maximum blend of 30%.
- The BSEC of blended samples increases with biodiesel blends. The average deviation of RPO with diesel is 41.4% from diesel.
- CO decreases with an increase in blend percentage. The maximum reduction in CO is obtained for RPE compared to diesel. The maximum deviation is found to be 57.47%, respectively, at 30% blending.
- CO2 increases with biodiesel blends. The increase in CO2 is higher for RPE. Diesel is considered the better source in the reduction of CO2. The average deviation of UHC is 49.16% at 30% blending.
- UHC increases with an increase in biodiesel blending. The decrease in UHC is found for RPE. Diesel is considered the better source in the reduction of UHC. The average deviation of UHC compared to diesel is 51.10% at 30% blending.
- NOx increase with biodiesel blends the reduction in NOx is higher for RPE. Diesel is considered the better source in the reduction of NOx. The increase in NOx is found to be 172.68% at 30% blending.

8.1.3 Statistical analysis

- ANOVA and regression analysis are carried out using Minitab V 19. The results reveal that the developed models' performance is good, with an R-square value of more than 70%. Load and blend are considered the most significant parameters in predicting the performance and emissions of the engine.
- Equations for predicting the performance and emission parameters are listed under section 5.2. A graph of experimental and predicted values is plotted to identify the relationship between experimental values and predicted values.

8.1.4 ANN Modelling

- ANN modeling using MatLab 2019a is carried out using an MLPNN network. The trial and error approach is used. The number of neurons are varied from 4 to

10 in increments of 1. The performance, output, and error for each neuron are recorded. The RMSE is computed. The models' performance is judged based on the least R-square value.

- It is found that the optimised model for predicting BTE, BSEC, CO, and NOx is the one with 6 neurons. The best model for predicting the UHC and CO_2 is the one with 5 neurons.

8.6 Field study

- Samples MPO, MWO, MPWO, and RPO with 20% blending are subjected to fuelling in a TATA make tipper. The observations revealed that the tipper's CO emission was reduced. But nitrogen oxides increase (NO, NO2, and NOx) in every form. The best reducer of CO emission is RPO, with deviations of 29.5% and 50.74% with diesel at both idle and high idle conditions, respectively. RPO increases NOx emissions. The deviations measured are 29.5% and 33%, respectively.

8.7 Scope for future work

- Dimensional analysis of the model to the prototype of lab scale engine with industrial tipper.
- Design and develop fuel filters, especially for biodiesel blends.
- Corrosive study of different metals subjected to biodiesel applications.

REFERENCES

Agatonovic-Kustrin, S., and Beresford, R. (2000). “Basic concepts of artificial neural network (ANN) modeling and its application in pharmaceutical research.” *Journal of Pharmaceutical and Biomedical Analysis*, 22(5), 717–727.

Ahamad, N., Sharma, A., and Singh, Y. (2018). “Performance and emission analysis of a diesel engine implementing polanga biodiesel and optimization using Taguchi method.” *Process Safety and Environmental Protection*, 120, 146–154.

Ahirwal, J., Maiti, S. K., and Satyanarayana Reddy, M. (2017). “Development of carbon, nitrogen and phosphate stocks of reclaimed coal mine soil within 8 years after forestation with Prosopis juliflora (Sw.) Dc.” *Catena*, 156(March), 42–50.

Ahmad, M. A., Yahya, W. J., Ithnin, A. M., Hasannuddin, A. K., Aiman, M., Bakar, A., Yasser, A., Fatah, A., Azwadi, N., Sidik, C., and Noge, H. (2018). “Combustion performance and exhaust emissions fuelled with non-surfactant water-in-diesel emulsion fuel made from different water sources.” (x), 24266–24280.

Al-esawi, N., and Qubeissi, M. Al. (2019). “The Impact of Biodiesel Fuel on Ethanol / Diesel Blends.” *energies*, 12(1), 1–11.

Al-lwayzy, S. H., and Yusaf, T. (2017). “Diesel engine performance and exhaust gas emissions using Microalgae Chlorella protothecoides biodiesel.” *Renewable Energy*, 101, 690–701.

Amarnath, H. K., & Prabhakaran, P. (2012). A study on the thermal performance and emissions of a variable compression ratio diesel engine fuelled with karanja biodiesel and the optimization of parameters based on experimental data. International Journal of Green Energy, 9(8), 841-863.

Aneeque, M., Alshahrani, S., Kareemullah, M., Afzal, A., Saleel, C. A., Soudagar, M. E. M., Hossain, N., Subbiah, R., and Ahmed, M. H. (2021). “The Combined effect of alcohols and calophyllum inophyllum biodiesel using response surface methodology optimization.”

Arunprasad, S., Iyer, H. J., Omkaar, K., Jayaganth, M., and and Palani, K. (2020). “Performance and Emission Characteristics of C . I Engine using Jatropha and Pongamia Mixed Biodiesel Performance and Emission Characteristics of C . I Engine using Jatropha and Pongamia Mixed Biodiesel.” *IOP Conf. Series: Materials Science and Engineering*, 954(1), 1–10.

Babu, A. V., Rao, B. V. A., and Kumar, P. R. (2009). “Transesterification for the preparation of biodiesel from crude-oil of pongamia pinnata.” *Thermal Science*, 13(3), 201–206.

Balat, M., and Balat, H. (2010). “Progress in biodiesel processing.” *Applied Energy*, 87(6), 1815–1835.

Bora, P., Konwar, L. J., Phukan, M. M., Deka, D., and Konwar, B. K. (2015). “Microemulsion based hybrid biofuels from Thevetia peruviana seed oil: Structural and dynamic investigations.” *Fuel*, 157, 208–218.

Cecrle, E., Depcik, C., Duncan, A., Guo, J., Mangus, M., Peltier, E., Stagg-williams, S., and Zhong, Y. (2012). “Investigation of the Effects of Biodiesel Feedstock on the Performance and Emissions of a Single-Cylinder Diesel Engine.”

Chauhan, B. S., Kumar, N., and Cho, H. M. (2012). “A study on the performance and emission of a diesel engine fueled with Jatropha biodiesel oil and its blends.” *Energy*, 37(1), 616–622.

Cirak, B., and Demirtas, S. (2014). “An Application of Artificial Neural Network for Predicting Engine Torque in a Biodiesel Engine.” 2(4), 74–80.

Damanik, N., Ong, H. C., Tong, C. W., Meurah, T., and Mahlia, I. (2018). “A review on the engine performance and exhaust emission characteristics of diesel engines fueled with biodiesel blends.” 15307–15325.

Datta, A., and Mandal, B. K. (2016). “Impact of alcohol addition to diesel on the performance combustion and emissions of a compression ignition engine.” *Applied Thermal Engineering*, 98, 670–682.

Debia, M., Couture, C., Njanga, P. E., Neesham-Grenon, E., Lachapelle, G., Coulombe, H., Hallé, S., and Aubin, S. (2017). “Diesel engine exhaust exposures in two underground mines.” *International Journal of Mining Science and Technology*, 27(4), 641–645.

Dhanarasu, M., Rameshkumar, K. A., and Maadeswaran, P. (2021). “Effect of acetone as an oxygenated additive with used sunflower oil biodiesel on performance , combustion and emission in diesel engine.” *Environmental Technology*, 0(0), 1–11.

Dhar, A., Kevin, R., and Agarwal, A. K. (2012). “Production of biodiesel from high-FFA neem oil and its performance, emission and combustion characterization in a single cylinder DICI engine.” *Fuel Processing Technology*, 97, 118–129.

Dwivedi, G., and Sharma, M. P. (2014). “Prospects of biodiesel from Pongamia in India.” *Renewable and Sustainable Energy Reviews*, 32, 114–122.

Ehsan, M., and Chowdhury, M. T. H. (2015). “Production of biodiesel using alkaline based catalysts from waste cooking oil: A case study.” *Procedia Engineering*, 105(Icte 2014), 638–645.

Ghobadian, B., Rahimi, H., Nikbakht, A. M., Najafi, G., and Yusaf, T. F. (2009). “Diesel engine performance and exhaust emission analysis using waste cooking biodiesel fuel with an artificial neural network.” *Renewable Energy*, 34(4), 976–982.

Godiganur, S., Suryanarayana Murthy, C. H., and Reddy, R. P. (2009). “6BTA 5.9 G2-1 Cummins engine performance and emission tests using methyl ester mahua (Madhuca indica) oil/diesel blends.” *Renewable Energy*, 34(10), 2172–2177.

Gui, M. M., Lee, K. T., and Bhatia, S. (2008). “Feasibility of edible oil vs. non-edible oil vs. waste edible oil as biodiesel feedstock.” *Energy*, 33(11), 1646–1653.

Habibullah, M., Masjuki, H. H., Kalam, M. A., Rizwanul Fattah, I. M., Ashraful, A. M., and Mobarak, H. M. (2014). “Biodiesel production and performance evaluation of coconut, palm and their combined blend with diesel in a single-cylinder diesel engine.” *Energy Conversion and Management*, 87, 250–257.

Hagan, M. T., and Menhaj, M. B. (1994). “Training feedforward networks with the

Marquardt algorithm.” *IEEE TRANSACTIONS ON NEURAL NETWORKS*, 5(6), 4–8.

Heydari-maleney, K., Taghizadeh-alisaraei, A., Ghobadian, B., and Abbaszadeh-mayvan, A. (2017). “Analyzing and evaluation of carbon nanotubes additives to diesohol-B2 fuels on performance and emission of diesel engines.” *Fuel*, 196, 110–123.

Hoekman, S. K., and Robbins, C. (2012). “Review of the effects of biodiesel on NOx emissions.” *Fuel Processing Technology*, 96, 237–249.

Hosamani, B. R., Abbas, S., and Katti, V. (2021). “Assessment of performance and exhaust emission quality of different compression ratio engine using two biodiesel mixture : Artificial neural network approach.” *Alexandria Engineering Journal*, 60(1), 837–844.

Hussan, J., Hj, M., Kalam, A., and Ali, L. (2013). “Tailoring key fuel properties of diesel e biodiesel e ethanol blends for diesel engine.” *Journal of Cleaner Production*, 51, 118–125.

Imtenan, S., Masjuki, H. H., Varman, M., Kalam, M. A., Arbab, M. I., Sajjad, H., and Ashrafur Rahman, S. M. (2014). “Impact of oxygenated additives to palm and jatropha biodiesel blends in the context of performance and emissions characteristics of a light-duty diesel engine.” *Energy Conversion and Management*, 83(2014), 149–158.

Kaisan, M. U., Anafi, F. O., Nuszkowski, J., Kulla, D. M., & Umaru, S. (2020). Calorific value, flash point and cetane number of biodiesel from cotton, jatropha and neem binary and multi-blends with diesel. *Biofuels*, *11*(3), 321-327.

Kalam, M. A., Masjuki, H. H., Jayed, M. H., and Liaquat, A. M. (2011). “Emission and performance characteristics of an indirect ignition diesel engine fuelled with waste cooking oil.” *Energy*, 36(1), 397–402.

Kannan, G. R., Balasubramanian, K. R., and Anand, R. (2013). “Artificial Neural Network Approach To Study The Effect Of Injection Pressure And Timing On Diesel Engine Performance Fueled With Biodiesel.”, *Energy*, 14(4), 507–519.

Khalife, E., Tabatabaei, M., Demirbas, A., and Aghbashlo, M. (2017). “Impacts of additives on performance and emission characteristics of diesel engines during steady state operation." *Progress in Energy and Combustion Science*, 59, 32–78.

Knothe, G., and Steidley, K. R. (2005). "Kinematic viscosity of biodiesel fuel components and related compounds . Influence of compound structure and comparison to petrodiesel fuel components." *Energy*, 84, 1059–1065.

Kumar, S. (2020). "Comparison of linear regression and artificial neural network technique for prediction of a soybean biodiesel yield." *Energy Sources, Part A: Recovery, Utilization and Environmental Effects*, 42(12), 1425–1435.

Liaquat, A. M., Masjuki, H. H., Kalam, M. A., Fattah, I. M. R., Hazrat, M. A., Varman, M., Mofijur, M., and Shahabuddin, M. (2020). "Effect of coconut biodiesel blended fuels on engine performance and emission characteristics." *Procedia Engineering*, 56, 583–590.

Lutz, E. A., Reed, R. J., Lee, V. S. T., and Burgess, J. L. (2017). "Comparison of personal diesel and biodiesel exhaust exposures in an underground mine." *Journal of Occupational and Environmental Hygiene*, 14(7), D102–D109.

M.R. Shukri, M.M. Rahman, D. R. and K. K. (2015). "Artificial Neural Network Optimization Modeling On Engine Performance Of Diesel Engine Using Biodiesel Fuel." *International Journal of Automotive and Mechanical Engineering*, 11(June), 2332–2347.

Mahalingam, A., Munuswamy, D. B., and Devarajan, Y. (2018). "Investigation On The Emission Reduction Technique In Acetone-Biodiesel Aspirated Diesel Engine." *Journal of Palm research*, 30(June), 345–349.

Mallikappa, D. N., Reddy, R. P., and Murthy, C. S. N. (2012). "Performance and emission characteristics of double cylinder CI engine operated with cardanol bio fuel blends." *Renewable Energy*, 38(1), 150–154.

Nair, J. N., Singh, T. S., and Dhana, V. (2021). "Effect of addition of bio-additive clove oil to ternary fuel blends (Diesel-Biodiesel-Ethanol) on compression ignition engine Effect of addition of bio-additive clove oil to ternary fuel blends (Diesel-Biodiesel-Ethanol) on compression ignition engin." *Journal of Physics: Conference Series*, 2070(012212), 1–10.

Ogunkunle, O., and Ahmed, N. A. (2021). “Overview of Biodiesel Combustion in Mitigating the Adverse Impacts of Engine Emissions on the Sustainable Human – Environment Scenario.”

Palash, S. M., Kalam, M. A., Masjuki, H. H., Arbab, M. I., Masum, B. M., and Sanjid, A. (2014). “Impacts of NO x reducing antioxidant additive on performance and emissions of a multi-cylinder diesel engine fueled with Jatropha biodiesel blends.” *Energy Conversion and Management*, 77(x), 577–585.

Palash, S. M., Kalam, M. A., Masjuki, H. H., Masum, B. M., Fattah, I. M. R., and Mo, M. (2013). “Impacts of biodiesel combustion on NOx emissions and their reduction approaches.” 23(x), 473–490.

Palash, S. M., Masjuki, H. H., Kalam, M. A., Atabani, A. E., Rizwanul Fattah, I. M., and Sanjid, A. (2015). “Biodiesel production, characterization, diesel engine performance, and emission characteristics of methyl esters from Aphanamixis polystachya oil of Bangladesh.” *Energy Conversion and Management*, 91, 149–157.

Pandian, M., Sivapirakasam, S. P., and Udayakumar, M. (2011). “Investigation on the effect of injection system parameters on performance and emission characteristics of a twin cylinder compression ignition direct injection engine fuelled with pongamia biodiesel – diesel blend using response surface methodology.” *Applied Energy*, 88(8), 2663–2676.

Patel, R. L., and Sankhavara, C. D. (2017). “Biodiesel production from Karanja oil and its use in diesel engine: A review.” *Renewable and Sustainable Energy Reviews*, 71(December 2016), 464–474.

Perumal, V., and Ilangkumaran, M. (2017). “Experimental analysis of engine performance, combustion and emission using pongamia biodiesel as fuel in CI engine” *Energy*, 129, 228–236.

Perumal, V., and Ilangkumaran, M. (2018). “Water emulsified hybrid pongamia biodiesel as a modi fi ed fuel for the experimental analysis of performance , combustion and emission characteristics of a direct injection diesel engine.” *Renewable Energy*, 121(x), 623–631.

Pohit, G., and Misra, D. (2013). “Optimization of Performance and Emission Characteristics of Diesel Engine with Biodiesel Using Grey-Taguchi Method.” 1(1), 1–8.

Prakash, R., Singh, R. K., and Murugan, S. (2013). “Experimental investigation on a diesel engine fueled with bio-oil derived from waste wood e biodiesel emulsions.” *Energy*, 55, 610–618.

Qi, D. H., Geng, L. M., Chen, H., Bian, Y. Z., Liu, J., and Ren, X. C. (2009). “Combustion and performance evaluation of a diesel engine fueled with biodiesel produced from soybean crude oil.” *Renewable Energy*, 34(12), 2706–2713.

Rahim Karami , Mohammad G. Rasul, M. M. K. K. 1and M. A. 1. (2019). “Performance analysis of direct injection diesel engine fueled with diesel-tomato seed oil biodiesel blending by anova and ann.” *energies Article*, 12(4421), 1–18.

Rajesh Kumar, B., and Saravanan, S. (2016). “Effects of iso-butanol/diesel and n-pentanol/diesel blends on performance and emissions of a di diesel engine under premixed LTC (low temperature combustion) mode.” *Fuel*, 170, 49–59.

Ramírez Verduzco, L. F. (2013). “Density and viscosity of biodiesel as a function of temperature: Empirical models.” *Renewable and Sustainable Energy Reviews*, 19, 652–665.

Rao, K. P., Babu, T. V., Anuradha, G., Rao, B. V. A., Bran, R., and Ester, M. (2017). “IDI diesel engine performance and exhaust emission analysis using biodiesel with an artificial neural network (ANN).” *Egyptian Journal of Petroleum*, 26(3), 593–600.

Rao, K. P., and Rao, B. V. A. (2017). “Parametric optimization for performance and emissions of an IDI engine with Mahua biodiesel.” *Egyptian Journal of Petroleum*, 26(3), 733–743.

Sajjadi, B., Raman, A. A. A., and Arandiyan, H. (2016). “A comprehensive review on properties of edible and non-edible vegetable oil-based biodiesel: Composition, specifications and prediction models.” *Renewable and Sustainable Energy Reviews*, 63, 62–92.

Sanjid, A., Masjuki, H. H., Kalam, M. A., Rahman, S. M. A., Abedin, M. J., and Palash, S. M. (2014). “Production of palm and jatropha based biodiesel and investigation of palm-jatropha combined blend properties , performance , exhaust emission and noise in an unmodi fi ed diesel engine.” *Journal of Cleaner Production*, 65, 295–303.

Saravanan, S., Rajesh Kumar, B., Varadharajan, A., Rana, D., Sethuramasamyraja, B., and Lakshmi Narayana rao, G. (2017). “Optimization of DI diesel engine parameters fueled with iso-butanol/diesel blends – Response surface methodology approach.” *Fuel*, 203, 658–670.

Sarıtas, I., Emre, H., and Og, H. (2010). “Expert Systems with Applications Prediction of diesel engine performance using biofuels with artificial neural network.” 37, 6579–6586.

Shahir, S. A., Masjuki, H. H., Kalam, M. A., Imran, A., Fattah, I. M. R., and Sanjid, A. (2014). “Feasibility of diesel-biodiesel-ethanol/bioethanol blend as existing CI engine fuel: An assessment of properties, material compatibility, safety and combustion.” *Renewable and Sustainable Energy Reviews*, 32, 379–395.

Shahir, V. K., Jawahar, C. P., and Suresh, P. R. (2015). “Comparative study of diesel and biodiesel on CI engine with emphasis to emissions - A review.” *Renewable and Sustainable Energy Reviews*, 45, 686–697.

Sharanappa, P., and Navindgi, M. C. (2017). “Physico-chemical properties of diesel-biodiesel-ethanol blends.” *International Journal of Scientific & Engineering Research*, 8(2), 506–510.

Shivakumar, Srinivasa Pai, P., and Shrinivasa Rao, B. R. (2011). “Artificial Neural Network based prediction of performance and emission characteristics of a variable compression ratio CI engine using WCO as a biodiesel at different injection timings.” *Applied Energy*, 88(7), 2344–2354.

Shrivastava, K., Thipse, S. S., and Patil, I. D. (2021). “Optimization of diesel engine performance and emission parameters of Karanja biodiesel-ethanol-diesel blends at optimized operating conditions.” *Fuel*, 293(May 2020), 120451.

Sianturi, R. U. D., and Fauziyah, E. (2020). “Performance and Emission Characteristics of C . I Engine using Jatropha and Pongamia Mixed Biodiesel Performance and Emission Characteristics of C . I Engine using Jatropha and Pongamia Mixed Biodiesel.” *IOP Conf. Series: Materials Science and Engineering*, 954, 1–9.

Sidhu, M. S., Roy, M. M., and Wang, W. (2018). “Glycerine emulsions of diesel-biodiesel blends and their performance and emissions in a diesel engine.” *Applied Energy*, 230(August), 148–159.

Simsek, S., and Uslu, S. (2020). “Investigation of the effects of biodiesel / 2-ethylhexyl nitrate (EHN) fuel blends on diesel engine performance and emissions by response surface methodology (RSM).” *Fuel*, 275(May), 118005.

Simsek, S., Uslu, S., and Simsek, H. (2022). “Proportional impact prediction model of animal waste fat-derived biodiesel by ANN and RSM technique for diesel engine.” *Energy*, 239, 122389.

Singh, A. N., and Singh, J. S. (2006). “Experiments on ecological restoration of coal mine spoil using native trees in a dry tropical environment, India: A synthesis.” *New Forests*, 31(1), 25–39.

Singh, P. J., Khurma, J., and Singh, A. (2010). “Preparation, characterisation, engine performance and emission characteristics of coconut oil based hybrid fuels.” *Renewable Energy*, 35(9), 2065–2070.

Sivaramakrishnan Kaliamoorthy, and R. Paramasivam. (2013). “Investigation on performance and emissions of a biodiesel engine through optimization techniques.” *Thermal Science*, 17(1), 179–193.

Srithar, K. (2017). “Experimental investigations on mixing of two biodiesels blended with diesel as alternative fuel for diesel engines.” *Journal of King Saud University - Engineering Sciences*, 29(1), 50–56.

Srivastava, N. K., Ram, L. C., and Masto, R. E. (2014). “Reclamation of overburden and lowland in coal mining area with fly ash and selective plantation: A sustainable ecological approach.” *Ecological Engineering*, 71, 479–489.

Subbaiah, G. V., and Gopal, K. R. (n.d.). “International Journal of Green Energy An Experimental Investigation on the Performance and Emission Characteristics of a Diesel Engine Fuelled with Rice Bran Biodiesel and Ethanol Blends.” (June 2013), 37–41.

Sureshkumar, K., Velraj, R., and Ganesan, R. (2008). “Performance and exhaust emission characteristics of a CI engine fueled with Pongamia pinnata methyl ester (PPME) and its blends with diesel.” *Renewable Energy*, 33(10), 2294–2302.

Thodda, G., Madhavan, V. R., and Thangavelu, L. (2020). “Environmental effects predictive modelling and optimization of performance and emissions of acetylene fuelled ci engine using ann and rsm predictive modelling and optimization of performance and emissions.” *Energy Sources, Part A: Recovery, Utilization, and Environmental Effects*, 00(00), 1–19.

Tiffany, D. (2016). “Economic analysis of biodiesel usage in underground mines.” *BioEnergy*, 1(January 1998), 922–932.

Torres-jimenez, E., and Svolj, M. (2010). “Physical and Chemical Properties of Ethanol - Biodiesel Blends for Diesel Engines.” *Energy & Fuels*, (13), 2002–2009.

Tosun, E., Aydin, K., and Bilgili, M. (2016). “Comparison of linear regression and artificial neural network model of a diesel engine fueled with biodiesel-alcohol mixtures.” *Alexandria Engineering Journal*, 55(4), 3081–3089.

Wakil, M. A., Kalam, M. A., Masjuki, H. H., Atabani, A. E., and Fattah, I. M. R. (2015). “Influence of biodiesel blending on physicochemical properties and importance of mathematical model for predicting the properties of biodiesel blend.” *Energy Conversion and Management*, 94, 51–67.

Wu-gao, Z., Li, D., Zhen, H., and Jian-guang, Y. (2005). “Physico-chemical properties of ethanol – diesel blend fuel and its effect on performance and emissions of diesel engines.” 30, 967–976.

Wu, G., Ge, J. C., and Choi, N. J. (2020). “Comprehensive review of the application characteristics of biodiesel blends in diesel engines.” *Applied Sciences*, 10(8015), 1–31.

Xue, J., Grift, T. E., and Hansen, A. C. (2011). “Effect of biodiesel on engine performances and emissions.” *Renewable and Sustainable Energy Reviews*, 15(2), 1098–1116.

Yusri, I. M., Mamat, R., Azmi, W. H., Omar, A. I., Obed, M. A., and Shaiful, A. I. M. (2017). “Application of response surface methodology in optimization of performance and exhaust emissions of secondary butyl alcohol-gasoline blends in SI engine.” *Energy Conversion and Management*, 133, 178–195.

Zaharin, M. S. M., Abdullah, N. R., Najafi, G., Sharudin, H., and Yusaf, T. (2017). “Effects of physicochemical properties of biodiesel fuel blends with alcohol on diesel engine performance and exhaust emissions: A review.” *Renewable and Sustainable Energy Reviews*, 79(May), 475–493.

Appendix-I

Sl. No.	Sample	Blend in %	Load in %	Density in g/cc	Kinematic Viscosity in Cst	Calorific value in MJ/Kg	BP in KW	Time for 10CC fuel consumption in s	Mass of the fuel consumed in Kg/s	BTE in %	BSEC (MJ/KW-Hr)	CO in %	CO_2 in %	UHC in PPM	NO_X in PPM
1	D	0	0	0.825	3.94	44.24	0.1	75	0.000110	2.93	122.89	0.08	1.8	26	7
2		0	25	0.825	3.94	44.24	1.3	65	0.000127	23.48	15.33	0.08	2.5	28	15
3		0	50	0.825	3.94	44.24	2.6	40	0.000206	28.90	12.46	0.09	5	30	85
4		0	75	0.825	3.94	44.24	4.0	31	0.000266	33.60	10.71	0.32	5.8	40	128
5		0	100	0.825	3.94	44.24	5.3	22	0.000375	31.79	11.32	0.96	7.6	58	229
6	DA	10	0	0.819	3.93	44.1	0.1	76	0.000108	3.00	120.01	0.07	1.8	24	15
7		10	25	0.819	3.93	44.1	1.3	65	0.000126	23.73	15.17	0.07	2.4	26	29
8		10	50	0.819	3.93	44.1	2.6	41	0.000200	29.94	12.02	0.08	5.3	28	118
9		10	75	0.819	3.93	44.1	4.0	32	0.000256	35.05	10.27	0.14	7.7	38	210
10		10	100	0.819	3.93	44.1	5.3	22	0.000372	32.13	11.21	0.9	8.4	52	256
11	DE	10	0	0.817	3.92	45.12	0.1	77	0.000106	2.98	120.90	0.07	2	24	12
12		10	25	0.817	3.92	45.12	1.3	66	0.000124	23.61	15.25	0.07	2.6	26	24
13		10	50	0.817	3.92	45.12	2.6	43	0.000190	30.76	11.70	0.08	5.6	27	123
14		10	75	0.817	3.92	45.12	4.0	32	0.000255	34.34	10.48	0.1	8	34	235
15		10	100	0.817	3.92	45.12	5.3	23	0.000355	32.91	10.94	0.89	8.6	50	273
16	MPO5	5	0	0.83	3.96	44.1	0.1	73	0.000114	2.84	126.62	0.04	1.6	21	11
17		5	25	0.83	3.96	44.1	1.3	59	0.000141	21.26	16.94	0.05	2.5	22	55
18		5	50	0.83	3.96	44.1	2.6	35	0.000237	25.22	14.28	0.08	4.9	26	96
19		5	75	0.83	3.96	44.1	4.0	28	0.000296	30.26	11.90	0.24	6.2	39	262
20		5	100	0.83	3.96	44.1	5.3	18	0.000461	25.94	13.88	0.85	8	45	297
21	MPO10	10	0	0.832	3.99	44.02	0.1	73	0.000114	2.84	126.70	0.04	2	18	24
22		10	25	0.832	3.99	44.02	1.3	58	0.000143	20.88	17.24	0.05	3.1	22	78

23		10	50	0.832	3.99	44.02	2.6	34	0.000245	24.48	14.70	0.09	5.2	21	123
24		10	75	0.832	3.99	44.02	4.0	27	0.000308	29.16	12.34	0.2	6.4	34	273
25		10	100	0.832	3.99	44.02	5.3	18	0.000462	25.92	13.89	0.82	8.4	36	300
26		15	0	0.836	4.12	43.95	0.1	73	0.000115	2.83	127.10	0.04	2.1	17	35
27		15	25	0.836	4.12	43.95	1.3	59	0.000142	21.17	17.00	0.05	3.3	22	83
28	MPO15	15	50	0.836	4.12	43.95	2.6	34	0.000246	24.40	14.75	0.09	5.3	21	230
29		15	75	0.836	4.12	43.95	4.0	27	0.000310	29.07	12.38	0.18	6.6	34	280
30		15	100	0.836	4.12	43.95	5.3	17	0.000492	24.40	14.75	0.63	8.8	38	307
31		20	0	0.839	4.3	43.62	0.1	73	0.000115	2.84	126.60	0.04	2.4	15	43
32		20	25	0.839	4.3	43.62	1.3	59	0.000142	21.26	16.93	0.05	3.3	18	85
33	MPO20	20	50	0.839	4.3	43.62	2.6	33	0.000254	23.78	15.14	0.08	5.8	22	260
34		20	75	0.839	4.3	43.62	4.0	25	0.000336	27.02	13.32	0.12	6.8	30	308
35		20	100	0.839	4.3	43.62	5.3	17	0.000494	24.50	14.69	0.56	9	37	345
36		25	0	0.843	4.5	42.62	0.1	72	0.000117	2.86	126.02	0.05	2.3	15	48
37		25	25	0.843	4.5	42.62	1.3	58	0.000145	21.29	16.91	0.05	3.3	18	88
38	MPO25	25	50	0.843	4.5	42.62	2.6	33	0.000255	24.22	14.86	0.07	6.1	19	272
39		25	75	0.843	4.5	42.62	4.0	25	0.000337	27.53	13.08	0.11	7.2	27	325
40		25	100	0.843	4.5	42.62	5.3	16	0.000527	23.49	15.33	0.58	9.8	33	370
41		30	0	0.846	4.8	41.24	0.1	69	0.000123	2.82	127.69	0.05	2.5	14	50
42		30	25	0.846	4.8	41.24	1.3	56	0.000151	21.17	17.01	0.05	3.6	17	94
43	MPO30	30	50	0.846	4.8	41.24	2.6	32	0.000264	24.19	14.88	0.07	6.1	19	291
44		30	75	0.846	4.8	41.24	4.0	23	0.000368	26.08	13.80	0.1	7.8	26	350
45		30	100	0.846	4.8	41.24	5.3	16	0.000529	24.19	14.88	0.56	10.6	29	405
46		5	0	0.824	3.96	44.8	0.1	73	0.000113	2.82	127.70	0.04	1.8	18	12
47		5	25	0.824	3.96	44.8	1.3	64	0.000129	22.86	15.75	0.05	2.5	21	56
48	MPA5	5	50	0.824	3.96	44.8	2.6	38	0.000217	27.15	13.26	0.08	5.3	23	97
49		5	75	0.824	3.96	44.8	4.0	28	0.000294	30.01	12.00	0.26	6.4	39	278
50		5	100	0.824	3.96	44.8	5.3	18	0.000458	25.72	14.00	0.82	8.1	44	300

51		10	0	0.826	3.99	44.35	0.1	72	0.000115	2.80	128.49	0.04	2.3	19	28
52		10	25	0.826	3.99	44.35	1.3	59	0.000140	21.24	16.95	0.04	3.5	22	81
53	MPA10	10	50	0.826	3.99	44.35	2.6	36	0.000229	25.92	13.89	0.06	5.6	25	125
54		10	75	0.826	3.99	44.35	4.0	28	0.000295	30.24	11.91	0.24	7	37	292
55		10	100	0.826	3.99	44.35	5.3	17	0.000486	24.48	14.71	0.75	9.2	44	312
56		15	0	0.829	4.12	43.8	0.1	71	0.000117	2.79	129.15	0.04	2.5	18	36
57		15	25	0.829	4.12	43.8	1.3	63	0.000132	22.88	15.73	0.05	3.3	18	84
58	MPA15	15	50	0.829	4.12	43.8	2.6	36	0.000230	26.15	13.77	0.06	5.4	20	231
59		15	75	0.829	4.12	43.8	4.0	27	0.000307	29.42	12.24	0.23	6	32	300
60		15	100	0.829	4.12	43.8	5.3	17	0.000488	24.69	14.58	0.69	9.4	36	320
61		20	0	0.834	4.22	43.7	0.1	71	0.000117	2.78	129.63	0.04	2.5	17	45
62		20	25	0.834	4.22	43.7	1.3	63	0.000132	22.79	15.79	0.05	3.6	18	89
63	MPA20	20	50	0.834	4.22	43.7	2.6	34	0.000245	24.60	14.63	0.06	5.8	19	279
64		20	75	0.834	4.22	43.7	4.0	27	0.000309	29.31	12.28	0.19	6.4	27	320
65		20	100	0.834	4.22	43.7	5.3	17	0.000491	24.60	14.63	0.55	9.8	33	367
66		25	0	0.837	4.4	43	0.1	70	0.000120	2.77	129.84	0.05	2.5	14	50
67		25	25	0.837	4.4	43	1.3	63	0.000133	23.08	15.60	0.05	4.1	16	96
68	MPA25	25	50	0.837	4.4	43	2.6	34	0.000246	24.91	14.45	0.07	6.1	18	284
69		25	75	0.837	4.4	43	4.0	26	0.000322	28.58	12.60	0.18	7.1	27	349
70		25	100	0.837	4.4	43	5.3	17	0.000492	24.91	14.45	0.55	10	28	373
71		30	0	0.84	4.65	42.32	0.1	69	0.000122	2.77	130.10	0.05	2.6	12	52
72		30	25	0.84	4.65	42.32	1.3	63	0.000133	23.37	15.40	0.05	4.1	15	116
73	MPA30	30	50	0.84	4.65	42.32	2.6	34	0.000247	25.22	14.27	0.11	6.2	16	302
74		30	75	0.84	4.65	42.32	4.0	25	0.000336	27.82	12.94	0.18	7.3	24	353
75		30	100	0.84	4.65	42.32	5.3	16	0.000525	23.74	15.16	0.56	10.5	26	425
76		5	0	0.832	3.94	44.22	0.1	75	0.000111	2.91	123.88	0.03	1.8	17	10
77	MPE5	5	25	0.832	3.94	44.22	1.3	66	0.000126	23.66	15.22	0.05	2.6	19	57
78		5	50	0.832	3.94	44.22	2.6	41	0.000203	29.39	12.25	0.07	5.6	22	102

79		5	75	0.832	3.94	44.22	4.0	29	0.000287	31.18	11.55	0.25	6.6	36	280
80		5	100	0.832	3.94	44.22	5.3	19	0.000438	27.24	13.22	0.76	9.5	42	310
81		10	0	0.832	3.98	44.5	0.1	74	0.000112	2.85	126.35	0.04	2.3	16	15
82		10	25	0.832	3.98	44.5	1.3	66	0.000126	23.51	15.31	0.05	3.8	18	86
83	MPE10	10	50	0.832	3.98	44.5	2.6	40	0.000208	28.49	12.63	0.07	5.8	23	130
84		10	75	0.832	3.98	44.5	4.0	29	0.000287	30.99	11.62	0.27	7.1	36	293
85		10	100	0.832	3.98	44.5	5.3	19	0.000438	27.07	13.30	0.7	9.6	43	317
86		15	0	0.834	4.08	44	0.1	74	0.000113	2.87	125.23	0.04	2.6	15	15
87		15	25	0.834	4.08	44	1.3	65	0.000128	23.36	15.41	0.06	3.8	18	86
88	MPE15	15	50	0.834	4.08	44	2.6	38	0.000219	27.31	13.18	0.07	6.1	20	240
89		15	75	0.834	4.08	44	4.0	28	0.000298	30.18	11.93	0.27	6.7	30	310
90		15	100	0.834	4.08	44	5.3	19	0.000439	27.31	13.18	0.62	9.6	35	330
91		20	0	0.835	4.15	43.9	0.1	73	0.000114	2.84	126.81	0.04	2.8	12	44
92		20	25	0.835	4.15	43.9	1.3	65	0.000128	23.38	15.40	0.05	3.8	16	87
93	MPE20	20	50	0.835	4.15	43.9	2.6	35	0.000239	25.18	14.30	0.09	5.9	16	285
94		20	75	0.835	4.15	43.9	4.0	28	0.000298	30.22	11.91	0.21	6.8	26	324
95		20	100	0.835	4.15	43.9	5.3	18	0.000464	25.90	13.90	0.55	10.1	32	375
96		25	0	0.839	4.35	43.12	0.1	73	0.000115	2.88	125.15	0.05	2.6	10	49
97		25	25	0.839	4.35	43.12	1.3	64	0.000131	23.33	15.43	0.05	4.2	11	102
98	MPE25	25	50	0.839	4.35	43.12	2.6	35	0.000240	25.51	14.11	0.06	6.2	14	291
99		25	75	0.839	4.35	43.12	4.0	27	0.000311	29.52	12.19	0.16	7.1	25	347
100		25	100	0.839	4.35	43.12	5.3	18	0.000466	26.24	13.72	0.52	10.4	26	395
101		30	0	0.841	4.46	42.6	0.1	73	0.000115	2.90	123.94	0.05	2.6	10	54
102		30	25	0.841	4.46	42.6	1.3	64	0.000131	23.56	15.28	0.05	4.2	11	119
103	MPE30	30	50	0.841	4.46	42.6	2.6	35	0.000240	25.76	13.97	0.09	6.7	15	329
104		30	75	0.841	4.46	42.6	4.0	27	0.000311	29.81	12.08	0.18	7.5	23	382
105		30	100	0.841	4.46	42.6	5.3	18	0.000467	26.50	13.58	0.49	10.8	25	429
106	MWO5	5	0	0.829	3.86	48.24	0.1	77	0.000108	2.74	131.16	0.05	2.0	21	10

107		5	25	0.829	3.86	48.24	1.3	66	0.000126	21.76	16.54	0.07	2.3	24	72
108		5	50	0.829	3.86	48.24	2.6	41	0.000202	27.04	13.31	0.09	4.3	27	180
109		5	75	0.829	3.86	48.24	4.0	28	0.000296	27.70	13.00	0.24	5.8	40	230
110		5	100	0.829	3.86	48.24	5.3	20	0.000415	26.38	13.65	0.90	7.3	48	259
111	MWO10	10	0	0.831	3.98	44.56	0.1	77	0.000108	2.96	121.44	0.05	1.8	19	15
112		10	25	0.831	3.98	44.56	1.3	65	0.000128	23.10	15.58	0.07	3.3	22	76
113		10	50	0.831	3.98	44.56	2.6	40	0.000209	28.37	12.69	0.08	5.3	25	196
114		10	75	0.831	3.98	44.56	4.0	28	0.000297	29.91	12.03	0.23	5.8	38	238
115		10	100	0.831	3.98	44.56	5.3	20	0.000416	28.49	12.64	0.78	8.9	45	262
116	MWO15	15	0	0.834	4.02	44.22	0.1	77	0.000108	2.98	120.95	0.05	1.8	18	31
117		15	25	0.834	4.02	44.22	1.3	66	0.000126	23.60	15.26	0.07	3.5	20	61
118		15	50	0.834	4.02	44.22	2.6	40	0.000209	28.48	12.64	0.09	5.5	24	130
119		15	75	0.834	4.02	44.22	4.0	26	0.000321	27.89	12.91	0.18	5.7	35	240
120		15	100	0.834	4.02	44.22	5.3	19	0.000439	27.17	13.25	0.60	8.9	42	280
121	MWO20	20	0	0.836	4.18	43.92	0.1	77	0.000109	2.99	120.42	0.05	1.9	16	43
122		20	25	0.836	4.18	43.92	1.3	66	0.000127	23.70	15.19	0.07	3.7	24	79
123		20	50	0.836	4.18	43.92	2.6	39	0.000216	27.77	12.97	0.09	5.8	24	150
124		20	75	0.836	4.18	43.92	4.0	26	0.000322	28.01	12.85	0.15	5.8	31	248
125		20	100	0.836	4.18	43.92	5.3	18	0.000464	25.86	13.92	0.60	8.9	41	301
126	MWO25	25	0	0.838	4.4	43.26	0.1	73	0.000115	2.87	125.43	0.05	1.9	16	46
127		25	25	0.838	4.4	43.26	1.3	60	0.000140	21.81	16.50	0.07	3.7	23	80
128		25	50	0.838	4.4	43.26	2.6	35	0.000240	25.38	14.18	0.09	5.9	21	162
129		25	75	0.838	4.4	43.26	4.0	24	0.000352	25.99	13.85	0.13	6.2	28	252
130		25	100	0.838	4.4	43.26	5.3	17	0.000493	24.73	14.55	0.54	8.8	38	320
131	MWO30	30	0	0.842	4.6	42.92	0.1	69	0.000122	2.72	132.26	0.05	2.0	15	46
132		30	25	0.842	4.6	42.92	1.3	56	0.000150	20.43	17.62	0.07	3.9	17	112
133		30	50	0.842	4.6	42.92	2.6	32	0.000263	23.35	15.42	0.09	6.3	21	183
134		30	75	0.842	4.6	42.92	4.0	26	0.000324	28.46	12.65	0.10	6.5	28	280

135		30	100	0.842	4.6	42.92	5.3	17	0.000495	24.81	14.51	0.54	8.8	30	357
136	MWA5	5	0	0.824	3.96	45.3	0.1	74	0.000111	2.83	127.38	0.05	2.1	18	11
137		5	25	0.824	3.96	45.3	1.3	65	0.000127	22.96	15.68	0.07	2.4	21	76
138		5	50	0.824	3.96	45.3	2.6	39	0.000211	27.55	13.06	0.09	4.6	23	189
139		5	75	0.824	3.96	45.3	4.0	30	0.000275	31.79	11.32	0.26	6.1	37	242
140		5	100	0.824	3.96	45.3	5.3	21	0.000392	29.67	12.13	0.87	7.7	45	272
141	MWA10	10	0	0.827	4	44.9	0.1	74	0.000112	2.84	126.72	0.04	2.2	17	16
142		10	25	0.827	4	44.9	1.3	60	0.000138	21.31	16.90	0.06	4.1	19	80
143		10	50	0.827	4	44.9	2.6	37	0.000224	26.28	13.70	0.07	6.6	22	206
144		10	75	0.827	4	44.9	4.0	30	0.000276	31.96	11.26	0.20	7.2	33	250
145		10	100	0.827	4	44.9	5.3	20	0.000414	28.41	12.67	0.68	11.0	39	275
146	MWA15	15	0	0.829	4.02	44.1	0.1	72	0.000115	2.81	128.23	0.04	2.2	16	33
147		15	25	0.829	4.02	44.1	1.3	57	0.000145	20.56	17.51	0.06	4.3	17	64
148		15	50	0.829	4.02	44.1	2.6	37	0.000224	26.69	13.49	0.08	6.8	21	137
149		15	75	0.829	4.02	44.1	4.0	29	0.000286	31.38	11.47	0.16	7.1	31	252
150		15	100	0.829	4.02	44.1	5.3	20	0.000415	28.86	12.48	0.52	11.0	37	294
151	MWA 20	20	0	0.831	4.16	43.2	0.1	72	0.000115	2.86	125.91	0.04	2.4	14	45
152		20	25	0.831	4.16	43.2	1.3	57	0.000146	20.94	17.19	0.06	4.6	21	83
153		20	50	0.831	4.16	43.2	2.6	35	0.000237	25.71	14.00	0.08	7.2	21	158
154		20	75	0.831	4.16	43.2	4.0	29	0.000287	31.96	11.27	0.13	7.2	27	260
155		20	100	0.831	4.16	43.2	5.3	19	0.000437	27.92	12.90	0.52	11.0	36	316
156	MWA 25	25	0	0.836	4.3	42.98	0.1	72	0.000116	2.86	126.02	0.04	2.4	14	48
157		25	25	0.836	4.3	42.98	1.3	57	0.000147	20.92	17.21	0.06	4.6	20	84
158		25	50	0.836	4.3	42.98	2.6	35	0.000239	25.69	14.01	0.08	7.3	18	170
159		25	75	0.836	4.3	42.98	4.0	28	0.000299	30.83	11.68	0.11	7.7	24	265
160		25	100	0.836	4.3	42.98	5.3	19	0.000440	27.89	12.91	0.47	10.9	33	336
161	MWA 30	30	0	0.838	4.59	42.92	0.1	72	0.000116	2.85	126.15	0.04	2.5	13	48
162		30	25	0.838	4.59	42.92	1.3	57	0.000147	20.90	17.23	0.06	4.8	15	118

163		30	50	0.838	4.59	42.92	2.6	35	0.000239	25.66	14.03	0.08	7.8	18	192
164		30	75	0.838	4.59	42.92	4.0	27	0.000310	29.70	12.12	0.09	8.1	24	294
165		30	100	0.838	4.59	42.92	5.3	18	0.000466	26.40	13.64	0.47	10.9	26	375
166		5	0	0.823	3.94	45.71	0.1	81	0.000102	3.07	117.28	0.04	2.3	17	9
167		5	25	0.823	3.94	45.71	1.3	70	0.000118	24.54	14.67	0.07	2.4	19	75
168	MWE5	5	50	0.823	3.94	45.71	2.6	44	0.000187	30.85	11.67	0.08	4.9	22	191
169		5	75	0.823	3.94	45.71	4.0	31	0.000265	32.60	11.04	0.25	6.2	32	252
170		5	100	0.823	3.94	45.71	5.3	20	0.000412	28.04	12.84	0.80	8.7	38	286
171		10	0	0.826	3.98	45.24	0.1	79	0.000105	3.01	119.45	0.04	2.5	15	17
172		10	25	0.826	3.98	45.24	1.3	69	0.000120	24.35	14.79	0.06	4.5	18	85
173	MWE10	10	50	0.826	3.98	45.24	2.6	42	0.000197	29.64	12.14	0.06	7.3	20	220
174		10	75	0.826	3.98	45.24	4.0	30	0.000275	31.76	11.34	0.18	8.0	30	267
175		10	100	0.826	3.98	45.24	5.3	20	0.000413	28.23	12.75	0.62	12.3	36	294
176		15	0	0.828	4	44.9	0.1	78	0.000106	2.99	120.36	0.04	2.5	14	35
177		15	25	0.828	4	44.9	1.3	68	0.000122	24.12	14.93	0.06	4.8	16	69
178	MWE15	15	50	0.828	4	44.9	2.6	40	0.000207	28.38	12.69	0.07	7.6	19	146
179		15	75	0.828	4	44.9	4.0	30	0.000276	31.92	11.28	0.14	7.9	28	270
180		15	100	0.828	4	44.9	5.3	19	0.000436	26.96	13.35	0.48	12.3	34	315
181		20	0	0.832	4.12	44.22	0.1	75	0.000111	2.91	123.88	0.04	2.6	13	48
182		20	25	0.832	4.12	44.22	1.3	67	0.000124	24.01	14.99	0.06	5.1	19	89
183	MWE20	20	50	0.832	4.12	44.22	2.6	39	0.000213	27.96	12.88	0.07	8.0	19	169
184		20	75	0.832	4.12	44.22	4.0	30	0.000277	32.26	11.16	0.12	8.0	25	279
185		20	100	0.832	4.12	44.22	5.3	19	0.000438	27.24	13.22	0.48	12.3	33	338
186		25	0	0.834	4.32	43.8	0.1	75	0.000111	2.93	123.00	0.04	2.6	13	52
187		25	25	0.834	4.32	43.8	1.3	66	0.000126	23.82	15.11	0.06	5.1	18	90
188	MWE25	25	50	0.834	4.32	43.8	2.6	37	0.000225	26.71	13.48	0.07	8.1	17	182
189		25	75	0.834	4.32	43.8	4.0	29	0.000288	31.41	11.46	0.10	8.5	22	283
190		25	100	0.834	4.32	43.8	5.3	19	0.000439	27.43	13.12	0.43	12.1	30	360

191		30	0	0.838	4.54	43	0.1	74	0.000113	2.93	122.97	0.04	2.8	12	52
192		30	25	0.838	4.54	43	1.3	66	0.000127	24.15	14.91	0.06	5.4	14	126
193	MWE30	30	50	0.838	4.54	43	2.6	36	0.000233	26.35	13.66	0.07	8.7	17	206
194		30	75	0.838	4.54	43	4.0	28	0.000299	30.74	11.71	0.08	9.0	22	315
195		30	100	0.838	4.54	43	5.3	18	0.000466	26.35	13.66	0.43	12.1	24	401
196		5	0	0.829	4	44.65	0.1	74	0.000112	2.85	126.32	0.05	1.6	20	10
197		5	25	0.829	4	44.65	1.3	61	0.000136	21.73	16.57	0.07	2.5	24	65
198	MPWO5	5	50	0.829	4	44.65	2.6	37	0.000224	26.36	13.66	0.09	4.6	26	145
199		5	75	0.829	4	44.65	4.0	29	0.000286	30.99	11.62	0.24	6.0	40	241
200		5	100	0.829	4	44.65	5.3	20	0.000415	28.50	12.63	0.88	7.7	46	273
201		10	0	0.832	4.08	44.5	0.1	74	0.000112	2.85	126.35	0.05	1.8	18	17
202		10	25	0.832	4.08	44.5	1.3	60	0.000139	21.36	16.86	0.07	3.3	22	76
203	MPWO10	10	50	0.832	4.08	44.5	2.6	36	0.000231	25.60	14.06	0.09	5.5	23	158
204		10	75	0.832	4.08	44.5	4.0	29	0.000287	30.99	11.62	0.20	6.6	35	260
205		10	100	0.832	4.08	44.5	5.3	20	0.000416	28.49	12.63	0.81	8.6	43	286
206		15	0	0.836	4.12	44	0.1	72	0.000116	2.79	129.02	0.05	1.9	18	33
207		15	25	0.836	4.12	44	1.3	58	0.000144	20.79	17.31	0.07	3.6	22	75
208	MPWO15	15	50	0.836	4.12	44	2.6	34	0.000246	24.38	14.77	0.09	5.6	22	189
209		15	75	0.836	4.12	44	4.0	27	0.000310	29.04	12.40	0.18	6.0	35	264
210		15	100	0.836	4.12	44	5.3	19	0.000440	27.24	13.21	0.64	9.0	41	300
211		20	0	0.839	4.25	43.5	0.1	74	0.000113	2.89	124.55	0.05	2.1	16	45
212		20	25	0.839	4.25	43.5	1.3	61	0.000138	22.04	16.33	0.07	3.5	23	80
213	MPWO20	20	50	0.839	4.25	43.5	2.6	35	0.000240	25.21	14.28	0.09	5.9	23	190
214		20	75	0.839	4.25	43.5	4.0	25	0.000336	27.03	13.32	0.15	6.0	31	287
215		20	100	0.839	4.25	43.5	5.3	18	0.000466	26.01	13.84	0.60	9.1	40	325
216		25	0	0.841	4.6	42.92	0.1	70	0.000120	2.76	130.22	0.05	2.0	16	45
217	MPWO25	25	25	0.841	4.6	42.92	1.3	56	0.000150	20.46	17.60	0.07	3.6	20	83
218		25	50	0.841	4.6	42.92	2.6	37	0.000227	27.03	13.32	0.09	5.9	21	193

219		25	75	0.841	4.6	42.92	4.0	23	0.000366	25.21	14.28	0.11	7.0	27	302
220		25	100	0.841	4.6	42.92	5.3	17	0.000495	24.84	14.49	0.55	9.4	35	347
221		30	0	0.843	4.8	42.12	0.1	69	0.000122	2.77	129.95	0.05	2.3	14	47
222		30	25	0.843	4.8	42.12	1.3	56	0.000151	20.80	17.31	0.07	3.7	17	110
223	MPWO30	30	50	0.843	4.8	42.12	2.6	32	0.000263	23.77	15.15	0.09	6.1	20	225
224		30	75	0.843	4.8	42.12	4.0	23	0.000367	25.62	14.05	0.10	7.2	27	310
225		30	100	0.843	4.8	42.12	5.3	16	0.000527	23.77	15.15	0.52	10.0	30	393
226		5	0	0.823	3.99	45.42	0.1	74	0.000111	2.82	127.56	0.04	1.9	18	11
227		5	25	0.823	3.99	45.42	1.3	64	0.000129	22.58	15.95	0.06	2.4	21	65
228	MPWA5	5	50	0.823	3.99	45.42	2.6	39	0.000211	27.52	13.08	0.08	4.9	22	141
229		5	75	0.823	3.99	45.42	4.0	28	0.000294	29.63	12.15	0.26	6.2	37	250
230		5	100	0.823	3.99	45.42	5.3	20	0.000412	28.22	12.76	0.83	7.5	43	282
231		10	0	0.826	4.04	45.34	0.1	74	0.000112	2.82	127.80	0.04	2.2	16	22
232		10	25	0.826	4.04	45.34	1.3	59	0.000140	20.77	17.33	0.05	3.7	18	79
233	MPWA10	10	50	0.826	4.04	45.34	2.6	37	0.000223	26.06	13.82	0.06	6.0	22	162
234		10	75	0.826	4.04	45.34	4.0	28	0.000295	29.58	12.17	0.22	7.0	27	267
235		10	100	0.826	4.04	45.34	5.3	19	0.000435	26.76	13.45	0.70	10.0	34	290
236		15	0	0.829	4.09	44.02	0.1	72	0.000115	2.81	127.99	0.04	2.3	16	34
237		15	25	0.829	4.09	44.02	1.3	56	0.000148	20.24	17.79	0.05	3.9	18	73
238	MPWA15	15	50	0.829	4.09	44.02	2.6	37	0.000224	26.74	13.46	0.07	6.2	19	181
239		15	75	0.829	4.09	44.02	4.0	27	0.000307	29.27	12.30	0.19	6.4	31	272
240		15	100	0.829	4.09	44.02	5.3	19	0.000436	27.46	13.11	0.60	10.1	38	302
241		20	0	0.832	4.2	43.22	0.1	72	0.000116	2.85	126.12	0.04	2.4	13	44
242		20	25	0.832	4.2	43.22	1.3	56	0.000149	20.54	17.53	0.05	4.0	20	85
243	MPWA20	20	50	0.832	4.2	43.22	2.6	35	0.000238	25.67	14.02	0.07	6.4	18	215
244		20	75	0.832	4.2	43.22	4.0	27	0.000308	29.70	12.12	0.16	6.7	27	286
245		20	100	0.832	4.2	43.22	5.3	19	0.000438	27.87	12.92	0.58	10.3	35	336
246	MPWA25	25	0	0.835	4.5	43.26	0.1	72	0.000116	2.84	126.69	0.05	2.4	11	48

247		25	25	0.835	4.5	43.26	1.3	56	0.000149	20.44	17.61	0.05	4.3	12	89
248		25	50	0.835	4.5	43.26	2.6	35	0.000239	25.55	14.09	0.07	6.6	15	224
249		25	75	0.835	4.5	43.26	4.0	26	0.000321	28.47	12.64	0.14	7.3	25	302
250		25	100	0.835	4.5	43.26	5.3	18	0.000464	26.28	13.70	0.50	10.3	28	345
251		30	0	0.838	4.69	42.52	0.1	72	0.000116	2.88	124.97	0.05	2.5	10	49
252		30	25	0.838	4.69	42.52	1.3	56	0.000150	20.72	17.37	0.05	4.4	11	115
253	MPWA30	30	50	0.838	4.69	42.52	2.6	35	0.000239	25.91	13.90	0.09	6.9	16	243
254		30	75	0.838	4.69	42.52	4.0	25	0.000335	27.76	12.97	0.13	7.6	24	319
255		30	100	0.838	4.69	42.52	5.3	17	0.000493	25.17	14.31	0.51	10.6	26	394
256		5	0	0.824	3.96	45.88	0.1	81	0.000102	3.05	117.86	0.04	1.8	17	9
257		5	25	0.824	3.96	45.88	1.3	70	0.000118	24.42	14.74	0.07	2.6	20	67
258	MPWE5	5	50	0.824	3.96	45.88	2.6	47	0.000175	32.79	10.98	0.08	5.3	22	154
259		5	75	0.824	3.96	45.88	4.0	36	0.000229	37.67	9.56	0.25	6.4	35	252
260		5	100	0.824	3.96	45.88	5.3	21	0.000392	29.30	12.29	0.79	9.1	41	280
261		10	0	0.826	3.97	45.66	0.1	78	0.000106	2.95	122.11	0.05	2.1	17	11
262		10	25	0.826	3.97	45.66	1.3	69	0.000120	24.12	14.92	0.07	4.0	20	84
263	MPWE10	10	50	0.826	3.97	45.66	2.6	40	0.000207	27.97	12.87	0.07	5.7	22	144
264		10	75	0.826	3.97	45.66	4.0	32	0.000258	33.56	10.73	0.27	7.3	33	252
265		10	100	0.826	3.97	45.66	5.3	20	0.000413	27.97	12.87	0.69	9.8	39	302
266		15	0	0.828	4.06	45	0.1	78	0.000106	2.98	120.63	0.05	2.4	16	14
267		15	25	0.828	4.06	45	1.3	68	0.000122	24.07	14.96	0.08	4.1	17	78
268	MPWE15	15	50	0.828	4.06	45	2.6	40	0.000207	28.31	12.72	0.07	6.2	19	153
269		15	75	0.828	4.06	45	4.0	32	0.000259	33.97	10.60	0.27	5.6	30	203
270		15	100	0.828	4.06	45	5.3	19	0.000436	26.90	13.38	0.63	9.8	34	313
271		20	0	0.833	4.18	44.12	0.1	75	0.000111	2.91	123.75	0.05	2.5	15	46
272	MPWE20	20	25	0.833	4.18	44.12	1.3	67	0.000124	24.04	14.98	0.07	4.0	18	82
273		20	50	0.833	4.18	44.12	2.6	39	0.000214	27.99	12.86	0.10	6.0	19	208
274		20	75	0.833	4.18	44.12	4.0	30	0.000278	32.29	11.15	0.26	6.0	26	302

275		20	100	0.833	4.18	44.12	5.3	19	0.000438	27.27	13.20	0.59	10.2	32	353
276	MPWE25	25	0	0.836	4.49	43.98	0.1	75	0.000111	2.91	123.80	0.05	2.1	13	46
277		25	25	0.836	4.49	43.98	1.3	65	0.000129	23.31	15.44	0.07	4.6	17	96
278		25	50	0.836	4.49	43.98	2.6	37	0.000226	26.54	13.56	0.08	6.0	17	206
279		25	75	0.836	4.49	43.98	4.0	28	0.000299	30.13	11.95	0.16	6.9	24	322
280		25	100	0.836	4.49	43.98	5.3	19	0.000440	27.26	13.21	0.49	10.0	29	370
281	MPWE30	30	0	0.838	4.65	42.92	0.1	74	0.000113	2.93	122.74	0.05	2.3	12	51
282		30	25	0.838	4.65	42.92	1.3	66	0.000127	24.20	14.88	0.07	4.3	14	139
283		30	50	0.838	4.65	42.92	2.6	35	0.000239	25.66	14.03	0.12	6.4	15	254
284		30	75	0.838	4.65	42.92	4.0	27	0.000310	29.70	12.12	0.18	6.9	23	338
285		30	100	0.838	4.65	42.92	5.3	19	0.000441	27.86	12.92	0.46	10.2	25	416
286	RPO5	5	0	0.83	3.96	44.52	0.1	66	0.000126	2.55	141.39	0.03	1.8	16	12
287		5	25	0.83	3.96	44.52	1.3	53	0.000157	18.91	19.03	0.04	2.8	17	60
288		5	50	0.83	3.96	44.52	2.6	32	0.000259	22.84	15.76	0.06	5.4	20	105
289		5	75	0.83	3.96	44.52	4.0	25	0.000332	26.76	13.45	0.17	6.8	29	286
290		5	100	0.83	3.96	44.52	5.3	17	0.000488	24.27	14.84	0.60	8.8	34	324
291	RPO10	10	0	0.86	4	44.1	0.1	62	0.000139	2.33	154.48	0.03	2.2	14	28
292		10	25	0.86	4	44.1	1.3	50	0.000172	17.38	20.71	0.04	3.4	17	90
293		10	50	0.86	4	44.1	2.6	29	0.000297	20.17	17.85	0.06	6.2	18	141
294		10	75	0.86	4	44.1	4.0	26	0.000331	27.12	13.27	0.14	7.0	26	314
295		10	100	0.86	4	44.1	5.3	17	0.000506	23.64	15.23	0.59	9.2	27	345
296	RPO15	15	0	0.89	4.19	43.76	0.1	60	0.000148	2.20	163.92	0.03	1.6	14	42
297		15	25	0.89	4.19	43.76	1.3	48	0.000185	16.25	22.15	0.04	2.5	18	99
298		15	50	0.89	4.19	43.76	2.6	27	0.000330	18.28	19.69	0.07	4.1	18	273
299		15	75	0.89	4.19	43.76	4.0	25	0.000356	25.39	14.18	0.14	5.0	27	333
300		15	100	0.89	4.19	43.76	5.3	17	0.000524	23.02	15.64	0.50	6.6	30	365
301	RPO20	20	0	0.92	4.42	43.25	0.1	57	0.000161	2.04	176.28	0.03	2.9	12	51
302		20	25	0.92	4.42	43.25	1.3	45	0.000204	14.91	24.14	0.04	4.0	14	100

303		20	50	0.92	4.42	43.25	2.6	25	0.000368	16.57	21.73	0.06	7.0	16	307
304		20	75	0.92	4.42	43.25	4.0	23	0.000400	22.87	15.74	0.09	8.2	24	363
305		20	100	0.92	4.42	43.25	5.3	16	0.000575	21.21	16.97	0.44	10.8	30	407
306	RPO25	25	0	0.94	5	42.9	0.1	56	0.000168	1.98	181.85	0.04	3.1	12	58
307		25	25	0.94	5	42.9	1.3	43	0.000219	14.06	25.60	0.04	4.1	14	106
308		25	50	0.94	5	42.9	2.6	25	0.000376	16.35	22.02	0.05	7.6	15	326
309		25	75	0.94	5	42.9	4.0	21	0.000448	20.60	17.48	0.09	9.0	22	390
310		25	100	0.94	5	42.9	5.3	15	0.000627	19.62	18.35	0.45	12.3	26	444
311	RPO30	30	0	0.96	5.2	42.1	0.1	53	0.000181	1.87	192.57	0.03	3.4	11	60
312		30	25	0.96	5.2	42.1	1.3	42	0.000229	13.70	26.27	0.03	4.7	14	113
313		30	50	0.96	5.2	42.1	2.6	24	0.000400	15.66	22.99	0.04	7.9	16	349
314		30	75	0.96	5.2	42.1	4.0	18	0.000533	17.62	20.43	0.06	10.1	22	420
315		30	100	0.96	5.2	42.1	5.3	13	0.000738	16.97	21.22	0.35	13.8	24	486
316	RPA5	5	0	0.828	3.97	44.71	0.1	67	0.000124	2.58	139.53	0.03	1.8	14	13
317		5	25	0.828	3.97	44.71	1.3	54	0.000153	19.23	18.72	0.03	2.8	15	66
318		5	50	0.828	3.97	44.71	2.6	32	0.000259	22.80	15.79	0.05	5.5	18	115
319		5	75	0.828	3.97	44.71	4.0	26	0.000318	27.78	12.96	0.16	7.0	26	314
320		5	100	0.828	3.97	44.71	5.3	18	0.000460	25.65	14.04	0.57	9.0	30	356
321	RPA10	10	0	0.85	3.97	44.19	0.1	63	0.000135	2.39	150.56	0.03	2.2	12	28
322		10	25	0.85	3.97	44.19	1.3	52	0.000163	18.26	19.72	0.03	3.5	18	92
323		10	50	0.85	3.97	44.19	2.6	29	0.000293	20.36	17.68	0.06	6.3	20	146
324		10	75	0.85	3.97	44.19	4.0	26	0.000327	27.38	13.15	0.14	7.2	28	323
325		10	100	0.85	3.97	44.19	5.3	17	0.000500	23.87	15.08	0.56	9.4	30	355
326	RPA15	15	0	0.89	4.04	43.9	0.1	62	0.000144	2.26	159.14	0.03	1.6	15	43
327		15	25	0.89	4.04	43.9	1.3	49	0.000182	16.54	21.77	0.04	2.5	19	103
328		15	50	0.89	4.04	43.9	2.6	27	0.000330	18.23	19.75	0.07	4.2	20	284
329		15	75	0.89	4.04	43.9	4.0	26	0.000342	26.33	13.68	0.14	5.1	30	346
330		15	100	0.89	4.04	43.9	5.3	17	0.000524	22.95	15.69	0.48	6.8	33	379

331	RPA20	20	0	0.91	4.6	43.6	0.1	58	0.000157	2.08	172.75	0.03	3.0	11	54
332		20	25	0.91	4.6	43.6	1.3	46	0.000198	15.29	23.55	0.04	4.1	13	107
333		20	50	0.91	4.6	43.6	2.6	26	0.000350	17.28	20.83	0.06	7.2	14	328
334		20	75	0.91	4.6	43.6	4.0	24	0.000379	23.93	15.04	0.09	8.4	22	389
335		20	100	0.91	4.6	43.6	5.3	17	0.000535	22.60	15.93	0.41	11.1	27	436
336	RPA25	25	0	0.94	4.71	43.3	0.1	58	0.000162	2.03	177.22	0.04	3.3	11	63
337		25	25	0.94	4.71	43.3	1.3	45	0.000209	14.58	24.69	0.04	4.3	13	116
338		25	50	0.94	4.71	43.3	2.6	25	0.000376	16.20	22.22	0.05	7.9	14	359
339		25	75	0.94	4.71	43.3	4.0	23	0.000409	22.35	16.10	0.08	9.4	19	429
340		25	100	0.94	4.71	43.3	5.3	16	0.000588	20.73	17.36	0.43	12.7	24	488
341	RPA30	30	0	0.95	4.8	42.3	0.1	54	0.000176	1.92	187.93	0.03	3.7	9	68
342		30	25	0.95	4.8	42.3	1.3	43	0.000221	14.11	25.51	0.03	5.1	11	127
343		30	50	0.95	4.8	42.3	2.6	24	0.000396	15.75	22.86	0.04	8.7	13	395
344		30	75	0.95	4.8	42.3	4.0	19	0.000500	18.70	19.25	0.06	11.2	17	475
345		30	100	0.95	4.8	42.3	5.3	15	0.000633	19.69	18.28	0.34	15.2	19	549
346	RPE5	5	0	0.826	3.94	44.82	0.1	68	0.000121	2.62	137.49	0.03	2.1	13	14
347		5	25	0.826	3.94	44.82	1.3	55	0.000150	19.59	18.38	0.03	3.3	14	72
348		5	50	0.826	3.94	44.82	2.6	33	0.000250	23.51	15.31	0.05	6.4	17	126
349		5	75	0.826	3.94	44.82	4.0	28	0.000295	29.92	12.03	0.15	8.1	25	343
350		5	100	0.826	3.94	44.82	5.3	18	0.000459	25.65	14.04	0.54	10.5	29	388
351	RPE10	10	0	0.84	3.96	44.5	0.1	65	0.000129	2.48	145.23	0.03	2.5	12	29
352		10	25	0.84	3.96	44.5	1.3	54	0.000156	19.05	18.90	0.03	3.8	18	95
353		10	50	0.84	3.96	44.5	2.6	30	0.000280	21.17	17.01	0.06	6.9	20	150
354		10	75	0.84	3.96	44.5	4.0	27	0.000311	28.57	12.60	0.13	7.9	28	333
355		10	100	0.84	3.96	44.5	5.3	18	0.000467	25.40	14.17	0.53	10.4	30	366
356	RPE15	15	0	0.85	4.02	44.32	0.1	64	0.000133	2.42	148.65	0.03	1.7	14	45
357		15	25	0.85	4.02	44.32	1.3	50	0.000170	17.50	20.57	0.04	2.6	18	106
358		15	50	0.85	4.02	44.32	2.6	28	0.000304	19.60	18.37	0.06	4.3	18	293

359		15	75	0.85	4.02	44.32	4.0	26	0.000327	27.30	13.19	0.13	5.2	27	356
360		15	100	0.85	4.02	44.32	5.3	17	0.000500	23.80	15.12	0.45	6.9	30	391
361	RPE20	20	0	0.91	4.2	43.92	0.1	60	0.000152	2.14	168.22	0.03	3.1	10	56
362		20	25	0.91	4.2	43.92	1.3	48	0.000190	15.84	22.73	0.04	4.3	12	111
363		20	50	0.91	4.2	43.92	2.6	28	0.000325	18.48	19.48	0.06	7.5	14	338
364		20	75	0.91	4.2	43.92	4.0	25	0.000364	24.74	14.55	0.08	8.8	20	401
365		20	100	0.91	4.2	43.92	5.3	17	0.000535	22.44	16.05	0.39	11.7	25	449
366	RPE25	25	0	0.93	4.5	43.6	0.1	59	0.000158	2.07	173.55	0.04	3.4	10	65
367		25	25	0.93	4.5	43.6	1.3	50	0.000186	16.26	22.14	0.04	4.5	12	118
368		25	50	0.93	4.5	43.6	2.6	26	0.000358	16.91	21.29	0.05	8.2	12	366
369		25	75	0.93	4.5	43.6	4.0	25	0.000372	24.39	14.76	0.08	9.7	17	438
370		25	100	0.92	4.5	43.6	5.3	16	0.000575	21.04	17.11	0.41	13.2	21	498
371	RPE30	30	0	0.92	4.62	42.7	0.1	57	0.000161	2.07	174.04	0.03	3.9	9	69
372		30	25	0.92	4.62	42.7	1.3	46	0.000200	15.44	23.31	0.03	5.4	11	130
373		30	50	0.92	4.62	42.7	2.6	25	0.000368	16.78	21.45	0.04	9.2	12	402
374		30	75	0.92	4.62	42.7	4.0	23	0.000400	23.16	15.54	0.06	11.7	17	484
375		30	100	0.93	4.62	42.7	5.3	16	0.000581	21.25	16.94	0.32	15.9	19	560

List of Publications based on Ph.D. Research Work

Sl. No.	Title of the paper	Authors (In the same order as in the paper. Underline the Research Scholar's name)	Name of the Journal/ Conference/ Symposium, Vol., No., Pages	Month &Year of Publications	Category *
1	A Comparative Study and Regression Analysis on Physico-Thermal Properties using Pongamia Pinnata-Waste Cooking Oil Methyl Ester Mixture	Balaji Rao K, B. M. Kunar, Ch. S. N. Murthy	Energy Sources, Part A: Recovery, Utilization, and Environmental Effects Vol. 1, 1-12 (Scopus)	May 2021	1
2	A Critical Review on Different Biodiesel Blends and their Application in Underground Mining Machineries	Balaji Rao K, B. M. Kunar, Ch. S. N. Murthy	International Conference on Recent Trends in Technology, Engineering and Applied Science (ICRTTEAS 2019),	12th to 13th April 2019.	4
3	A Comparative Assessment and Statistical Analysis of Performance and Emissions of Diesel Engine Fuelled with Emulsified Methyl Esters of Pongamia Pinnata diesel blends	Balaji Rao K, B. M. Kunar, Ch. S. N. Murthy	Advances in Energy, Environment for Sustainable Development-2022	07-08 January, 2022	4
4	Statistical Analysis and Comparative Assessment on the Performance and Emissions of a Diesel Engine Fuelled using Diesel-Ethanol and Diesel-Acetone Blends	Balaji Rao K, B. M. Kunar, Ch. S. N. Murthy	Environmental Quality Management	Communicated	1

*Category: 1: Journal paper, full paper reviewed 2: Journal paper, Abstract reviews 3: Conference/Symposium paper, full paper reviewed
4: Conference/Symposium paper, abstract reviewed 5: Others (including papers in Workshops, NITK Research Bulletins, Short notes etc.)
(If the paper has been accepted for publication but yet to be published, the supporting documents must be attached.)

Balaji Rao K
Research Scholar

Dr. B. M. Kunar & Prof. Ch. S. N. Murthy (Retd.)
Research Guides

BIODATA

1. Name : Balaji Rao K

2. Father's Name : Krishna Murthy K

3. Mather's Name : Vimala Bai K

3. Date of Birth : 01-05-1983

4. Nationality : Indian

5. Marital Status : Married

6. Present Position : Research Scholar, NITK, Surathkal

7. Address for Communication : # 2429, 1st Main, 3A cross,
Vivekanandnagar, Bangarpet, Kolar (DT),

8. Mobile : (+91)-9483774273

9. E-mail : balajiada@gmail.com

10. Academic Qualifications:

Degree	Specialization	Year	College	University	%/CGPA
M. Tech (Full Time)	Engineering Design	2012-2015	Er. Perumal Manimekalai College of Engineering and Technology, Hosur	Anna University, Chennai	*7.35 (CGPA)*
B. E (Full Time)	Mechanical Engineering	2002-2006	Bangalore College of Engineering and Technology, Bangalore	Visveswaraya Technological University, Belgaum	*63.11%*

11. Work Experience: (7 Years)

From	To	Designation	Organization
June 2015	Dec 2017	Assistant Professor (Mechanical Engg.)	Dr. T. Thimmaiah Institute of Technology, Karnataka
Sep 2009	June 2012	Lecturer (Mechanical Engg.)	Dr. T. Thimmaiah Institute of Technology, Karnataka
Apr 2008	Sep 2009	Consultant Engineer	Aeronautical Development Agency, Bangalore
Mar 2007	Dec 2007	Lecturer (Mechanical Engg.)	CMR institute of Technology, Bangalore